Characterising the temperature dependence of anaerobic CH_4 and CO_2 production from intact and drained New Zealand peatlands

A thesis

submitted in partial fulfilment

of the requirements for the degree

of

Master of Science (Research) in Environmental Sciences

at

The University of Waikato

by

Alice Rose Wheatley-Wilson

THE UNIVERSITY OF
WAIKATO
Te Whare Wānanga o Waikato

2021

Abstract

Understanding the temperature response of anaerobic microbial processes in wetlands is important in determining consequences for carbon dynamics and the production of methane (CH_4) under climate warming scenarios. Natural wetlands, including peatlands, contribute roughly 30% of global CH_4 emissions, making them the largest natural source of CH_4. The transfer of carbon-based greenhouse gases (C-GHG) to the atmosphere produced from the significant amounts of organic matter stored in anaerobic environments could cause a positive feedback to climate warming. This is concerning for peatlands as these environments hold enormous global carbon stocks and given projected global temperature increases. The consensus of previous work suggests that climate warming will result in the acceleration of organic matter decomposition, stimulating CH_4 and carbon dioxide (CO_2) emissions from peatlands. However, the poorly constrained temperature response of CH_4 production continues to plague ecosystem models, due to a lack of understanding of the parameters controlling this process.

Despite the importance of wetlands as global sources of CH_4, there is uncertainty among CH_4 production versus temperature models in these environments. Verifying models over a larger temperature range enables us to extract information from a dataset and capture important features such as the temperature optimum or point of rate decline. Therefore, to extract meaningful information on the temperature response of wetland methane production, we collected data on the response across a large temperature range to capture the full curvature of the response. We generated detailed temperature response curves of CH_4 production from two New Zealand peatlands. As far as we are aware, these data are unique in the international literature and provide new information for interpreting ecosystem-scale fluxes.

To improve our understanding, we quantified the temperature response of anaerobic organic matter decomposition into CH_4 and anaerobic CO_2 for both an intact and a drained New Zealand peatland. We also compared anaerobic CH_4 and CO_2 production rates across different vegetation types by examining different locations within the intact site. Understanding the difference in C-GHG production potential from contrasting land uses has important implications for managing peat soils and when considering the effects of rewetting drained systems and for comparing the relative net climate forcing of each ecosystem. We developed a methodology for anaerobic peat sampling and performed laboratory incubations for both intact and drained peat. Peat samples were incubated for four days in a temperature gradient block

ranging from 8.5–51°C, with 18 discrete temperatures that allowed three replicates at each temperature.

Using Macromolecular Rate Theory (MMRT), we derived temperature response metrics for anaerobic CH_4 and CO_2 production, including the temperature optimum (T_{opt}) and the inflection point (T_{inf}). The T_{opt} for CH_4 production ranged from 30.1–32.8°C and T_{inf} values ranged from 23.3–25.6°C. The temperature response did not significantly differ between sites for CH_4, and each peak was relatively tightly constrained, with a sharp increase in production rates at around 15–20°C, followed by a rapid decline in rates above the T_{opt}. On the other hand, the anaerobic CO_2 production curves were less constrained by temperature and differed across sites. Both T_{opt} and T_{inf} were higher for anaerobic CO_2 compared to CH_4, with T_{opt} ranging from 35.4–44°C and T_{inf} ranging from 25–32.2°C.

Overall, this study observed that anaerobic CH_4 and CO_2 production in intact and drained peatlands in New Zealand showed a response with temperature that was well described using MMRT. Despite differences in curvature, temperature metrics did not significantly differ between sites. Anaerobic CO_2 was produced at much higher rates than CH_4, however, the source of the CO_2 is unclear. Additionally, the molar ratio of CO_2:CH_4 increased dramatically above methanogenic T_{opt}. This may provide a positive feedback to the carbon cycle and have important implications for the rewetting of drained peat.

Acknowledgments

Firstly, I would like to thank my supervisors, Jordan Goodrich and Dave Campbell. Jordan, it was such a pleasure working with you and getting to know you. I am so glad I was your student. You are so easy to get along with and I always enjoyed having a chat and a laugh with you. Thank you for being so generous with your time and patiently working through this thesis with me – you have taught me so much. I would recommend a good natured, easy-going supervisor like you to anyone.

Dave, without you I probably would not have decided to do this strange masters thing. Thank you for introducing me to the world of research and teaching me a fact or two about peat. Your experience in research and passion for peat is inspiring, thank you for guiding me throughout this process. While on the topic of passionate geniuses, thank you Louis Schipper for teaching me all about MMRT and always being encouraging about my results and progress. Louis and Dave, I always appreciated the frequent check-ins on the way in or out of the office; it was always nice to have that support and understanding.

To my favourite masters pals and field work helpers: Emily Fensham, Ally Van de Laar, and Olivia Adamson. Such amazing friends and inspiring, intelligent young women. Emily, so glad to have begun my science journey with one of my best friends. Thanks for so many great memories - my tummy still hurts from laughing at you falling thigh deep into peat. Ally, thanks for being my office and masters buddy. I am so grateful we have had each other's company and advice throughout this whole process. To Olivia, thanks for being a ray of sunshine and constant source of positivity, your fun-loving attitude to life is contagious.

And the boyfriend of the year award goes to...Christopher Perry. Thank you for supporting me in so many ways, a shoulder to stress-cry on, someone to put things into perspective, and someone who always makes me laugh. Not to mention, doing my experiments for me when I broke my wrist, and even keeping complaints to a slightly above minimum level while doing it!

Thank you Holly Harvey-Wishart and Chris Morcom for lab and field gear; to Aaron Wall for your GIS skills and for bringing baby Evelyn into the office; my cousin Danielle for being the other (smarter and cooler) scientist in the family; Ben Roche for navigating the maze of online learning and zoom calls with me during lockdown, Georgie Glover-Clark and Kristyn Numa for your guidance into the world of being a masters student; Cheryl Ward for being a wizard with Microsoft Word; all of the WaiBER folk: Chris, Dori, Seb, Gimhani, Reza, Adam,

Thomas, Helena, and Seger; and to Charlotte Alster, Vic Arcus, and Terry Isson for being excited about all things MMRT.

Thank you to J.D. and R.D. Wallace Ltd. for permitting access to one of their farms, and to farm manager Shaun Olsen and Board Chairman Harry Snell. Thank you to the Brewster family for permitting access to Kopuatai via their farm. I would also like to acknowledge the Department of Conservation and Ngāti Hako, the kaitiaki of Kopuatai. This project was supported with funding from the University of Waikato and SSIF funding for Crown Research Institutes from the Ministry of Business, Innovation and Employment's Science and Innovation Group via Manaaki Whenua Landcare Research.

I dedicate this thesis to my family and friends. Mum, you have taught me that strong (and tiny) women can do anything. To be such a trusted and respected leader in your field has always inspired me, growing up I have always wanted to be as hard-working, intelligent, and accomplished as you. Dad, known to some as "Garry, the running legend", and known to me as the best dad in the world. Thank you for always supporting me with everything I do and for always being proud of me. My brother Tim, thanks for buying me food, you are the brother that every student needs and definitely my favourite brother. Katie and Diane, thank you for being my best friends and my Waikanae home away from home. Finally, thank you to all my loving, adventurous, and amazing friends, for reminding me to take a break!

Table of Contents

Abstract i
Acknowledgments iii
Table of Contents v
Chapter 1 Introduction 1
1.1 Global carbon cycle and peatlands 1
1.2 Temperature response of wetland CH_4 production 2
1.3 Southern Hemisphere peat bogs 3
1.4 Thesis aim 4
1.5 Thesis objectives 5
1.6 Outline 6
Chapter 2 Literature Review 7
2.1 Introduction 7
2.2 Global atmospheric methane 7
2.2.1 Climate change and wetlands 8
2.3 Peat definitions and characteristics 9
2.3.1 Peat carbon budgets 10
2.3.2 Waikato peat bogs 12
2.3.3 Drained peat 13
2.4 Mechanisms controlling peatland methane flux 14
2.4.1 Production 14
2.4.1.1 Microbial respiration 14
2.4.1.2 Moisture 16
2.4.1.3 Redox potential 19
2.4.1.4 Substrate availability 19
2.4.2 Methane transport 22
2.4.3 Consumption 23
2.4.4 Anaerobic CO_2 production 23
2.5 Temperature response of methane production 24
2.5.1 Temperature dependence of peat carbon decomposition 24
2.5.2 Temperature control terminology 25
2.5.3 CH_4 production rate vs. temperature studies 26
2.5.4 Other factors influencing temperature response 27

2.5.5 Temperature versus rate models 32
2.5.5.1 Arrhenius and Q_{10} 32
2.5.5.2 Macromolecular rate theory 33
2.6 Methods in literature for measuring soil CH_4 production 37
2.7 Knowledge gaps and implications 39
Chapter 3 Methods and site description 40
3.1 Site description 40
3.1.1 Kopuatai 40
3.1.2 Moanatuatua 43
3.2 General methods 45
3.2.1 Peat sample collection 45
3.2.1.1 Kopuatai peat sampling methods 46
3.2.1.2 Drained peat sampling methods 48
3.2.2 Sample preparation 49
3.2.2.1 Flushing samples 49
3.2.2.2 Homogenization 50
3.2.2.3 Substrate additions 50
3.2.3 Incubation 50
3.2.3.1 Incubation length 52
3.2.3.2 Pre-incubation 53
3.2.4 Headspace sampling 54
3.2.5 Sample analysis 55
3.2.6 Data processing 56
3.2.6.1 Curve fitting 59
Chapter 4 Characterising the temperature dependence of CH_4 production in New Zealand peatlands 60
4.1 Abstract 60
4.2 Introduction 60
4.3 Site description and methods 62
4.3.1 Site description 62
4.3.2 Peat sample collection 64
4.3.3 Sample preparation and incubation 64
4.3.4 Headspace sampling 66
4.3.5 Sample processing and analysis 67

4.3.6 Data analysis 67
4.4 Results 68
4.4.1 Climate and hydrological conditions 68
4.4.2 Depth profiles of CH_4 and CO_2 71
4.4.3 Temperature dependence of CH_4 production 72
4.4.4 Temperature dependence of anaerobic CO_2 production 79
4.4.5 Ratio of CO_2:CH_4 production 83
4.5 Discussion 84
4.5.1 Temperature dependence of CH_4 production 84
4.5.2 Temperature dependence of anaerobic CO_2 production 91
4.5.3 Anaerobic CO_2:CH_4 production ratio 95
4.5.4 Utility of MMRT in describing temperature dependence 97
4.5.5 Method review and applicability to other systems 99
4.6 Conclusion 102
Chapter 5 Conclusion 104
5.1 Findings 104
5.2 Implications for rewetting drained peatlands 106
5.3 Future work 107
5.4 Recommendations 108
References 110
Appendices 122
Appendix A 122
Appendix B 127

Chapter 1
Introduction

1.1 Global carbon cycle and peatlands

Methane (CH_4) and carbon dioxide (CO_2) account for approximately 55% of the natural greenhouse gas (GHG) effect and, of that, 15–25% is from CH_4 (Etminan *et al.*, 2016). Natural wetlands, including peatlands, contribute roughly 30% of global CH_4 emissions, making them the largest natural source of CH_4 (Kirschke *et al.*, 2013; Saunois *et al.*, 2020). The greenhouse effect is the process of atmospheric warming caused by greenhouse gases (GHG) absorbing thermal energy in the troposphere. Anthropogenic warming caused by increases in GHG emissions from human activities has destabilized the natural greenhouse effect and disrupted climate cycles (Turner *et al.*, 2019). Anthropogenic warming has also induced the acceleration of decomposition (Duffy *et al.*, 2021), which is concerning for peatlands as these environments are enormous global carbon stocks (Loisel *et al.*, 2021). The transfer of significant amounts of organic matter stored in anaerobic environments to the atmosphere leads to a positive feedback to climate change (Eville, 1991; Davidson & Janssens, 2006; Portner *et al.*, 2010; Schuur *et al.*, 2015). Saunois *et al.* (2020) found 149 $TgCH_4\ yr^{-1}$ to 181 $TgCH_4\ yr^{-1}$ originated from wetlands from data collected between 2008 to 2017, using bottom-up and top-down approaches respectively. This is a source of concern and uncertainty in a changing climate (Yvon-Durocher *et al.*, 2014; Saunois *et al.*, 2020). Emissions are still poorly constrained due to differences in magnitude and spatial heterogeneity within and across sites and a poor understanding of their controls (Dalal *et al.*, 2007; Dinsmore *et al.*, 2009; Turetsky *et al.*, 2014; Kolton *et al.*, 2019). Despite the importance of wetlands as global sources of CH_4, there seems to be more uncertainty among wetland emission models than there is in the projected climate variables used to drive them. Understanding the factors regulating methane emissions from peatlands is important for making projections of the shift of carbon from natural soils to the atmosphere and necessary for mitigation and ecosystem modelling (Bartlett *et al.*, 1989; van Winden *et al.*, 2012). Of particular concern it the poorly constrained temperature response of CH_4 production, which continues to plague ecosystem models due to a lack of understanding of the parameters controlling this process.

Davidson and Janssens (2006) suggest the temperature sensitivity of belowground organic matter decomposition should be described and modelled using a set of principles outlining environmental constraints and kinetic theory. The consensus of previous work suggests that

climate warming will result in the acceleration of organic matter decomposition, stimulating CH_4 and CO_2 emissions from peatlands (Davidson & Janssens, 2006; Weedon *et al.*, 2013; Kolton *et al.*, 2019; Hopple *et al.*, 2020). This is concerning considering the high global warming potential of CH_4 (28–34 times that of CO_2 over a 100-year time frame) (Myhre *et al.*, 2013). To make better predictions on carbon sensitivity using models, we need to reduce the high level of uncertainty from temperature response functions used in current models (Portner *et al.*, 2010).

1.2 Temperature response of wetland CH_4 production

Microbial respiration from aerobic systems is well studied but modelling this response with temperature has been subject to debate for decades (Lloyd & Taylor, 1994; Fang & Moncrieff, 2001; Davidson & Janssens, 2006). In contrast, there is a paucity of knowledge on the temperature response of organic matter turnover from anaerobic systems, including peatlands. Models used to make projections are often parameterized using data published decades ago and from a limited number of sites (e.g., Dunfield *et al.*, 1993). Most temperature response studies are often limited to a handful of temperatures and rarely cover the full range needed to capture accurate temperature response curves. To extract meaningful information on the temperature response of wetland CH_4 production, we require improved data across a larger temperature range that captures the full curvature. Verifying models over a larger temperature range enables us to extract important features such as the temperature optimum (T_{opt}) (Portner *et al.*, 2010).

In addition to having more detailed and better data on temperature response, there is also confusion about which model most accurately characterises this response. The continued use of exponential and Q_{10} functions may be a reasonable first approximation of temperature response at low temperatures, however, these models do not predict a T_{opt} or account for changes in relative temperature sensitivity (Schipper *et al.*, 2014). Macromolecular rate theory (MMRT) is a temperature response model developed to describe enzyme-mediated biological reactions (Hobbs *et al.*, 2013), that may also successfully model gas production rates from peat. MMRT is derived from thermodynamic first principles and accounts for changes in the heat capacity (ΔC_p) of enzymes to explain temperature sensitivity, including at the higher and lower temperatures that Q_{10} fails to capture (Schipper *et al.*, 2014).

The methodology used to quantify the temperature dependence in soil respiration studies ranges from lab incubations and in-field static-chamber installations to ecosystem scale measurements using the eddy covariance technique. Lab incubations are particularly

advantageous because environmental and physical soil properties can be controlled. Recent advances in aerobic respiration studies have been made using the temperature gradient block method, which involves incubating a series of small soil samples across a linear temperature gradient within a solid block of aluminium, and quantifying the resulting gas production as a measure of soil organic matter decomposition. This same methodology can be adapted to study the temperature dependence of CH_4 production rates (Kolton *et al.*, 2019) by focussing on maintaining *in situ* anaerobic conditions throughout the measurement process (Dunfield *et al.*, 1993; Yavitt *et al.*, 2006; Hopple *et al.*, 2020). Alongside CH_4, other anaerobic respiration studies have measured anaerobic CO_2 production to assess C-GHG loss partitioning patterns (Waddington *et al.*, 2001; Wilson *et al.*, 2017; Conrad, 2020; Liu *et al.*, 2021). Understanding the production ratio of anaerobic CO_2 and CH_4 from peatlands may have important implications for positive feedbacks between the carbon cycle and global warming given the higher potency of CH_4 as a GHG, relative to CO_2 (Yvon-Durocher *et al.*, 2014).

1.3 Southern Hemisphere peat bogs

The Northern Hemisphere hosts the greatest global peatland area where the majority of carbon-related peat studies are conducted. There is a need to expand this discussion more comprehensively to Southern peatlands where climate, soil, vegetation, and carbon exchange patterns differ from their Northern Hemisphere counterparts. Southern Hemisphere wetlands contribute ~50% to global wetland CH_4 emissions, and while most of these originate from tropical peatlands, understanding CH_4 fluxes from the full spectrum of ecosystems is important in closing the global CH_4 budget.

The few Northern Hemisphere peatland studies demonstrating the thermal response of CH_4 production across a wide temperature range include Dunfield *et al.* (1993) sampled from Hudson Bay, Canada and Kolton *et al.* (2019) from Minnesota, U.S.A. Other CH_4 production temperature response studies exist for peatlands (Svensson, 1984; Waddington *et al.*, 2001; Freitag & Prosser, 2009; Hanson *et al.*, 2016; Wilson *et al.*, 2016b; Sjögersten *et al.*, 2018; Deng *et al.*, 2019; Hopple *et al.*, 2020), including permafrost peat (Yavitt *et al.*, 2006; Metje & Frenzel, 2007; Treat *et al.*, 2014; Tveit *et al.*, 2015) and for other land uses (e.g., rice paddies) (Schulz *et al.*, 1997; Yao & Conrad, 2000; Glissman *et al.*, 2004; Duc *et al.*, 2010). However, Dunfield *et al.* (1993) & Kolton *et al.* (2019) are unique in using more than eight set temperatures across a temperature range larger than 35°C. Therefore, both of these studies

captured the full curvature of CH_4 production with temperature, including the T_{opt} (~30°C). As for Southern Hemisphere peatlands, no such published studies presently exist.

Because of this, we still need to develop a methodology for sampling and incubating peat from New Zealand systems, including both intact and drained systems. Peatlands in New Zealand include the limited area of intact systems or relatively intact systems and their drained counterparts. Increased demand for land has generated pressure for intact systems to be drained and developed for alternative land uses (Deverel *et al.*, 2016). The large carbon reservoirs in intact peatlands are converted to sources of atmospheric CO_2 when systems are drained, significantly altering carbon dynamics and flux pathways. While CH_4 emissions may be reduced after drainage, understanding C-GHG fluxes from drained peatlands is important as CO_2 emissions originating from these peatlands account for approximately 5% of all anthropogenic GHG emissions despite covering less than 1% of global land surface area (Joosten *et al.*, 2012). Drainage may also alter the temperature response of microbes by complicating other controls on CH_4 emissions, such as water table regimes and substrate availability (Hargreaves & Fowler, 1998; Le Mer & Roger, 2001).

Understanding the difference in production potential of C-GHGs from contrasting land uses has important implications for managing peat soils and when considering the effects of rewetting drained systems. Examining different locations within an intact site could provide insight into how CH_4 and anaerobic CO_2 production differ spatially and under certain vegetation types. Production of C-GHGs may also change temporally across seasons, and spatially, with depth. The response of CH_4 and anaerobic CO_2 production to rising temperatures as well as the overall impact of climate change is poorly understood. By assessing C-GHG emissions from these contrasting peatland systems, we can reduce uncertainty around the relative importance of C-GHG emissions/uptake to net climate forcing from each ecosystem (Dalal *et al.*, 2007; Goodrich *et al.*, 2017; Kolton *et al.*, 2019).

1.4 Thesis aim

The overarching aim of this thesis is to quantify the temperature response of anaerobic organic matter decomposition to CH_4 from peat soils and investigate differences among vegetation communities. The first part of this research was focussed on developing the techniques and methods for anaerobic sampling and temperature gradient block incubations for New Zealand peat. This involved adapting the temperature gradient block at the University of Waikato to assess production under anaerobic conditions for both natural and drained peat rather than

aerobic soil samples. Secondly, the aim was to quantify the relationship between CH_4 production and temperature from New Zealand peat systems and provide a new perspective on the effects of global temperature increases on peatlands due to climate change. Generating detailed temperature response curves for CH_4 production from temperate Southern Hemisphere bogs is unique in the international literature and should provide new information for interpreting ecosystem-scale fluxes. In addition, we used MMRT as a tool for extracting temperature response metrics for CH_4 production from New Zealand peat. These results broaden the scope for applying MMRT, a tool that has previously been successful in describing individual enzyme rate and aerobic CO_2 production at various scales, and ecosystem photosynthesis. Finally, the comparison of CH_4 production between an intact site and a drained site could provide insight into the quantity and movement of carbon associated with land use. Comparing multiple sites within the intact peatland also paints the picture of how vegetation structure can cause spatial variation in production of CH_4 and anaerobic CO_2.

1.5 Thesis objectives

We will achieve the overall aims of this study by creating a robust yet versatile methodology for sampling peat and performing laboratory-based incubations to measure anaerobic gas production rates. In order to achieve and expand on these aims, the following objectives were to:

i) develop a simple and reproducible technique for anaerobic peat sampling and performing laboratory incubations for both intact and drained peat by adapting the University of Waikato soils laboratory temperature gradient block to suit anaerobic incubation of peat;
ii) quantify CH_4 production rates originating from peat over a large temperature range (8.5-51°C);
iii) characterize the temperature response curve and predict the temperature optima for peatland CH_4 production based on the theoretical framework of MMRT;
iv) compare peatland CH_4 production rates to anaerobic CO_2 production rates;
v) present New Zealand peat system data on CH_4 and CO_2 production rates for intact versus drained systems and discuss why these data are an important contribution to the discussion on rewetting drained systems;
vi) identify issues surrounding C-GHG production from peat and discuss what implications this may have under a warming climate;

1.6 Outline

Chapter 2 outlines the relevant literature and current knowledge gaps around the cycling of C-GHGs released from peat, the environmental drivers and controls regulating these flux pathways, the effects of temperature on C-GHGs, and a review of temperature models and methodological techniques used in anaerobic peat studies.

Chapter 3 introduces the study sites and describes the methodology used in this study. To compare the C dynamics of an intact versus a drained system, we chose two study sites, the largely intact Kopuatai peat bog and a drained dairy farm site on the former Moanatuatua peat bog.

Chapter 4 is laid out in the format of a journal article with an abstract, introduction, results, discussion, and conclusion. This chapter describes and compares the temperature response of anaerobic CH_4 and CO_2 production from both intact and drained peat sites and discusses the success of the methodology used in this study.

Chapter 5 concludes the thesis and summarises the main findings in relation to results found in previous studies. The implications of rewetting drained peat on C-GHG production were also outlined in this section, as well as recommendations for further research in this area.

Chapter 2

Literature Review

2.1 Introduction

Natural wetlands globally contribute 15–25% to the greenhouse gas (GHG) effect and roughly 30% of the global methane (CH_4) budget, making them the largest natural source of CH_4 to the atmosphere (Etminan *et al.*, 2016; Saunois *et al.*, 2020). Wetland CH_4 production represents a positive contribution to radiative forcing in the atmosphere (Portner *et al.*, 2010; Yvon-Durocher *et al.*, 2014; Neubauer & Megonigal, 2015) due to the high global warming potential (GWP) of CH_4 (28–34 times that of CO_2 over a 100-year time frame) (Myhre *et al.*, 2013). Rates of CH_4 production from saturated organic soils are controlled by a number of environmental variables including temperature, water table depth (WTD), and substrate availability (Moore & Dalva, 1993; Knox *et al.*, 2021). This chapter provides background information surrounding this topic including peatland classification and characteristics, hydrological and biogeochemical regimes, as well as carbon cycling and implications for climate change. These concepts and classifications lead to a more detailed section on the response of peatland CH_4 production to temperature. Following this is a section on peat sampling and incubation methodologies from international studies and the best way of adapting these to suit New Zealand peat systems. This study is the first of its kind to focus on CH_4 production in New Zealand peat.

2.2 Global atmospheric methane

The global carbon (C) cycle refers to the exchange of carbon between the soil, hydrological, biological, and atmospheric systems as a consequence of natural and anthropogenic energy cycling (Moore & Dalva, 1993; Davidson & Janssens, 2006). Carbon undergoes a series of reactions in each of these environments aided by chemical, physical, and biological factors. In the soil, these factors influence the creation, transformation, and decomposition of carbon. For example, soil microbial (or heterotrophic) respiration reduces C compounds for decomposition into an energy source and drives the flux of these compounds from soils to the atmosphere (Castro *et al.*, 1995; Dalal *et al.*, 2007; Schädel *et al.*, 2020).

Two carbon-based GHGs (C-GHG) released from the soil that influence the earth's climate and the global C cycle, are CH_4 and CO_2 (Moore & Dalva, 1993). After CO_2, CH_4 is the second most important GHG in the atmosphere (28–34 times that of CO_2 over a century) (Myhre *et al.*, 2013). The largest biological source of CH_4 is production from anaerobic environments such as wetlands where soils are saturated and oxygen-limited (Le Mer & Roger, 2001; Saunois *et al.*, 2020). Saunois *et al.* (2020) estimated 149 Tg CH_4 yr^{-1} originated from wetlands using data collected from 2008 to 2017. On the other hand, the largest biological sink for methane is consumption via microbial activity in soils and sediments.

2.2.1 Climate change and wetlands

Imbalances in the global carbon cycle have led to the accumulation of CO_2 and CH_4 in the lower troposphere, trapping longwave radiation and causing global temperatures to rise (Fiore *et al.*, 2002). Wetlands are important for regulating the C cycle (Frolking & Roulet, 2007) and there is evidence that CH_4 emissions from wetlands have been strongly responsive to climate changes in the past, indicating they will continue to be responsive to climate changes in the future (Bridgham *et al.*, 2013). A warmer climate may then cause an increase in GHG production from wetland soils, prompting a positive feedback to global warming (Updegraff *et al.*, 1998; Gedney *et al.*, 2004; Van Huissteden *et al.*, 2006).

Soil microbes in peatlands are particularly sensitive to climate change (Tfaily *et al.*, 2014). The effects of anthropogenically induced global climate change continue to disturb natural ecosystem processes by promoting changes in microbial activity and altering the cycling of C (Basiliko *et al.*, 2012). Rising temperatures, increased GHG emissions, and changes in climate regimes are just some of these effects (Tfaily *et al.*, 2014). In particular, rising temperature has a major influence on the biological and physiological activity rates of organisms in soil and will potentially stimulate microbial decomposition of peat (Davidson & Janssens, 2006). Soil microbes play a key role in the fixing, cycling, storage, and sequestration of carbon, and understanding these processes helps explain past changes to global atmospheric CH_4 and make future scenario projections (Dlugokencky *et al.*, 2011). The pattern of global atmospheric methane over time shows a steady increase over the past 30 years, with the exception of 2000–2007 (Figure 2.1). Methane emissions began increasing again from 2007 after a stable period beginning in 2000, thought to be caused by increased temperatures in mid to high latitude wetlands promoting increased methane emissions (van Winden *et al.*, 2012; Turner *et al.*, 2019). Some climate models predict that by the end of the 21st century, temperatures will be elevated up to 6–10°C and likely to stimulate more C-GHG emissions from peat (Zhang & Wang, 2017).

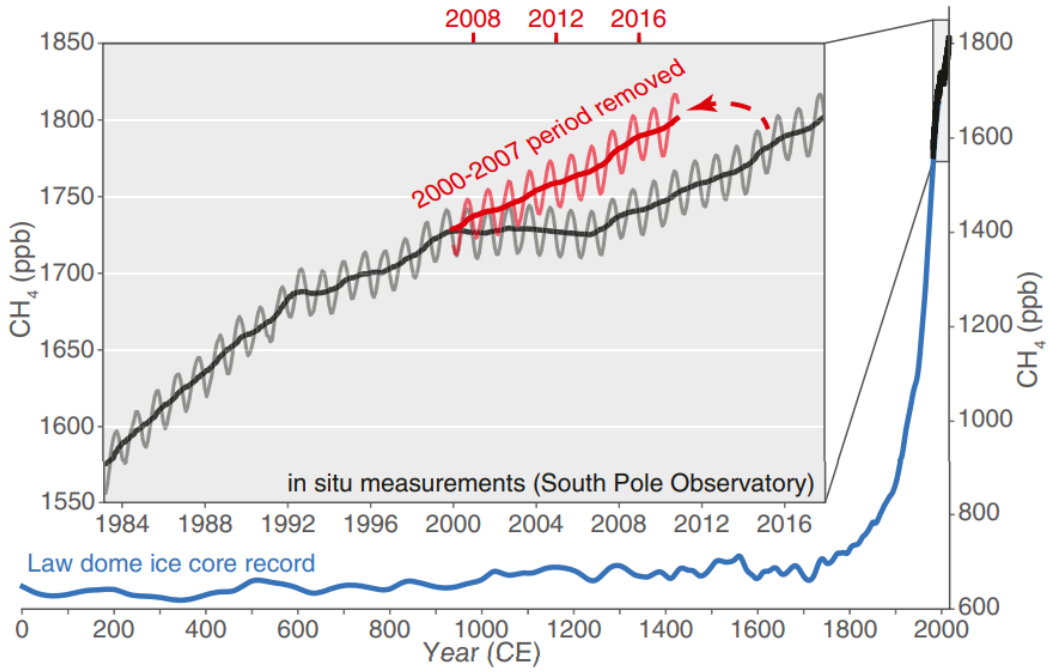

Figure 2.1 Pattern of global atmospheric methane over time showing direct observations (black), deseasonalized observations (grey), the Law Dome ice core record (blue), and simulation of removal of the 7-year stabilization period (red). Sourced from Turner *et al.* (2019).

2.3 Peat definitions and characteristics

Natural peatlands cover approximately 3% of the global terrestrial area but store up to 50% of the total terrestrial soil carbon (Yu *et al.*, 2010; Huang *et al.*, 2021). The flux of C-GHGs are sensitive to climate in peatlands, although this degree of sensitivity is uncertain due to scaling processes across landscapes and regions (e.g., Lehmann *et al.*,2016; Dinsmore *et al.*,2009). Even less is known about C-GHG flux rates and variability, size of carbon stocks, and flux sensitivity to climate and environmental change in Southern Hemisphere systems (Baird *et al.*, 2004; Broder *et al.*, 2012; Goodrich *et al.*, 2017).

By definition, peatlands are a type of wetland that forms ‘peat’, a term describing the organic substrate formed by the accumulation of partially decomposed plant matter at least 30 cm deep (Clymo, 1984; Yang *et al.*, 2017). The United States Department of Agriculture (USDA) soil taxonomic system classifies peat as a Histosol, which is an obligate hydric soil that is organic and very poorly drained (Tiner & Ralph, 2016; Yang *et al.*, 2017). Generally, peatlands are classified into three categories: (1) minerotrophic, (2) ombrotrophic, and (3) transition, depending on their hydrological and geochemical regime (Mitsch & Gosselink, 2000). Minerotrophic peatlands are referred to as fens; ombrotrophic peatlands are referred to as bogs, and transition peatlands are an intermediary between these two (McGlone, 2009; Lin *et al.*,

2012). In addition to carbon storage, peatlands also provide many important functions at both the local and global scale, including regulating atmospheric gases and improving water quality (Fisher & Reddy, 2013). Peatlands are also biologically diverse, boasting a variety of plant species including; shrubs mosses, and small trees, while animal species range from invertebrates, amphibians such as frogs, waterfowl, and even small mammals (Mitsch & Gosselink, 2000).

Peat bogs predominantly undergo a vertical exchange of water in the forms of precipitation and evaporation but have some lateral water outputs via seepage and overland flow, whereas fens receive stream or groundwater input (Scott, 1996; Smith, 2003). Peat bogs also characteristically have a low (acidic) pH and low nutrient content due to limited inputs, in contrast to fens (Mitsch & Gosselink, 2000). Below the water table exists the oxygen-depleted catotelm, where slow anaerobic degradation of organic matter takes place. However, the boundary of saturated peat is subject to change with capillary action (Clymo, 1984). The water table is located where pore water exists at atmospheric pressure, whereas capillary water is held at less than atmospheric pressure via suction (Schwärzel *et al.*, 2006; Fritz *et al.*, 2008). Climate also drives water table and temperature changes, which in combination regulate soil carbon fluxes (e.g., Van Huissteden *et al.*, 2006; Goodrich *et al.*, 2017).

2.3.1 Peat carbon budgets

Undisturbed peatlands are CO_2 sinks and CH_4 sources, while the relative strength of each determines their influence on climate (Frolking & Roulet, 2007). The overall rate of carbon accumulated within or lost from an ecosystem is referred to as the net ecosystem carbon balance (NECB). NECB can be simplified into an equation suited to wetland C exchange pathways (Eq. 2-1) (Chapin *et al.*, 2006).

$$\mathrm{NECB} = \mathrm{NEP} - F_{\mathrm{CH4}} - F_{\mathrm{DOC}} \quad (2\text{-}1)$$

Net ecosystem CO_2 production (NEP) represents the difference between gross primary production (GPP) and ecosystem respiration (ER). F_{CH4} represents the net ecosystem exchange of methane and F_{DOC} refers to the dissolved organic carbon export. Photosynthesis and respiration regulate the exchange of carbon between the soil and the atmosphere. The assimilation of CO_2 by autotrophs (photosynthesis) represents gross primary production (GPP), which is counterbalanced by ecosystem respiration (ER), which refers to the loss of CO_2 via

autotrophic and heterotrophic respiration (Chapin *et al.*, 2006). The effects of F_{DOC} and F_{CH4} on Eq. 2-1 are reduced during dry years, but these differences typically do not substantially change the overall NECB (Goodrich *et al.*, 2017), however, this may not be the case for all systems (Dinsmore *et al.*, 2010).

A positive NECB indicates net C uptake by the system, suggesting the ecosystem is a carbon sink. Most peatland ecosystems tend to be a stronger C sink during summer due to increased growth conditions and warmer temperatures. On the other hand, New Zealand bogs tend to have a larger NECB than Northern Hemisphere bogs due to year-round growing conditions and relatively mild climate conditions supporting a short season of C loss and driving a relatively larger annual NEP (Goodrich *et al.*, 2017). Peatlands may be at risk of becoming a source when ER increases in a warmer and drier climate, as some future climate predictions suggest (van Winden *et al.*, 2012; Turner *et al.*, 2019).

Generally, peatlands sequester CO_2 and emit CH_4, which depending on the balance, causes a cooling or warming influence on the climate system. These climate system impacts are compared using the global warming potential (GWP) methodology, which suggests CH_4 has 28–34 times the radiative forcing strength of CO_2 over a 100-year time frame (Myhre *et al.*, 2013). Methane initially dominates the radiative forcing signal from peatlands for the first ~50 years of peatland formation; however, the effect stabilizes due to a relatively short atmospheric lifetime of ~12 years (Frolking *et al.*, 2006). CO_2 continues to accumulate beyond this period and has longer-lasting effects in the atmosphere, providing a net cooling effect over time as C sequestration dominates the system. Changes to the ratio of CO_2 sink to CH_4 source resulting from climate change or land use may affect the climate influence of peatlands and cause a positive feedback to anthropogenic climate forcing (Yvon-Durocher *et al.*, 2014; Neubauer & Megonigal, 2015; Huang *et al.*, 2021).

Figure 2.2 illustrates this relationship as a stable level of CH_4 radiative forcing in the first 50–100 years of bog formation, followed by a rapid decline in the radiative influence of CH_4 after this period. On the same timeline, CO_2 forcing is relatively stable but slowly decreasing due to its longer lifetime in the atmosphere (Frolking *et al.*, 2006; Frolking & Roulet, 2007). Frolking and Roulet (2007) found that only 0.3% of total emitted methane still existed in the atmosphere after 4000 years of constant fluxes, while 20% of CO_2 sequestered as peat has not returned to the atmosphere. Changes in the ratio of CO_2 sink to CH_4 source resulting from climate or land use may affect the climate influence of peatlands (Wilson *et al.*, 2016a; Hopple *et al.*, 2020).

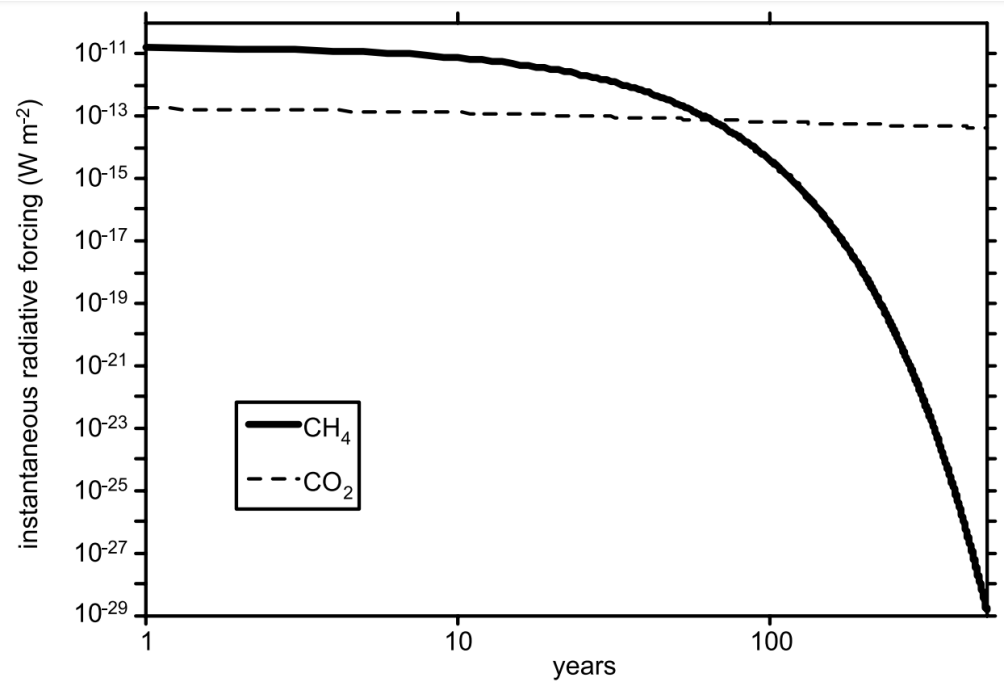

Figure 2.2 Example of the relationship between temporal evolution of instantaneous radiative forcing (W m^{-2}) of methane (solid line) versus CO_2 (dashed line) into the atmosphere. Sourced from Frolking et al. 2006).

2.3.2 Waikato peat bogs

The majority of research into peatlands has been undertaken in Northern Hemisphere boreal zones, environments characterised by excess moisture and below freezing winter temperatures (Eville, 1991; Bellisario *et al.*, 1999; Frolking *et al.*, 2006; Yavitt & Seidman-Zager, 2006; Frolking & Roulet, 2007). In the Southern Hemisphere, New Zealand's peatland systems are characterised by a mild, temperate climate, year-round growing conditions, and large annual NEP (Campbell *et al.*, 2014; Goodrich *et al.*, 2017). Despite their differences in climate, hydrology, and vegetation, Northern and Southern Hemisphere bogs share similar mechanisms controlling the pathways of C between the soil and the atmosphere (Goodrich *et al.*, 2015; Lehmann *et al.*, 2016). However, Goodrich *et al.* (2015) found annual total CH_4 fluxes from a northern New Zealand peat bog were notably higher than Northern Hemisphere systems. Therefore, it is worth expanding global peatland datasets to include more research on Southern Hemisphere peatland systems, and understand how the mechanisms driving carbon feedbacks/pathways differ from their Northern Hemisphere counterparts.

New Zealand peat bogs are located in both the North and South Island, predominantly in the Waikato and Southland (Scott, 1996). This study focuses on ombrotrophic peat bogs and their drained counterparts in the Waikato Basin. Peat bogs now only occupy 5% of land area in the Waikato region, after drainage of >90% of peatlands here (Scott, 1996; Ausseil *et al.*, 2015). Two intact peat bogs remaining in the region are Kopuatai and Moanatuatua. Kopuatai peat

dome spans 90 km^2 (9,665 ha) in the middle of the Hauraki catchment, located South of the Firth of Thames (Scott, 1996; McGlone, 2009). On the other hand, Moanatuatua spans 114 ha, but once covered 7,500 ha before being drained and converted to agricultural land. This conversion has created issues of land subsidence and artificial lowering of the water table within the native bog remnant (Clarkson *et al.*, 2004; Campbell *et al.*, 2021). New Zealand raised bogs are characterised by rush species of the Restionaceae family, including greater jointed rush (*Sporadanthus ferrugineus*), as well as wire rush species including *Empodisma robustum* (Wagstaff & Clarkson, 2012). Patches of *Sphagnum* moss also persist at Moanatuatua and Kopuatai (Smith, 2003), but do not contribute significantly to peat formation. The New Zealand Land Cover Database suggests freshwater wetlands in New Zealand cover 249,214 ha (Dymond *et al.*, 2021) and these unique and biodiverse ecosystems are host to an array of native species as well as provide important ecosystem functions (Scott, 1996).

2.3.3 Drained peat

Increasing demand for productive land has led to the widespread drainage of peatlands. Globally, around 65 Mha of peatlands have been modified from their natural conditions to develop land for agriculture, forestry, and other anthropogenic uses (Kaat & Joosten, 2009). Draining peat exposes organic matter to aerobic decomposition, causing increased CO_2 emissions and modifying the physical properties of the peat (Campbell *et al.*, 2021). Drained peat differs in characteristics from natural peat, although both are categorized as peat soils (Charman, 2002). Natural peat is mainly comprised of slowly decomposing plant material, while drained peat soil is an organic soil derived from aerated peat, that only contains remnants of partly decomposed plant matter (Charman, 2002).

The significant fraction of sequestered global carbon in deep peat has been destabilized over the past century by drainage and aeration (Wilson *et al.*, 2016b). The draining of peat causes an imbalance in the radiative forcing patterns of CO_2 and CH_4, causing peatlands to act as a CO_2 source as ER surpasses GPP while decreasing CH_4 production (Laine *et al.*, 1996; Van Huissteden *et al.*, 2006). The intensity and duration of the drainage determine the degree of oxidation and the extent of irreversible surface subsidence effects (Tiner & Ralph, 2016). The CO_2 loss from drained peat due to oxidation continues over time (Deverel *et al.*, 2016; Tiner & Ralph, 2016), however, C-GHGs lost from drained peatlands are poorly understood. There is uncertainty around the strength of other flux pathways such as the fate of DOC transported downstream and the strength of CH_4 fluxes from peat versus drainage ditches (Laine *et al.*, 1996; Whalen, 2005; Yang *et al.*, 2017). Laine *et al.* (1996) provided a schematic

representation of the pathways of CO_2 and CH_4 throughout the profile of both a natural (undrained) and drained system (Figure 2.3). The diagram illustrates how aerobic and anaerobic zones influence the oxidation state of mineralized carbon based on the depth and location of the layer. For example, litter decay within the aerobic zone produces CO_2, while decay in the anaerobic zone produces CH_4. When this CH_4 enters the aerobic zone, the majority is oxidized to CO_2 (Laine *et al.*, 1996).

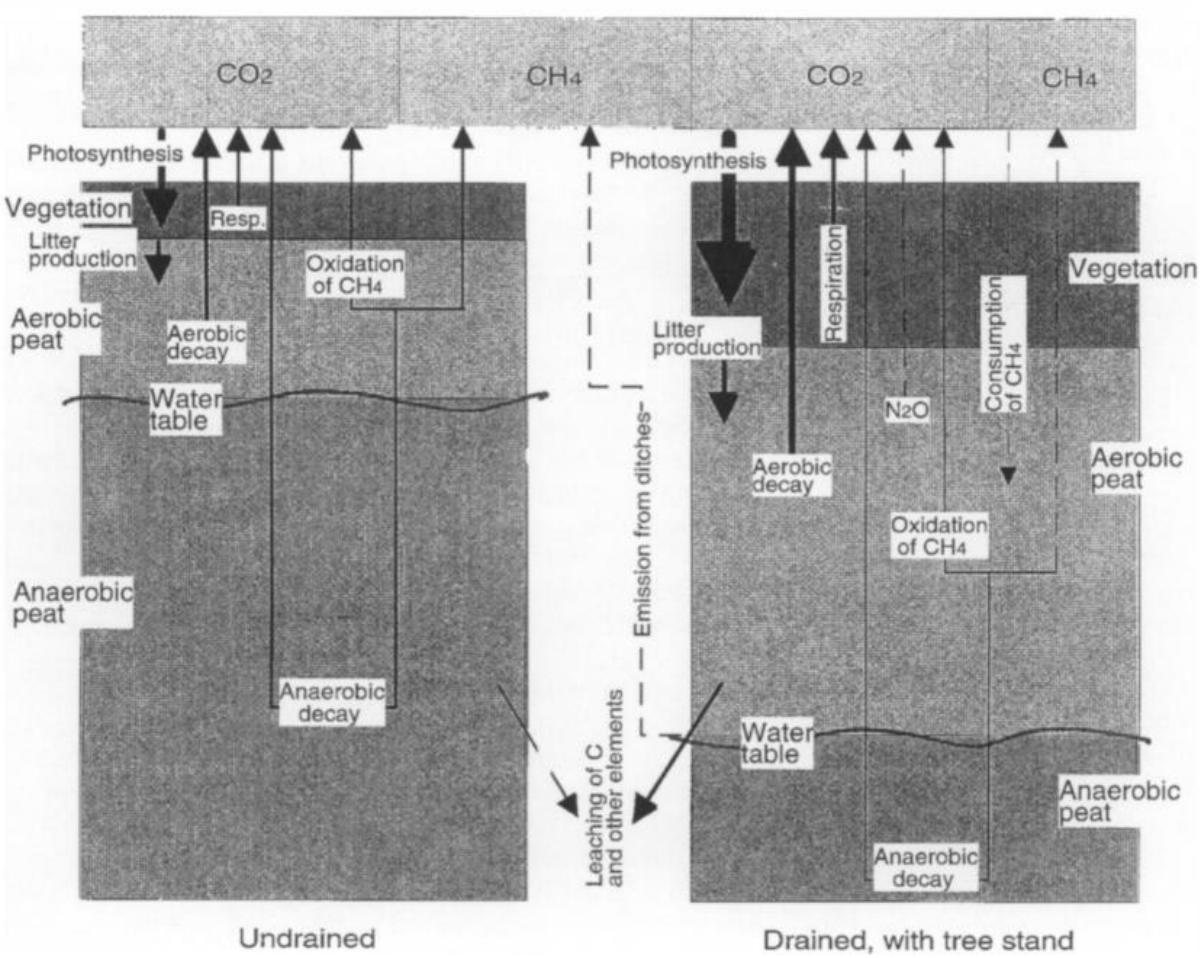

Figure 2.3 Schematic presentation of the GHG balances of undrained and drained peatland sites. Sourced from Laine *et al.* (1996).

2.4 Mechanisms controlling peatland methane flux

2.4.1 Production

2.4.1.1 Microbial respiration

Peatland CH_4 production refers to the microbially-driven process of organic matter decomposition into CH_4 (Le Mer & Roger, 2001). Microbes play a critical role in the process

of decomposition and transformation of dead organic material into reusable forms for other organisms (Gougoulias *et al.*, 2014). Photo- and chemo-autotrophs fix atmospheric carbon and synthesize it into organic matter. Heterotrophic microbes in the peat reverse this process by decomposing organic matter and utilizing carbon as a metabolic substrate for biomass production. The remaining metabolites return to the atmosphere as respiration products (Keller & Takagi, 2013; Gougoulias *et al.*, 2014). For unsaturated peat where oxygen is abundant, the main respiration product is CO_2. Oxygen is quickly depleted in saturated peat, so microbial populations shift towards communities that can utilize alternative electron acceptors (Gougoulias *et al.*, 2014). Methane production is driven by both syntrophic and competitive interactions for key substrates and in a classic anaerobic food chain based on thermodynamics, CO_2 is the final terminal electron acceptor (TEA) that reduces to CH_4 (Keller & Bridgham, 2007; Bridgham *et al.*, 2013; Wilson *et al.*, 2017; Conrad, 2020).

Anaerobic microbes are adapted to prolonged wetness and low oxygen levels, so decomposition is slow, and reactions yield less energy (Tiner & Ralph, 2016; Wilson *et al.*, 2017; Kolton *et al.*, 2019). There are two main pathways for CH_4 production in anoxic environments, including hydrogenotrophic (Eq. 2-2) and acetoclastic (Eq. 2-3) methanogenesis (Kolton *et al.*, 2019; Conrad, 2020).

$$4H_2 + CO_2 \rightarrow CH_4 + 2H_2O \quad (2\text{-}2)$$

$$2CH_3COOH \rightarrow 2CH_4 + 2CO_2 \quad (2\text{-}3)$$

The ratio of these two pathways is constrained by the stoichiometry of organic matter degradation and fermentation processes, which eventually result in the production of acetate and H_2 at a ratio of ≥67% acetoclastic and ≤33% hydrogenotrophic methanogenesis. These ratios reflect a perfectly efficient breakdown of organic matter; however, this is rarely the case and the partitioning is usually more complex (Conrad, 2020). Environmental constraints including moisture, redox potential, substrate availability, and temperature regulate microbial function (Schimel & Holland, 2005). For example, at low temperatures, acetoclastic

methanogenesis may dominate and at high temperatures, hydrogenotrophic methanogenesis may dominate (Chin *et al.*, 1999; Conrad, 2020). A more in-depth look into temperature controls on CH_4 production will be discussed in Section 2.5. The following section highlights three additional controls on CH_4 production.

2.4.1.2 Moisture

Moisture influences microbial respiration and decomposition rates by limiting oxygen supply and substrate diffusion (Schimel & Holland, 2005; Bridgham *et al.*, 2013). Low peat moisture reduces substrate diffusion, so organisms cannot readily access carbon substrate (Fang & Moncrieff, 2001; Schimel & Holland, 2005). High moisture content limits oxygen diffusion which lowers redox potential (Eh), encourages anaerobic conditions and subsequently slows microbial decomposition of organic matter (Schimel & Holland, 2005; Davidson & Janssens, 2006).

The key environmental controls on soil moisture are rainfall, evaporation, and soil texture (Schimel & Holland, 2005). Peat formation and accretion is dependent on precipitation and shifts in WTD as peat forms when precipitation exceeds evaporation and organic matter begins to accumulate. This imbalanced vertical transfer of water and the resulting shallow water table is typical of bogs (Section 2.3) (Tiner & Ralph, 2016). These unique hydrological controls select for specific microbial communities that determine organic matter decomposition rates (Clymo, 1984; Tiner & Ralph, 2016). Peat beneath the water table hosts microbial communities adapted to anaerobic conditions associated with high moisture content and low oxygen content, whereas, aerobic microbes are more likely to persist above the water table where oxygen can diffuse more readily (Le Mer & Roger, 2001). While both aerobic and anaerobic communities exist abundantly in permanently wet zones, dry zones or dry periods stimulate the activity of aerobic microbes and discourage methanogens. The rate of methanogenic activity is generally greatest a few centimetres below the water table level when the water level remains constant (Yang *et al.*, 2017). Seasonal fluctuations in WTD create a highly variable zone where changing redox conditions and substrate availability influence syntrophic microbial interactions (Moore & Dalva, 1993; Dalal *et al.*, 2007; Yang *et al.*, 2017). As the WTD rises, facultative anaerobes replace aerobic microbes, slowing decomposition. This slow decomposition causes organic matter to accumulate at the surface and forms peat. The opposite occurs when the WTD drops, exposing peat to aerobic microbes and increasing the rate of decomposition (Le Mer & Roger, 2001).

The heterogeneity and natural topography of peatlands determine hot spots for CH_4 and CO_2 emissions, based on soil saturation levels. Peatlands often have a hummock and hollow topography in which hollows are generally wetter, while hummocks remain dry. Methane is more likely to be produced in saturated hollows while aerobic hummocks tend to limit methanogenesis (van Winden *et al.*, 2012). Yang *et al.* (2017) describe how this heterogeneous relationship between WTD and peat C-GHG emissions differs from classic wetland emission models (Figure 2.4). Classic models assume the peat beneath the water table is anoxic and therefore, only producing CH_4. However, O_2 availability and depth do not solely regulate CH_4 dynamics. The emerging model assumes that anaerobic oxidation of methane (AOM) can still occur in saturated zones within the peat and that methanogenesis can still occur in anaerobic microsites in unsaturated peat (Blazewicz *et al.*, 2012; Yang *et al.*, 2017). Heterogeneity in peatland ecosystems enables the process of methanogenesis to occur simultaneously with other anaerobic respiration pathways when TEAs are available (Keller & Bridgham, 2007; Yang *et al.*, 2017). The classic model and other literature suggest very simply that CH_4 production rates are negatively correlated with CO_2 production rates as a function of changing WTD (Yang *et al.*, 2017). For example, Moore & Dalva (1993) found that for a water table situated at 40 cm depth, CO_2 fluxes increased by 4.3 times, while CH_4 emissions decreased by 5 times compared to surface-saturated profiles. The emerging model suggests the production and oxidation ratios do not simply increase or decrease relative to water table depth and in fact, both processes function to some degree at all levels of saturation (Yang *et al.*, 2017). The classic model assumes CH_4 oxidation is highest in unsaturated peat and becomes non-existent in saturated peat, while the emerging model implies that CH_4 oxidation is a function of CH_4 production and there are exceptions to the rules when it comes to the controls on CH_4 production dynamics (Yang *et al.*, 2017).

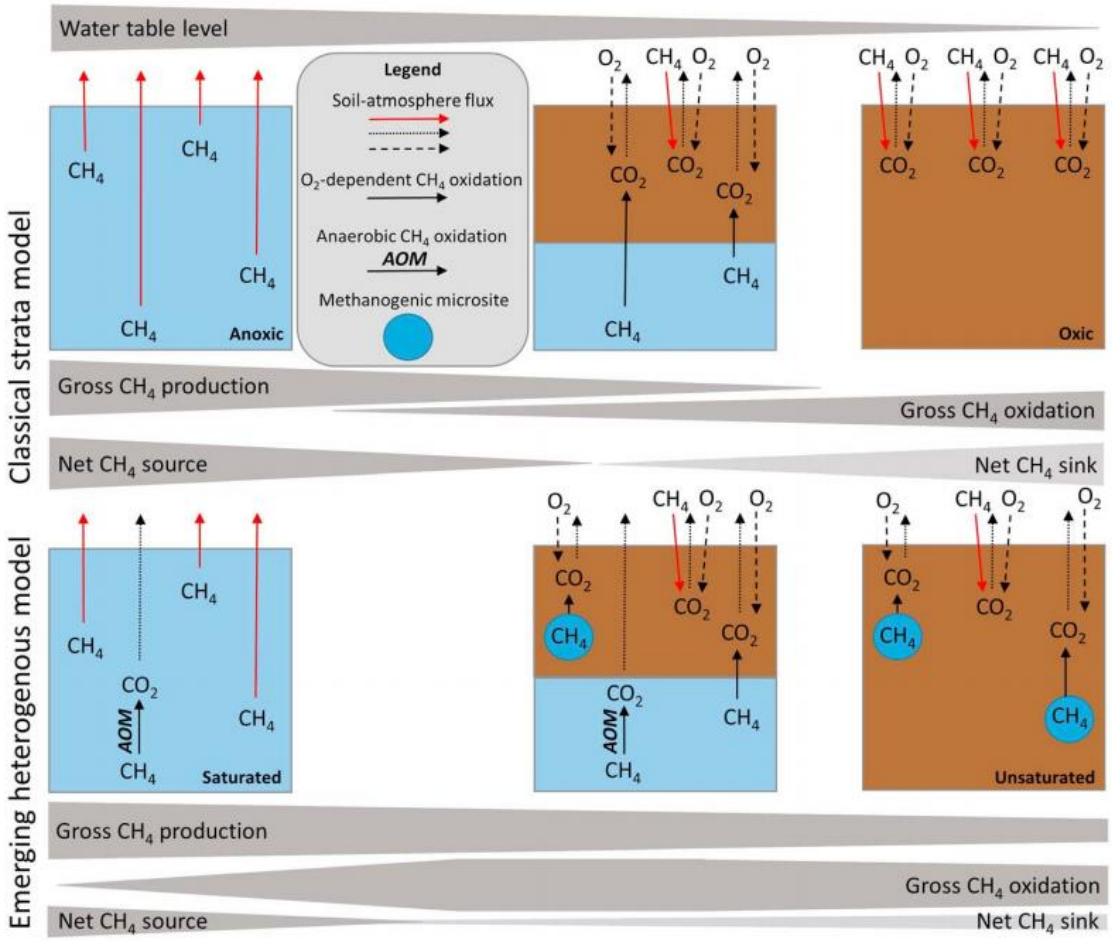

Figure 2.4 The classical strata model of the effects of the water table on the magnitude of CH_4 production and oxidation rates versus the emerging heterogeneous model. The relative magnitude of gross CH_4 production versus CH_4 oxidation and net source versus net sink is indicated by the width of the grey bars. Sourced from Yang *et al.* (2017).

Figure 2.4 suggests that disturbed or drained peatlands exhibit different CH_4 flux characteristics and mechanisms to undisturbed peatlands. Lowered water table and the resulting increase in temperature, altered hydro-geochemical conditions, and available labile carbon supply cause a decrease in CH_4 emissions. Evidence for this in disturbed systems, such as rice paddies, shows drying and rewetting of peat stimulates a pulse in CH_4 production due to the introduction of nutrients and decomposition products (Turetsky *et al.*, 2014). Methanogens are particularly sensitive to water table fluctuations, as Goodrich *et al.* (2015) found that low CH_4 production during a drought year remained low during the following summer season. The extreme conditions created a lag in CH_4 flux recovering upon rewetting, as the physicochemical properties of the soil changed (Kettunen *et al.*, 1999; Turetsky *et al.*, 2014; Goodrich *et al.*, 2015; Kolton *et al.*, 2019). Draining peat often significantly reduces CH_4 production relative to intact bogs as increasing the depth of the oxic zone limits the zones of methanogenesis and increases CH_4 oxidation rates (Huang *et al.*, 2021). On the other hand, CH_4 emissions from

drained sites may match those at undisturbed sites as maximum production rates tend to increase from drainage ditches (Dalal *et al.*, 2007; Turetsky *et al.*, 2014). The consistently low water table in drained peat alters soil characteristics including increased bulk density and decomposition rates, increased risk of land subsidence, and creation of an unsupportive environment for natural wetland plants. Increased bulk density also decreases the storage potential of both peat water and CH_4 (Turetsky *et al.*, 2014).

2.4.1.3 Redox potential

The reduction-oxidation (redox) potential of the soil acts as a master switch for microbial production and consumption of gases and is a function of soil moisture (Bridgham *et al.*, 2013). Soil moisture largely determines oxygen (O_2) diffusion rate in peat, and microbes utilize available O_2 as an electron acceptor (Schimel & Holland, 2005). In saturated peat, redox reactions follow a sequence determined by thermodynamic energy output (Keller & Bridgham, 2007; Bridgham *et al.*, 2013). Oxygen is the most energetically favourable electron acceptor and anaerobic conditions develop after all O_2 has been depleted. Anaerobes begin utilising the remaining TEAs in the system, which significantly reduces the rate of organic matter decomposition (Le Mer & Roger, 2001). Methane production is the final step in the sequential pathway of reduction where carbon is in its most reduced form (Bridgham *et al.*, 2013; Tiner & Ralph, 2016).

Methanogens are competitively suppressed in the presence of more favourable TEAs in order of highest redox potential/energy yield. Denitrifiers, manganese–, iron–, and sulfate–reducers compete with methanogens for carbon and hydrogen substrates (Van Huissteden *et al.*, 2006; Dalal *et al.*, 2007; Keller & Bridgham, 2007; Gougoulias *et al.*, 2014; Kolton *et al.*, 2019). However, after long-term peat saturation and depletion of all other TEAs, methanogenesis dominates. An example of this environment is the waterlogged and O_2 depleted catotelm, located beneath the water table in the peat profile. Anoxic environments such as the catotelm are depleted of TEAs, therefore microbes must decompose organic matter by fermentation, hydrolysis, and methanogenesis in order to liberate a C source (Conrad, 2020).

2.4.1.4 Substrate availability

The reduction of TEAs into a respiratory product (e.g., CO_2 to CH_4) is only part of the microbial respiration equation. The other part involves substrate acting as an electron donor to provide the microbe with energy (Dalal *et al.*, 2007; Bridgham *et al.*, 2013). To understand the

pathways of CH_4 cycling in peatlands and the sources of anaerobic CO_2, it is necessary to understand how specific microbial groups or processes progressively mineralize specific carbon pools (Figure 2.5). Firstly, polymers (e.g., soil organic matter and cellulose) hydrolyse to form monomers (e.g., simple sugars such as glucose). This is followed by the fermentation of these simple sugars into short-chain fatty acids and alcohols (e.g. ethanol, acetate) and secondary fermentation (acetogenesis) of either: acetate to H_2 and CO_2 or alcohols to acetate (Megonigal *et al.*, 2004; Bridgham *et al.*, 2013). Bacteria accomplish these functions (hydrolysis, fermentation, and acetogenesis) and methanogenic archaea then utilise the fermentation products (H_2 + CO_2, acetate, formate, methylated compounds, and alcohols) as simple C-compound substrates for methanogenesis. In peatland environments where there is significant organic matter, H_2, CO_2, and acetate tend to be the dominant methanogenic substrates and there are two major pathways of CH_4 production associated with these substrates: acetotrophy and the reduction of CO_2 by H_2 (Dalal *et al.*, 2007; Conrad, 2020). As stated in Section 2.4.1.1, stoichiometry suggests acetotrophic (or acetoclastic) methanogenesis generates two-thirds of CH_4, while hydrogenotrophic methanogenesis contributes the other third, however, this is rarely the case *in situ*. Various constraints regulate this ratio including environmental factors (e.g., pH, temperature, and organic matter), substrate availability, incomplete degradation processes, and alternative fates of fermentation products (Bridgham *et al.*, 2013; Conrad, 2020). Substrate quality may also differ across sites with differing botanical origins and hydrological regimes. For example, Bergman *et al.* (2000) found that for sites with low WTD, organic matter was subjected to aerobic degradation, and therefore plant litter inputs reaching the anaerobic zone were of poor quality, causing relatively low CH_4 production.

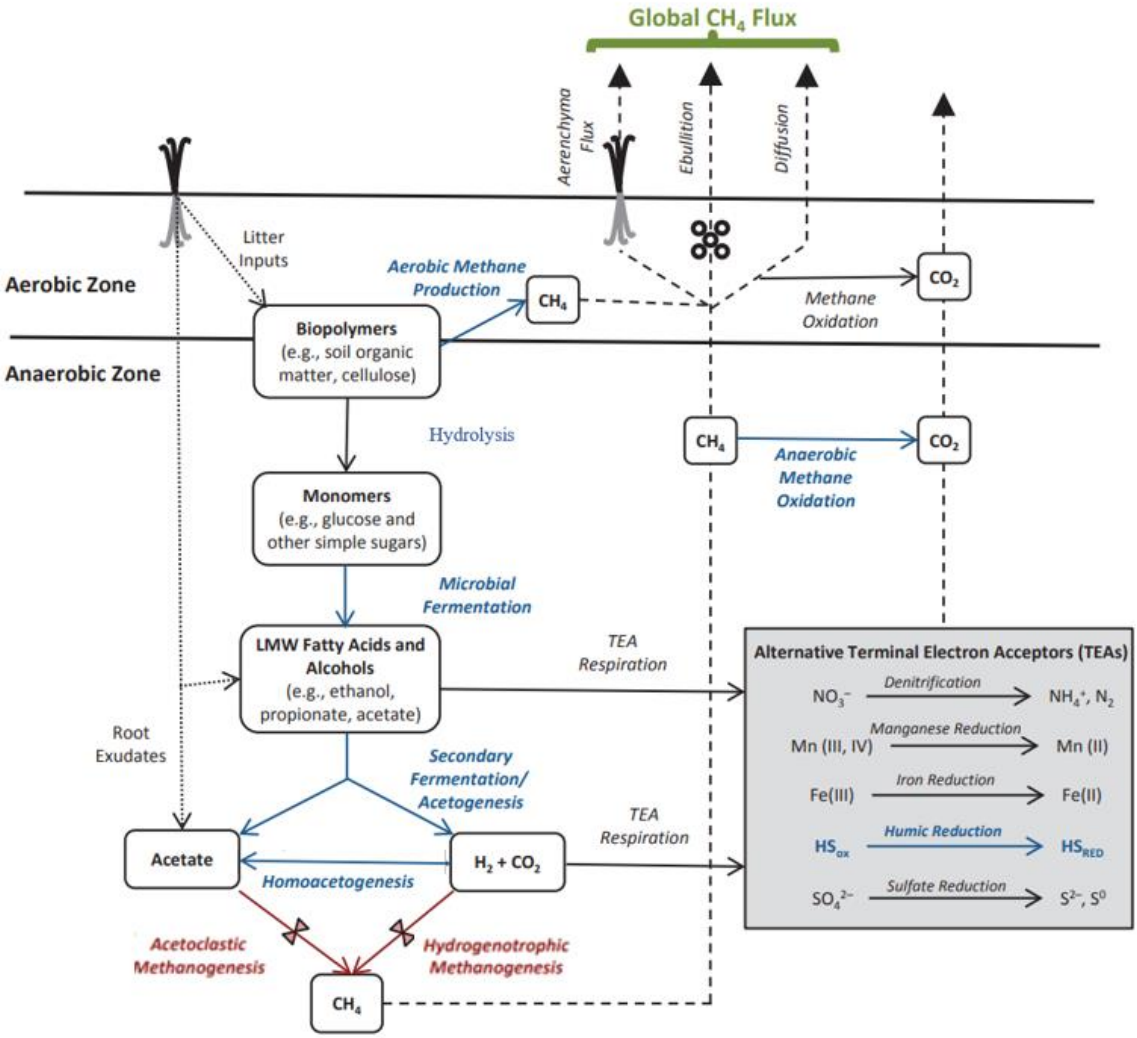

Figure 2.5 Methane cycling pathways in wetland ecosystems. Carbon inputs from the plant community (dotted lines) introduce carbon into the soil system. Carbon pools (white boxes) are progressively mineralized by microbial processes or groups (solid arrows) into gaseous end products (CH_4 and CO_2) that are emitted to the atmosphere via different flux pathways (dashed lines). Adapted from Bridgham *et al.* (2013).

Vegetation type significantly affects organic matter decomposition in wetlands and is often used as a proxy for C quality (Inglett *et al.*, 2012; Liu *et al.*, 2021). Granberg *et al.* (1997) suggest the degree of organic matter degradation may be a function of different plant communities. The dominant vegetation in New Zealand peatlands, *Empodisma robustum*, is an "ecosystem engineer" that captures rain and incoming nutrients first, restricting downward percolation to the remaining peat (Scott, 1996; Clarkson *et al.*, 2004). Plants supply the peat with substrate through root exudates and dead organic litter, which stimulates methanogenesis (Inglett *et al.*, 2012; Turetsky *et al.*, 2014; Tiner & Ralph, 2016). Recent deposition of organic material introduces new substrates onto surface layers and the quality of these substrates regulates peat decomposition rate as well as being an important environmental constraint on

carbon loss (Clymo, 1984; Waddington *et al.*, 2001; Wilson *et al.*, 2016b). Easily degradable (labile) carbon in the form of simple substrates are depleted first; meanwhile, more difficult to degrade (recalcitrant) substrates such as lignin are decomposed at a much slower rate. Continued deposition indicates the upper layers always have fresh, labile carbon for microbes to readily degrade and the lower layers in the peat profile always remain depleted of this labile carbon (Waddington *et al.*, 2001; Davidson & Janssens, 2006; Inglett *et al.*, 2012). Peat CH_4 production tends to be higher when labile carbon substrates such as cellulose are abundant, while rates are lower in peat with more recalcitrant carbon substrates such as lignin (Megonigal *et al.*, 2004; Inglett *et al.*, 2012).

2.4.2 Methane transport

Methane produced in the peat can escape to the atmosphere via diffusion, ebullition (bubble release), and plant-mediated transport through specialized aerenchyma tissues (Granberg *et al.*, 1997; Bridgham *et al.*, 2013). In some systems, CH_4 transfer occurs mostly via plants, which allows CH_4 to bypass aerobic peat layers between plant roots and the saturated peat. Wetland plants have adapted this feature to enable O_2 exchange to the roots to survive in hypoxic conditions (Dalal *et al.*, 2007; Sorrell & Brix, 2013; Turetsky *et al.*, 2014; Tiner & Ralph, 2016). This pathway is spatially variable depending on vegetation type, as not all plants possess aerenchyma (Le Mer & Roger, 2001; Inglett *et al.*, 2012). Methane ebullition can also bypass CH_4 oxidizers but is notoriously variable through both space and time. The solubility of CH_4 decreases with temperature as warmer water holds less dissolved CH_4, increasing bubble formation and the potential for ebullition (Moore & Dalva, 1993; Le Mer & Roger, 2001). The activity of dissolved gases is determined by pore water solubility and the equilibrium between chemical phases or ion exchange complexes in soil (Fisher & Reddy, 2013). Other environmental constraints influence ebullition flux both spatially and temporally, including seasonal temperature shifts, changes in atmospheric pressure, and precipitation (Le Mer & Roger, 2001; Fisher & Reddy, 2013). The rate of diffusion of dissolved gases in water is 1/10,000 that in air, so the pathway of diffusion for CH_4 is heavily controlled by soil moisture content and WTD. Additionally, the diffusion pathway is vulnerable to CH_4-oxidizing bacteria in aerobic peat layers (Clymo, 1984; Le Mer & Roger, 2001).

2.4.3 Consumption

Methanotrophy, also known as CH_4 consumption, is performed by methanotrophic bacteria in largely aerobic zones of the peat, generally within the surface layers (Le Mer & Roger, 2001; Van Huissteden *et al.*, 2006). Before entering the atmosphere, methanotrophs consume CH_4 to form CO_2. Figure 2.5 highlights where in the peat profile CH_4 is most commonly oxidized to CO_2 (Bridgham *et al.*, 2013). Between 10–90% of CH_4 is consumed by methanotrophs at or close to the peat surface before escaping to the atmosphere (Le Mer & Roger, 2001). Methanotrophs are found in the aerobic peat layer above the water table, inside the roots of submerged plants, and in the aerobic rhizosphere of plants with aerenchyma. Methane provides the C substrate or energy source for methanotrophs, which then rely on the availability of oxygen for their activity (Granberg *et al.*, 1997; Watson *et al.*, 1997; Dalal *et al.*, 2007).

Water table depth and peat saturation patterns strongly influence CH_4 oxidation, and both CH_4 production and oxidation can occur simultaneously in saturated peat (Dalal *et al.*, 2007). Figure 2.4 shows CH_4 production generally increases with soil water content, whereas consumption decreases rapidly in completely saturated peat, as oxygen and CH_4 are limited by diffusion (Bridgham *et al.*, 2013). This suggests peat saturation facilitates the shift between the two microbial populations, which may not be surprising considering both methanogens and methanotrophs are ubiquitous in peat and occur in close proximity to each other (Dalal *et al.*, 2007). Methanotrophy is most efficient in submerged or water-saturated peat where there are frequent shifts in WTD that promote intermittent methanogenic activity (Dalal *et al.*, 2007). When production is higher than consumption, the peat zone becomes a CH_4 source and when consumption is higher, the peat zone becomes a sink (Le Mer & Roger, 2001).

2.4.4 Anaerobic CO_2 production

There are relatively few studies on anaerobic CO_2 production, but these are especially limited for wetland soils (Waddington *et al.*, 2001; Liu *et al.*, 2021). In freshwater peatland ecosystems, devoid of all other electron acceptors, CO_2 becomes the final electron acceptor, which oxidizes to CH_4 (Bridgham *et al.*, 2013). However, anaerobic CO_2 is released during various phases of CH_4 production, including as a reactant in hydrogenotrophic methanogenesis (Eq. 2-2) and as a product of acetoclastic methanogenesis (Eq. 2-3) (Bridgham *et al.*, 2013). CH_4 may also undergo anaerobic methane oxidization (AOM) which leads to the production of CO_2. Other anaerobic respiration studies have used the ratio of anaerobic CO_2 production and CH_4 production together to assess C loss partitioning patterns (Wilson *et al.*, 2016b; Hopple *et al.*,

2020). Equimolar CH_4 and CO_2 are produced for every molecule of organic matter degraded during methanogenesis, however, anaerobic CO_2:CH_4 often exceeds this predicted 1:1 ratio. There is confusion around why this occurs and some explanations link the increased CO_2 production to upstream fermentation processes prior to methanogenesis (Wilson *et al.*, 2017; Conrad, 2020). Conrad (2020) suggested that environmental constraints including temperature, pH, organic matter quality, and alternative fates of CH_4 precursors regulate this ratio. Despite these observations, there tends to be a general decrease in this ratio with temperature (Wilson *et al.*, 2017; Hopple *et al.*, 2020). This may have important implications for positive feedbacks between the carbon cycle and climate change given the higher potency of CH_4 as a GHG, relative to CO_2 (Myhre *et al.*, 2013; Neubauer & Megonigal, 2015)

2.5 Temperature response of methane production

2.5.1 Temperature dependence of peat carbon decomposition

Temperature is an important environmental control on soil organic carbon decomposition, including anaerobic CH_4 production (Davidson & Janssens, 2006; Sierra *et al.*, 2015). However, there is uncertainty around the trajectory of wetland CH_4 emissions and global climate feedbacks with increased global temperatures (Moore & Dalva, 1993; Dlugokencky *et al.*, 2011; Zhang & Wang, 2017). As climate warming continues, it is becoming more important to understand what drives the variation in soil C dynamics (Schipper *et al.*, 2014), in order to improve the accuracy of future predictions of C-GHG emissions from peatlands. Peatlands store a significant amount of carbon in deep recalcitrant peat that if destabilized by temperature increases, has the potential to increase C-GHG emissions and create a positive feedback loop to climate warming (Davidson & Janssens, 2006; Riley *et al.*, 2011; van Winden *et al.*, 2012). Liu *et al.* (2021) predict a 37.5% increase in global wetland GHG emissions with a temperature rise of 1.5°C. This concerning prediction is a driving force behind continuing to further understand and quantify the effects of temperature on wetlands as a source of C-GHG (Wilson *et al.*, 2016b).

The relationship between temperature and microbial respiration in soils has been well studied; however, the majority of these studies focus on aerobic CO_2 (Davidson & Janssens, 2006; Sierra *et al.*, 2015; Kolton *et al.*, 2019). A point of confusion in temperature dependence studies is the response and sensitivity of decomposition at higher temperatures (≥25°C). Figure 2.6 illustrates potential theoretical responses including Arrhenius and MMRT responses (described in detail in Section 2.5.5) to show the difference between a response with and

without a decline in rates at high temperature. The temperature dependence for anaerobic C-GHG production, including CH_4, has rarely been measured across such a large temperature range. To address this knowledge gap and help reduce uncertainties of the temperature response in wetland CH_4 production, we need to incorporate these higher temperatures and include more measurements across this larger temperature range to capture the full response curvature (Portner *et al.*, 2010; Sierra *et al.*, 2015).

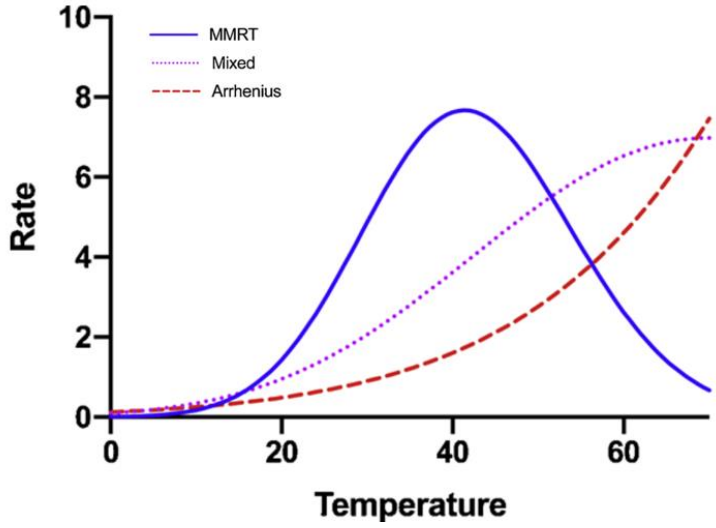

Figure 2.6 Conceptual figure adapted from Schipper *et al.* (2014) to show the Arrhenius response (red) most commonly used in soil temperature versus rate studies. This is compared to theoretical macromolecular rate theory (MMRT) curvature (blue) (discussed further in Section 2.5.5.2) and a mixture of the two (purple).

2.5.2 Temperature control terminology

Soil respiration can be divided into two components: root respiration and soil organic matter decomposition[1]. In a steady-state system, soil respiration is equal to decomposition (Davidson & Janssens, 2006), and throughout this thesis, these two terms are used interchangeably.

The decomposition of organic matter has both intrinsic and apparent temperature sensitivity. Intrinsic sensitivity describes inherent kinetic properties such as activation energy, ambient temperature, and decomposability, while apparent sensitivity describes the observed response under environmental constraints. Constraints may include soil particle aggregation, water saturation, and anaerobic decomposition, presence of phenolic compounds inhibiting enzymes responsible for decomposition, changes in soil-water film thickness altering C substrate diffusion, the composition of plant inputs, and land use change (Davidson & Janssens, 2006;

[1] In this study, we focus on soil organic matter decomposition, which is alternatively termed microbial or heterotrophic soil respiration.

Sierra *et al.*, 2015). This work will focus on incubations of small peat samples which likely still has components of both intrinsic and apparent temperature sensitivity.

2.5.3 CH_4 production rate vs. temperature studies

Most studies investigating temperature dependence of CH_4 production in peatlands carry out measurements using ≤5 temperatures over a relatively small range in temperatures (Bergman *et al.*, 1998; Hargreaves & Fowler, 1998; Treat *et al.*, 2014; Hanson *et al.*, 2016; Wilson *et al.*, 2016a; Hopple *et al.*, 2020). The temperature dependence of peatland CH_4 production has been studied primarily using incubation studies, including studies addressing higher temperatures (Svensson, 1984; Dunfield *et al.*, 1993; Yao & Conrad, 2000; Yavitt *et al.*, 2006; Metje & Frenzel, 2007; Freitag & Prosser, 2009; Blake *et al.*, 2015; Sjögersten *et al.*, 2018; Deng *et al.*, 2019; Kolton *et al.*, 2019). Dunfield *et al.* (1993) demonstrated that CH_4 production had optimum production rates at temperatures between 25–30°C with low production in the low temperature range. Similarly, results from Kolton *et al.* (2019) suggest that CH_4 production rates had a maximum at 30°C, while rates above 30°C and below 4°C were negligible.

Table 2.1. outlines published datasets that measure the response of CH_4 production to temperature including comparisons between sampling methods, temperature ranges, and temperatures of highest CH_4 production. Some of these studies also include results on the temperature dependence of anaerobic CO_2 production (e.g., Liu *et al.* 2021). There are notable differences in incubation length, depth of sampling, and study type highlighting the contrasting experimental methods among studies. These study sites are mostly located in the Northern Hemisphere. While the majority of the studies listed focus on peatlands, marshes, subarctic mires, and permafrost, included also are samples collected from lake sediments, rice paddies, and one manure slurry sample from a cattle and pig farm. Some incubation studies have investigated temperatures across a large temperature gradient, but few above 30°C (Hamdi *et al.*, 2013). For those studies with incubations above 30°C, all found a decrease in CH_4 production somewhere after this point. This response was found in peatlands (Dunfield *et al.*, 1993; MacDonald *et al.*, 1998; Yavitt *et al.*, 2006; Freitag & Prosser, 2009; Sjögersten *et al.*, 2018; Deng *et al.*, 2019; Kolton *et al.*, 2019), including permafrost and subarctic peat (Metje & Frenzel, 2007; Blake *et al.*, 2015; Tveit *et al.*, 2015) as well as other land uses including a rice paddy soil (Yao & Conrad, 2000), slurry (Elsgaard *et al.*, 2016), and lake sediments (Schulz *et al.*, 1997; Glissman *et al.*, 2004; Duc *et al.*, 2010). For the studies that did not incubate at temperatures higher than 30°C, CH_4 production increased with temperature up to

that point (Bergman *et al.*, 1998; Hargreaves & Fowler, 1998; Treat *et al.*, 2014; Hanson *et al.*, 2016; Wilson *et al.*, 2016a; Hopple *et al.*, 2020).

Results on the temperature dependence of anaerobic CO_2 production in the literature are scarce, with highly variable temperature optima or linear relationships (Yao & Conrad, 2000; Waddington *et al.*, 2001; Glissman *et al.*, 2004; Metje & Frenzel, 2007; Tfaily *et al.*, 2014; Treat *et al.*, 2014; Tveit *et al.*, 2015; Hanson *et al.*, 2016; Wilson *et al.*, 2016a; Sjögersten *et al.*, 2018; Deng *et al.*, 2019; Hopple *et al.*, 2020; Schädel *et al.*, 2020; Liu *et al.*, 2021). It is difficult to attribute the formation and sources of CO_2 under anaerobic conditions and determine what fraction is derived from CH_4 production (Bridgham *et al.*, 2013; Wilson *et al.*, 2017; Conrad, 2020). Despite many of these incubation studies having a small temperature range with ≤5 measurement temperatures, these studies have nonetheless been critical in improving our understanding of temperature dependence of C-GHG production and the microbially-mediated turnover of organic matter, which is crucial in making predictions for ecosystem response to climate change.

2.5.4 Other factors influencing temperature response

Soil warming studies suggest interactions between microbial activity, soil moisture, and substrate supply are crucial in determining the temperature response of C-GHG release from soils (Sierra *et al.*, 2015). Controls on the temperature response of CH_4 production include (1) soil moisture, (2) microbial communities, (3) substrate quality, and (4) CH_4 consumption, as outlined below:

(1) Goodrich *et al.* (2015) and Brown *et al.* (2014) found that although temperature was the dominant driver of CH_4 production, this was only the case when soils were sufficiently saturated.

(2) The influence of temperature on methanogenic pathways is largely dependent on the soil microbes that produce and oxidize acetate. Temperature can control methanogenic pathways by influencing the thermodynamics of fermentative production of H_2 and acetate, and by affecting microbial community composition (Megonigal *et al.*, 2004; van Winden *et al.*, 2012; Conrad, 2020). Microorganisms may also adapt and acclimatize to temperature changes in the soil, however, the degree to which this occurs and why, is still debated (Chin *et al.*, 1999; Riley *et al.*, 2011).

(3) The quality of substrate also influences temperature dependence, as low quality substrates are proposed to have a stronger temperature dependence than high quality

substrates. The decomposition rate for high quality substrates tends to be weaker but showed increases as temperature decreased for low quality substrates (Bosatta & Ågren, 1999).

(4) Methane consumption plays a role in controlling CH_4 production (Section 2.4.3) and temperature controls both processes. Castro *et al.* (1995) found that, like CH_4 production, CH_4 consumption rates increased in late spring and early summer. Methane consumption increased as temperature increased between –5 to 10°C, but remained relatively constant at temperatures between 10 and 20°C (Castro *et al.*, 1995).

Table 2.1 Publications focussed on the environmental response of CH_4 and CO_2 production with temperature from a range of climate zones/biomes.

Author (in order of publication date)	Location	Study type/ scale	Environment/ biome	Depth (cm)	Incubation temperature (°C)	Incubation length	CH_4 pro-duction	Anaer-obic CO_2 pro-duction	Highest CH_4 production temperature (°C)	Highest CO_2 production temperature (°C)
Svensson (1984)	Sweden	Incubation	Subartic mire	10–15	2, 5, 20, 15, 20, 24, 28, 37	3–6 months pre-incubation 1–2.5 months incubation	✓	–	20	–
Dunfield *et al.* (1993)	Canada	Incubation	Peatland	0–20	0–35	9 days	✓	–	30	–
Schulz *et al.* (1997)	Lake Constance Germany	Incubation	Pre alpine lake, profundal	4–12	2–49	2 month pre-incubation ≤14 day incubation	✓	–	35	–
Bergman *et al.* (1998)	Sweden	Incubation	Mixed mire	20–120	2–20	4 weeks pre-incubation ≤52 days incubation	✓	–	20	–
Macdonald *et al.* (1998)	Loch More, Scotland	Chamber	Blanket bog	30x40 cm monoliths	5–30	Unspecified	✓	–	30	–
Yao & Conrad (2000)	Italy, Phillipines Luisiana, Maligaya	Incubation	Rice paddy soil	Un specified	4.7–49.5	16 days	✓	✓	35–40	40
Waddington *et al.* (2001)	Quebec	Incubation	Peatland: undisturbed and drained	0–80	4, 12, 20	48 hours	–	✓	–	20
Glissman *et al.* (2004)	Lake Dagow, Germany	Incubation	Eutrophic Lake	0–10	4, 10, 15, 25, 30	73 days	✓	✓	30	30
Yavitt *et al.* (2006)	Canada	Incubation	Peatland complex	0–40	10, 22, 33, 45	73 days	✓	✓	33	Variable between sites
Metje & Frenzel (2005, 2007)	Siberia	Incubation	Permafrost peat	20–40	0–60	4 months pre-incubation 28 days incubation	✓	✓	30	Decline at 30°C, increase 40–58

Table 2.1 continued.

Author (in order of publication date)	Location	Study type/ scale	Environment/ biome	Depth (cm)	Incubation temperature (°C)	Incubation length	CH_4 pro-duction	Anaer-obic CO_2 pro-duction	Highest CH_4 production temperature (°C)	Highest CO_2 production temperature (°C)
Freitag & Prosser (2009)	North Wales, UK	Incubation	Peatland	0–20	0–40	2–6 months pre-incubation 6 days incubation	✓	–	25–30	–
Duc *et al.* (2010)	Sweden	Incubation	Lake sediments	5	4, 10, 20, 30	6 days	✓	–	30	–
Treat *et al.* (2014)	Alaska	Incubation	Arctic permafrost peat	0–100	–5, –0.5, 4, 20	30 day incubation	✓	✓	20	20
Tveit *et al.* (2015)	Svalbard, Norway	Incubation	Arctic permafrost peat	10–15	0–30	171 day pre-incubation, 26–39 days incubation	✓	✓	30	–
Blake *et al.* (2015)	Norway	Incubation	Arctic wetland	≤600	5, 20, 30, 40, 50, 60, 70	0–7 days	✓	–	30	–
Elsgaard *et al.* (2016)	Denmark	Incubation	Slurry	NA	5–52	3–41 hours	✓	–	33–37 for slurry after 17 hours	–
Hanson *et al.* (2016)	Minnesota USA	Chamber	Peatland	0 (CO_2), –20 (CH_4)	–7–25 (CO_2) –1–18 (CH_4)	4 years	✓	✓	18	25
Wilson *et al.* (2016)	Minnesota USA	Incubation	Peatland	25	2–17	13 months	✓	✓	16–17	11
Sjögersten *et al.* (2018)	Western Panama	Chamber, incubation	Tropical Ombrotrophic domed peatland	0–10	20, 25, 30, 35	Unspecified	✓	✓	35	35
Kolton *et al.* (2019)	Minnesota USA	Incubation	Peatland	10–30	0–40	10 days pre-incubation 4 weeks incubation	✓	✓	30	Variable over time: 4–7 and 20–23, 33 at 0.04 days, 4 at 6.8 days

Table 2.1 continued.

Author (in order of publication date)	Location	Study type/ scale	Environment/ biome	Depth (cm)	Incubation temperature (°C)	Incubation length	CH_4 pro-duction	Anaer-obic CO_2 pro-duction	Highest CH_4 production temperature (°C)	Highest CO_2 production temperature (°C)
Deng *et al.* (2019)	Tibet	Incubation	Wetland, adjacent to oligosaline alkaline lake	Un specified	10, 20, 30, 45	100 days	✓	✓	30	45 for first 60 days, 30 from days 60–100
Hopple *et al.* (2020)	Minnesota USA	Incubation Chamber (*in situ*)	Peatland	0–200	0–20	5 years	✓	✓	20	20
Liu *et al.* (2021)	China	Incubation	River delta, marsh	0–30	10, 20, 30	1 week pre-incubation 70 day incubation	–	✓	–	30

2.5.5 Temperature versus rate models

Mechanistic models of complex CH_4 flux pathways are needed for making predictions of future CH_4 emission rates and long-term C-GHG loss from peatlands (Reddy *et al.*, 2013). However, the most widely used mathematical models for estimating the temperature response of respiration in soil often lack parameters defining meaningful biological characteristics (Schipper *et al.*, 2014; Kolton *et al.*, 2019).

2.5.5.1 Arrhenius and Q_{10}

There is a wide range of mathematical models proposed to capture biochemical responses to changing temperature in soil (Lloyd & Taylor, 1994; Davidson & Janssens, 2006; Sierra, 2012). Many studies base these models on the Arrhenius function:

$$k = \mathrm{A}\ exp^{\left(\frac{-E_A}{RT}\right)} \quad (2\text{-}4)$$

Where k is the reaction rate, A is a pre-exponential factor, E_A is the activation energy (Joules mol^{-1}), R is the universal gas constant (8.314 J K^{-1} mol^{-1}), and T is temperature (Kelvin). Eq. 2-4 suggests an exponential increase in rates of respiration as temperature increases. However, biochemical reactions (mediated by enzymes) have an intrinsic temperature optimum (T_{opt}) after which there is a decline in reaction rate. Because the Arrhenius model was originally developed to describe chemical reaction rates and does not allow for a T_{opt}, this model may not always accurately represent the relationship between reaction rate and temperature even at temperatures below T_{opt} (Davidson & Janssens, 2006).

Another flawed aspect of many temperature response studies is the metric for relative temperature sensitivity. This is often calculated as Q_{10}, an empirical function used extensively in respiration or soil decomposition studies representing the ratio of rates determined 10°C apart (Eq. 2-5):

$$Q_{10} = \left(\frac{R_1}{R_2}\right)^{\frac{10}{T_2 - T_1}} \quad (2\text{-}5)$$

Where R_1 and R_2 represent reaction rates at temperatures T_1 and T_2. Estimates of Q_{10} in CH_4 production studies are highly variable. Dalal *et al.* (2007) found that CH_4 production had a

variable Q_{10} of 1.1 to 28 across many sites, averaging at around 4.0. Segers and Kengen (1998) synthesized 1046 laboratory experiments on CH_4 production rates using wetland soils and found an average Q_{10} of 4.1 (±0.4) and range from 1.5 to 28. Temporal and spatial variation in Q_{10} values for CH_4 production in saturated soils may be a function of the microbial community or microbial adaptation to local conditions (Le Mer & Roger, 2001; Riley *et al.*, 2011). For example, Turetsky *et al.* (2014) found that Q_{10} varied with depth and environmental conditions. Measurements of Q_{10} also tend to overestimate values at low temperatures and decline with temperature increases (Riley *et al.*, 2011). Despite this, global climate models often fix Q_{10} for CH_4 production at ~2, which fails to capture the changing relative temperature sensitivity with temperature (Schipper *et al.*, 2014). Small changes in the prescribed Q_{10} have a big impact on future emission projections (Riley *et al.*, 2011). Riley *et al.* (2011) modelled a 50% increase in CH_4 flux estimates when using a Q_{10} of 4, in comparison to a Q_{10} of 2. While Arrhenius and Q_{10} functions can estimate the relationship between rate versus temperature to a point, soil rate versus temperature models need a stronger theoretical basis for representing changing temperature sensitivity and for capturing a T_{opt} (Schipper *et al.*, 2014).

2.5.5.2 Macromolecular rate theory

Macromolecular rate theory (MMRT) (Hobbs *et al.*, 2013) uses the thermodynamic properties of biological macromolecules, specifically enzymes, to describe the temperature dependence of reaction rates ranging in scale from single enzymes to ecosystems, including photosynthesis, leaf and soil respiration (Hobbs *et al.*, 2013; Schipper *et al.*, 2014; Liang *et al.*, 2018; Prentice *et al.*, 2020). Unlike Arrhenius and Q_{10} functions, MMRT accommodates a T_{opt}. The decline in rates above T_{opt} has previously been explained by enzyme denaturation; however, denaturation occurs at temperatures higher than those commonly observed in soils (Hobbs *et al.*, 2013). The theory underpinning MMRT is that the activation energy (E_A) of enzyme-catalysed reactions is temperature dependent. A large negative change in enzyme heat capacity (ΔC_p) between the ground state and transition state causes the temperature dependence of E_A and explains the decline in rates above T_{opt} (Hobbs *et al.*, 2013; Schipper *et al.*, 2014).

To expand on this, the relationship between rate and temperature is most simply described by the Arrhenius function as mentioned above (Eq. 2-4). The Arrhenius function utilizes the concept of E_A, which describes the energy barrier over which reactants must rise to transform into products, also known as the 'transition state' (Hobbs *et al.*, 2013). Gibbs, Maxwell, and Boltzmann later substituted E_A for the change in Gibbs free energy (ΔG) (Schipper *et al.*, 2014). ΔG can be calculated using the difference between the change in enthalpy (ΔH) and entropy

(ΔS) in a reaction (ΔG = ΔH – ΔS). Erying and Polyani developed 'transition state theory' which quantified the pre-exponential term, *A*, to develop the Arrhenius theory further where $A=k_BT/h$, k_B is Boltzmann's constant, and *h* is planks constant (Schipper *et al.*, 2014). This theory expands on the original Arrhenius equation to produce Eq. 2-6 and simplified to Eq. 2-7 and can be simplified by taking the natural log of either side of the equation (Hobbs *et al.*, 2013; Schipper *et al.*, 2014):

$$k = \frac{k_B T}{h} e^{\left(\frac{-\Delta G^{\ddagger}}{RT}\right)} \tag{2-6}$$

$$\ln(k) = \ln\left(\frac{k_B T}{h}\right) - \frac{\Delta G^{\ddagger}}{RT} \tag{2-7}$$

It is assumed that ΔG is independent of temperature for small molecules in solution; however, this is not the case for macromolecules such as enzymes, which have large heat capacities (C_p). C_p is defined as the temperature dependence of enthalpy (H) and entropy (S). There are significant changes in heat capacity (ΔC_p) during catalysed reactions. Large values of ΔC_p cause pronounced temperature dependence of ΔG in Eq. 2-8 as follows (Schipper *et al.*, 2014):

$$\begin{aligned} \Delta G^{\ddagger} &= \Delta H^{\ddagger} - T\Delta S^{\ddagger} \\ &= \left[\Delta H^{\ddagger}_{T0} + \Delta C_p^{\ddagger}(T - T_0)\right] - T\left[\Delta S^{\ddagger}_{T0} + \Delta C_p^{\ddagger}(\ln T - \ln T_0)\right] \end{aligned} \tag{2-8}$$

Activation enthalpy (ΔH) varies linearly with temperature and activation entropy (ΔS) changes with the natural log of temperature, while the state of temperature dependence depends largely on ΔC_p. Large and negative ΔC_p cause rates to deviate from Arrhenius behaviour whereas when $\Delta C_p = 0$, MMRT collapses to the Arrhenius equation. Combining Eq. 2-7 and Eq. 2-8 produces the equation for MMRT (Hobbs *et al.*, 2013):

$$\begin{aligned} \ln(k) = ln\left(\frac{k_B T}{h}\right) - \frac{\Delta H^{\ddagger}_{T_0}}{RT} - \frac{\Delta C_p^{\ddagger}(T - T_0)}{RT} + \frac{\Delta S^{\ddagger}_{T_0}}{R} \\ + \frac{\Delta C_p^{\ddagger}(\ln T - \ln T_0)}{R} \end{aligned} \tag{2-9}$$

Where T_0 is a reference temperature, and $\Delta H^{\ddagger}$ T_0 and $\Delta S^{\ddagger}$ T_0 are the difference in enthalpy and entropy respectively, at T_0. If $\Delta H^{\ddagger}$ and $\Delta S^{\ddagger}$ are temperature dependent, ΔC_p will not be zero and the relationship between rate and temperature will show curvature (Hobbs *et al.*, 2013). Figure 2.7 visualizes the difference between the Arrhenius function, Lloyd & Taylor model (Lloyd & Taylor, 1994), and MMRT curves showing the change in shape and curvature with varying ΔC_p values. The Lloyd & Taylor model is an Arrhenius-derived model described in more detail in Lloyd and Taylor (1994).

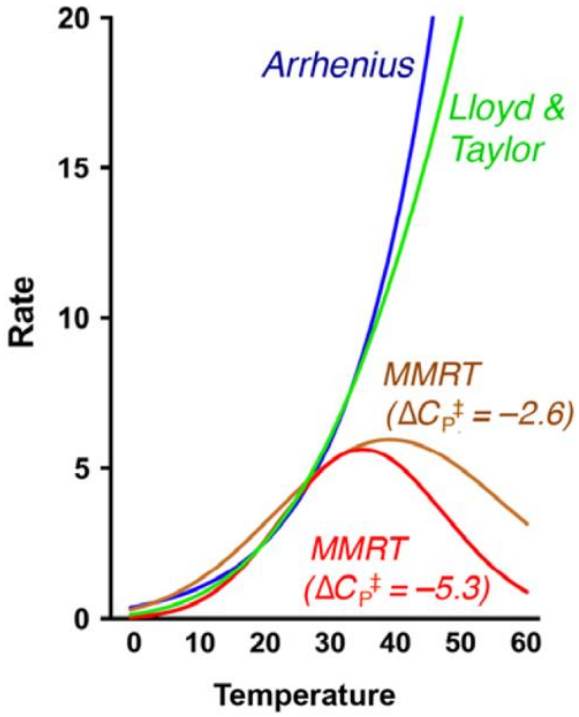

Figure 2.7 Relationship between temperature and reaction rate for Arrhenius, Lloyd & Taylor, and MMRT models. MMRT curves show the variation in curvature based on ΔC_p values.

Two important parameters can be derived from MMRT. The T_{opt}, which describes the temperature at which the production rate is maximal, and the inflection point (T_{inf}), which represents the temperature where the increase in rate is maximal (Schipper *et al.*, 2019). These metrics are important in understanding and predicting climate scenarios, nutrient cycling, and greenhouse gas production rates (Alster *et al.*, 2020). Duffy *et al.* (2021) extended the use of these parameters, to the temperature dependence of global carbon metabolism for projecting the temperature tipping point of the terrestrial biosphere. This provides an example of the relevance and interpretability of the T_{opt} and T_{inf} metrics. These metrics provide the framework for comparison on all scales, for synthesizing information, and for reforming our understanding of the temperature response across scales. Beginning with enzyme function, the "inflection point hypothesis" proposes that organism function and rates are fastest when enzymes within

the organism align their inflection point (T_{inf}) (Prentice *et al.*, 2020). For mesophilic organisms, this is somewhere around 37°C (Figure 2.8). When the environmental temperature is beyond this temperature, enzyme rates within the organism become unsynchronized, potentially leading to a decline in function and rates that may be catastrophic at larger scales.

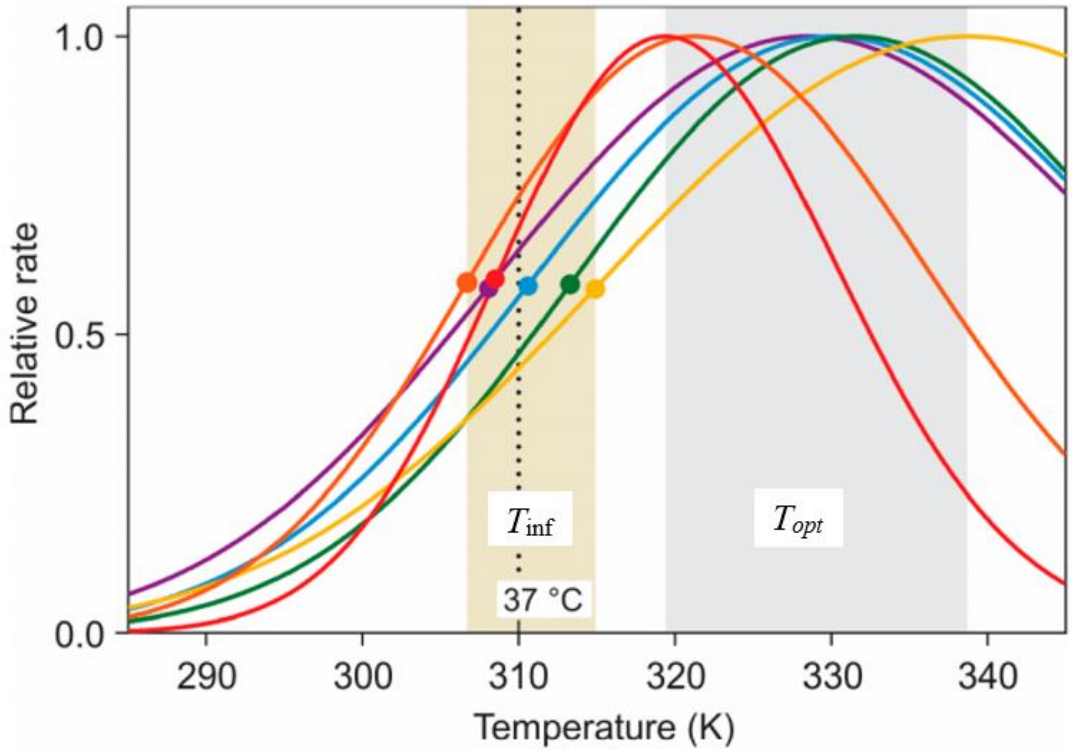

Figure 2.8 Temperature profiles for enzymes from *E. coli* showing the inflection point of each enzyme (circles) within the range of T_{inf} values (beige band) in comparison to the larger span of T_{opt} values (grey band). Sourced from Prentice et al., (2020).

The importance of using T_{opt} and T_{inf} parameters for modelling temperature response at the enzyme (Hobbs *et al.*, 2013; Prentice *et al.*, 2020) and global scale (Duffy *et al.*, 2021), suggests temperature response could also be extrapolated to the community and ecosystem scale. Schipper *et al.* (2014) suggests that a group of organisms with varying T_{opt} values within a given environment create a 'community T_{opt}'. This community T_{opt} is what we measure during soil incubation, chamber, or tower studies and was captured during soil incubations performed by Numa *et al.* (2021). The community or environmental T_{opt} would align with enzyme T_{inf}, within the beige band in Figure 2.8. This suggests that the environmental T_{inf} would be around ambient environmental temperatures (~20–25°C); however, despite beginning to understand the alignment of T_{opt} in soil microbial studies, T_{inf} is still poorly constrained. Figure 2.99 displays temperature response data from five FluxNet sites collated by Goodrich (2021). The curves at each of these sites represent an example of a community T_{opt}, or in this case, a larger

scale ecosystem T_{opt} derived from all the temperature dependent processes occurring in these ecosystems.

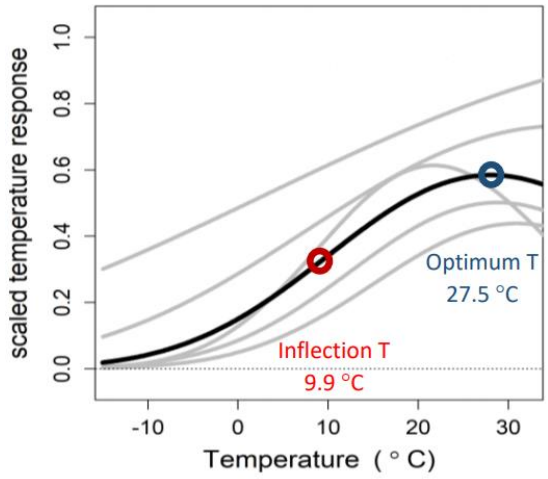

Figure 2.9 Preliminary CH_4 curve (black) including inflection and optimum temperature points derived from five FluxNet wetland sites (grey). Sourced from Goodrich, 2021 (unpublished).

2.6 Methods in literature for measuring soil CH_4 production

Methods utilized to measure CH_4 production and flux include micrometeorological techniques such as eddy covariance at the larger scale and in-field chamber techniques, mesocosms, and laboratory incubations, at the smaller scale.

Quantifying CH_4 production requires anaerobic conditions imitating those found *in situ* (Le Mer & Roger, 2001). Field chamber measurements may best represent *in situ* conditions; however, other environmental factors may confound the temperature dependence of soil C-GHG production results. Enclosed chambers also heat soils above normal and indiscriminately measure other transport mechanisms (Hargreaves & Fowler, 1998; Treat *et al.*, 2014). On the other hand, laboratory incubation studies interrogate soil respiration rates by eliminating potentially confounding variables (Dunfield *et al.*, 1993; Kolton *et al.*, 2019; Hopple *et al.*, 2020). With this in mind, it is important to capture the *in situ* conditions of the soil as accurately as possible using appropriate sampling methods (Bridgham & Ye, 2013). Methanogens are notoriously sensitive to environmental changes and can take time to adjust to new conditions. Any disturbance to the soil including removal, potentially alters the natural state of the soil, suggesting that the least amount of perturbation is best (Moore & Dalva, 1993). Sampling saturated soil with simple augers is not feasible due to the soft, unconsolidated nature of the material. Selecting a sampling technique that accurately represents a soil at a site requires appropriate sampling equipment. Polyvinylchloride (PVC) piping or stainless-steel corers are

appropriate for sampling peat and peat soils (Casado *et al.*, 2013). Experimental objectives and the statistical sampling design determine the location and depth of sampling. Generally, biological populations become less concentrated further away from the surface and most activity is assumed to occur in the near surface soil layers (Casado *et al.*, 2013).

Sampling containers may cause physical, chemical, or biological reactions with wetland soil samples between the time of sampling and analysis. This is a particular issue for anaerobic soils, where the process of methanogenesis is limited by abundant oxygen. Gas impermeable containers should be used to avoid contamination and for flushing the sample with N_2 gas to remove oxygen (Casado *et al.*, 2013). Soil storage time after sampling is debated, some studies suggest storage time after sampling should be kept to a minimum to best represent *in situ* conditions (Bridgham & Ye, 2013; Hopple *et al.*, 2020), while other studies suggest a long storage period to encourage the settling of methanogens (Blazewicz *et al.*, 2012; Treat *et al.*, 2014). Preparing samples for incubation often requires a pre-incubation period for soil microbes to recover from sampling disturbance. The range of pre-incubation durations is variable among studies, with some studies suggesting anything above 2 weeks is sufficient, and others suggesting 60 days or longer is more appropriate (Dunfield *et al.*, 1993; Hamdi *et al.*, 2013; Kolton *et al.*, 2019). Methanogens are sensitive to change and a lag period between the time of disturbance to the time of recovery is often observed in incubation studies. Soil preparation methods for respiration studies generally involve homogenizing the soil by sieving to less than 2 mm and removing any large roots, stones, and other material because these may contribute to an overestimation of microbial biomass (Rinklebe & Langer, 2013). On the other hand, modifications to soil structure such as homogenizing and sieving may unfavourably alter substrate availability and gas exchange, thus changing the effect of moisture and temperature on respiration and decomposition (Sierra *et al.*, 2015). Dunfield *et al.* (1993) found that blending reduced variation between replicates but significantly increased CH_4 production compared to unblended controls.

Methane and CO_2 are commonly analysed by gas chromatography (GC) and infrared gas analysis (IRGA), respectively. Headspace samples are periodically removed using a syringe, before injection into the GC or IRGA for analysis (Dalal *et al.*, 2007; Bridgham & Ye, 2013). Wecking *et al.* (2020) assessed the applicability of a field-based Quantum Cascade Laser (QCL) to measure chamber results for N_2O production and Hamill (2019) used this method for CH_4 chamber studies. The QCL quantifies gas samples instantaneously and accurately, proving to be an effective tool as a substitute for GC equipment.

2.7 Knowledge gaps and implications

Anthropogenic activities have led to increased GHG emissions and disrupted natural climate cycles (Duffy *et al.*, 2021). Some climate change models project a 6–10°C increase in temperatures by the end of the 21st century (Zhang & Wang, 2017). We currently depend on the large and persistent terrestrial global carbon sink to mitigate anthropogenic emissions of CO_2 and regulate global environmental change to meet the Paris Climate Accord (Duffy *et al.*, 2021). However, many of the world's ecosystems, including peatlands, which are a large carbon reservoirs, are vulnerable to increased temperatures that stimulate the release of C-GHGs (Davidson & Janssens, 2006). We need a clearer understanding of the loss of C-GHGs from soils as temperature increases, particularly on the variability of C-GHG loss from peatlands as CH_4 emissions. Modelling is a tool that should be utilized when assessing and predicting the effects of climate change and the carbon balance of peatlands (Van Huissteden *et al.*, 2006). By using temperature models, we can make projections on the temperature response of global peatland systems. However, we are currently missing data from a wide range of global peat ecosystems across a wide temperature range. A wide temperature range is needed to capture the full curvature of the temperature response and fit production models to these data for informing future predictions (Turetsky *et al.*, 2014). Southern Hemisphere systems have limited representation in CH_4 temperature response studies over a large temperature range and no such study exists for New Zealand systems. This research aims to capture the temperature response across a range of New Zealand systems from intact to drained peatlands, to add to the global understanding, and to better inform models for New Zealand and Southern Hemisphere systems. Additionally, the differences in temperature response between intact and drained peatlands should better inform us of the implications of rewetting drained systems, in terms of CH_4 and anaerobic CO_2 emissions and the potential GWP associated with each system.

Chapter 3

Methods and site description

3.1 Site description

Peat samples were collected from two sites in the Waikato region as endpoints in the spectrum of peatland degradation from 'pristine' to 'farmed'. In order to capture the full range of New Zealand peat conditions, we chose to compare an intact site (Kopuatai) to a drained farm site.

3.1.1 Kopuatai

Kopuatai peat dome is an ombrotrophic restiad peat bog located in the Hauraki Plains within the Waikato region of Te Ika-a-Māui, Aotearoa/New Zealand (37°25.11′S, 175°33.19′E), ~45 km to the northeast of Hamilton (Figure 3.1). The bog spans ~90 km^2 (9,665 ha) making it the largest remaining undisturbed raised peat bog in New Zealand (Newnham *et al.*, 1995; Goodrich *et al.*, 2017). Peat accumulation began 13,500 years ago leading to peat depths up to 14 m (Newnham *et al.*, 1995). Being an ombrotrophic bog, water and nutrient sources are almost solely limited to precipitation inputs. This causes the peat to be highly acidic (pH ~4), and nutrient-poor. Distinctive vegetation zones corresponding to water table depth and nutrient availability exist throughout Kopuatai, although this is dominated by species of the Restionaceae vascular plant family. Jointed wire rush (*Empodisma robustum*) is the main peat-forming plant and most abundant species by area at Kopuatai. *E. robustum* communities are found throughout the bog and are most dominant towards the centre of the dome. Greater jointed rush (*Sporadanthus ferrugineus*) is also present as well as sedge species (*Machaerina spp.)* (Agnew *et al.*, 1993; Wagstaff & Clarkson, 2012). These plants have special adaptations to withstand bog conditions, for example, *E. robustum* is adapted to retain water at the bog surface using a thick mulch layer beneath the canopy to insulate surface peat from solar radiation (Campbell and Williamson, 1997). Woody shrubs including Manuka (*Leptospermum scoparium*) are predominantly found towards the fringes of the bog, where conditions are more mesotrophic due to changes in land use and development. Drained peatland used for agriculture predominantly surrounds the perimeter of Kopuatai (Pronger *et al.*, 2014). We sampled multiple sites at Kopuatai bog to explore spatial variability driven by vegetation type. Woody shrub species at the perimeter of the bog give way to wire rush and sedge species towards the centre, therefore representative sites included: 1) wire rush (*E. robustum* – dominant vegetation

at Kopuatai), 2) sedge (*Machaerina spp.*), and 3) woody manuka scrub (*L. scoparium*). The three sampling sites were located within ~1 km of a long-term eddy covariance (EC) tower. Mean annual precipitation (1981-2010) for Kopuatai, measured at an official climate station 11 km to the east of the study site was 123.2 cm, and mean annual air temperature was 13.7°C (NIWA, 2019).

Figure 3.1 ArcGIS image showing the location of Kopuatai Peat bog (top right) in relation to Hamilton city (bottom left). Inset image showing close up of the location of sampling sites (pink) and EC tower (orange) within the bog (outlined in red).

3.1.2 Moanatuatua

Moanatuatua is an ombrotrophic peat bog located in the Hamilton Basin (37°55.50′S, 175°22.20′E), 17 km southwest of Hamilton City. Peat accumulation began ~13,000 years ago in a depression formed by an ancient path of the Waikato River upon an impermeable layer of volcanic ash deposits (Campbell, 1964). Once estimated to cover 75 km^2 of land, a remnant of this bog spans only 1.1 km^2 due to extensive draining and land use change (Clarkson et al., 2004). This extensive drainage has caused a drop in the water table at Moanatuatua peat reserve, which now unnaturally sits as much as 80 cm beneath the surface, causing issues of land subsidence at the site (Campbell et al., 2014).

The surrounding drained land, known as Moanatuatua drained peatland, was converted between the 1930s and 1980s into dairy pasture and blueberry orchards, which continue to dominate the present-day land use. The study site in this location is a drained site used for dairy pasture approximately 2.5 km away from Moanatuatua bog remnant, referred to throughout this thesis as Site DP or the drained pasture site. Figure 3.2 outlines the current size of the Moanatuatua bog remnant and the distance from the drained peat. Campbell *et al.* (2021) outline the drainage history and current management practices at Site DP. The site chosen for sampling was drained in 1975 and is characterised by closely spaced (~30 m apart) shallow surface drains. Site DP is classified as "deep-drained" (WTD ≥30 cm) according to IPCC (2014) and during the year of study had a WTD of 65.7 cm. Mean annual precipitation (1981-2010) measured at a nearby site was 116.7 cm and mean annual air temperature was 13.8°C (NIWA, 2019).

Site DP was rotationally grazed throughout the year. Ryegrass (*Lolium perenne*) and white clover (*Trifolium repens*) dominate the pasture species. The site was chosen based on the close proximity to eddy covariance (EC) instruments installed in the paddock for ease of access and ancillary data (Campbell *et al.*, 2021).

Site names are denoted as 'Site' followed by letter description of peatland type (I for intact Kopuatai peatland, D for drained peatland) and of the vegetation dominating the site (E for *E. robustum*), M for manuka (*L. scoparium*), S for sedge of (*Machaerina spp.*), P for pasture) (e.g., Site DP).

Figure 3.2 Location of drained peat sampling site at the drained site (green triangle), in relation to the remaining intact bog remnant, Moanatuatua (red outline).

3.2 General methods

A key objective in this study was to develop the methodology for sampling and processing New Zealand peat to measure anaerobic CH_4 and CO_2 production. Laboratory studies interrogate respiration production rates using different protocols by controlling variables such as temperature range and incubation length. However, experimental design differs among studies, making it difficult to make direct comparisons to other literature (Kolton *et al.*, 2019). The methodology chosen in this study was based on similar research methods for anaerobic peat samples and incubation studies (Dunfield *et al.*, 1993; Kolton *et al.*, 2019; Hopple *et al.*, 2020).

Lab incubations involved firstly collecting peat samples at each site and transporting them back to the laboratory, maintaining anaerobic conditions where possible throughout these steps. Secondly, incubating samples for a minimum of four days, and collecting gas headspace samples every 24 hours during this time. Finally, processing samples on an infrared gas analyser (IRGA) to quantify CO_2 and a quantum cascade laser (QCL) to quantify CH_4 and assessing the outputs using MATLAB and R.

3.2.1 Peat sample collection

A key first step in this project was identifying the most effective and pragmatic peat-sampling techniques for New Zealand peat. As the first study performing anaerobic CH_4 and CO_2 production incubations with New Zealand peat, we set out to determine suitable strategies. Assessing methods used in other publications on peat sampling methods was a helpful guide as the aim when designing these techniques was to limit potential disturbance effects during sampling. Such effects are a concern during incubation studies as they can render samples unrepresentative of *in situ* conditions. Disturbance effects include isolation from surrounding peat, exposure to oxygen, and fluctuating temperatures (Hodgkins *et al.*, 2015; Treat *et al.*, 2015). Although these impacts are undesirable, a study assessing the ratio of CH_4:CO_2 production rates for *in situ* field measurements and incubations by Hodgkins *et al.* (2015) found the effect of sampling disturbances on peat was unlikely to dramatically alter results. Variables to consider when sampling included the depth of peat sampling, the practicality of coring equipment, and the size and number of samples. The variation and versatility in sampling techniques utilized in this study accounted for the differing peat characteristics of both intact and drained peat. These two peat soil types are distinct in ways that meant sampling techniques used for one site, did not necessarily work for the other.

3.2.1.1 Kopuatai peat sampling methods

The surface layers of the intact peat (≤50 cm) were sampled using a 9.2 cm diameter cylindrical stainless-steel corer with a removable handle and serrated bottom edge. We placed the corer perpendicular to the surface with the serrated edge down and sliced it into the peat by twisting the removable handle from side to side (Figure 3.3a). This technique cuts into the peat while avoiding compression. After manoeuvring the core to the desired depth, we removed it from the peat, leaving behind just the core. Removing the core involved simply gripping the top few centimetres of the core and gently pulling it upwards, away from the surrounding peat (Figure 3.3b).

After coring the peat, the intact core was laid onto a wooden cutting board and sliced (Figure 3.3c) into ~0.5×2 cm sub-cores at the desired depth. A serrated bread knife proved to be the most effective at cutting the peat without compressing it, as found in methods from Hopple *et al.* (2020). We then manoeuvred these sub-cores into Hungate tubes by carefully twisting the sub-core and using a glass stirring rod to push the core gently into the tube (Figure 3.3d), careful to avoid compressing the peat. Tubes were immediately sealed, ready for transport back to the lab. We performed this process as quickly as possible to limit the air exposure time for the samples.

Figure 3.3 Stages in the intact peat coring process including (a) using the cylindrical core, (b) removing the peat core from the surrounding peat, (c) cutting peat to fit into a sampling container, and (d) manoeuvring a peat sample into a Hungate tube.

We focussed on the peat layer between –5 to –20 cm, within the hypothesized zone of maximum production for CH_4 based on an ecosystem-scale study by Goodrich *et al.* (2015). Often shallow peat depths, less than ≤20 cm, are chosen for study as CH_4 production seems to be high and meaningful to the resulting flux, perhaps explained by substrate availability and shallow WTD (Svensson, 1984; Dunfield *et al.*, 1993; Schulz *et al.*, 1997; MacDonald *et al.*, 1998; Glissman *et al.*, 2004; Freitag & Prosser, 2009). The zone of maximum CH_4 production is generally associated with mean WTD or the rhizosphere of dominant plant species, which influences the presence of alternative electron acceptors and the availability of substrate.

Goodrich *et al.* (2015) found that daily mean CH_4 flux was highest when the WTD was approximately 2–3 cm on either side of –10 cm. The 2012 mean WTD and hypothesized zone of maximum production was –7.65 cm (Goodrich *et al.*, 2015). This layer is within the shallow root zone, which supposedly produces the largest CH_4 flux, perhaps because of root exudation of labile C (Van Huissteden *et al.*, 2006; Goodrich *et al.*, 2015). Due to the high WTD and the unconsolidated nature of the deeper peat layers at our sampling sites, using the cylindrical core was not suitable for peat deeper than 50 cm.

3.2.1.2 Drained peat sampling methods

At the drained peat site, we took samples from ~30–35 cm. This layer is situated above the water table in both winter (mean WTD –50 cm) and summer (mean WTD –100 cm), but still within the capillary zone, where the peat was still near saturation. The capillary zone extends the zone of saturation above the water table (Campbell *et al.*, 2021). We also sampled peat beneath the summer WTD (–100 cm) as a comparison between saturated and surface layers, shown in the results section. In contrast to the intact site, here we dug pits and took small sub-cores at the desired depths. By simply digging an open pit, we were able to take dozens of replicates at each depth by coring the peat from all sides. To test the effects of sub-core size on incubation results, we initially used 6×5 cm bulk density cores placed into mason jars as a comparison to smaller Hungate tubes used at the intact site. Hungate tubes produced less variable results and proved to be less bulky to transport into the field, so we decided against using mason jars. To limit oxygen exposure, we used a 4 ml syringe with a sawed-off and sharpened bottom to extract peat from the side of the pit and plunged the peat into a Hungate tube (Figure 3.4).

Before settling on the drained peat sampling methods described above, we performed a preliminary method experiment using a Russian D-corer to collect peat up to 1 m depth, which gave us insight into how many samples we could take using this method and the degree of peat degradation with depth. With some force, we manoeuvred the D-corer into the peat and by twisting the top handle in a 180° rotation; a half cylindrical-shaped core becomes secured in the corer. After removing the D-corer from the peat, we gently twisted the sub-coring syringes into the core (Figure 3.4b), then removed and plunged the sub-core directly into the Hungate tubes, which we immediately sealed (Figure 3.4c). Using this method, there was only an initial exposure to oxygen when the D-corer opens, while the rest of the process was anaerobic. We decided against pursuing this method because it was labour intensive and multiple cores would have been necessary for replicates from each depth.

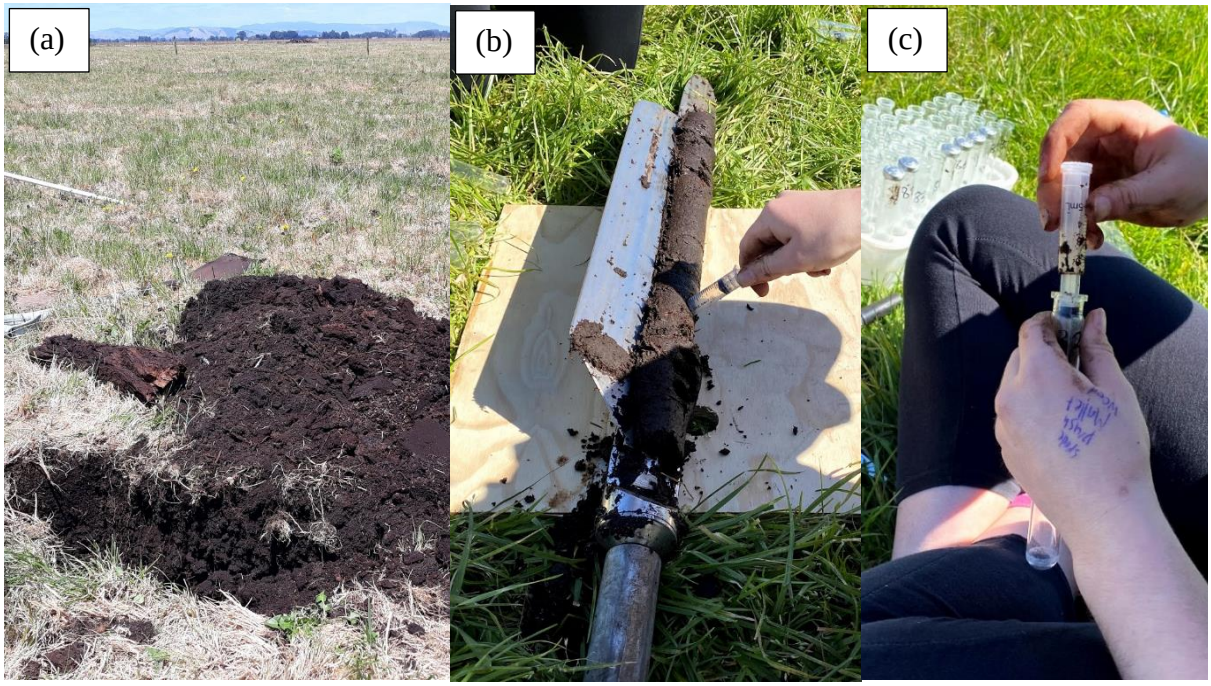

Figure 3.4 Drained peat coring process beginning with (a) digging an open pit and (b) using a syringe with a sawed-off and sharpened bottom to core peat from the side of the pit (or pictured here using preliminary D-coring method) and (c) plunging the core into the Hungate tube.

3.2.2 Sample preparation

3.2.2.1 Flushing samples

We prepared the peat samples for incubation by flushing the container holding the peat with nitrogen (N_2) gas to remove any existing oxygen. This created a starting time for calculating production and ensured the system was anaerobic (Yavitt *et al.*, 2006; Kolton *et al.*, 2019; Hopple *et al.*, 2020). We performed this process in the laboratory using a multi-hose needle manifold with an input and output needle inserted into each Hungate tube. The manifold system was attached to an N_2 gas cylinder and samples were purged with N_2 after arriving back from the field, within 5 hours of collection. Flush times varied for each sample container with Hungate tubes (15 ml) receiving approximately 3 minutes worth of flushing, while mason jars (500 ml) were flushed for 5 minutes. Flushing the Hungate tubes for 3 minutes removed any detectable CH_4 and CO_2. We initially flushed samples in the field to limit exposure time to ambient oxygen stored within the container during sampling; however, the practicality of sampling outweighed the need for maintaining anaerobic conditions and this did not seem to impact incubation results. In particular, carrying a gas tank into the intact bog site was not

feasible or justifiable when flushing in the lab was an available option so we flushed all samples in the laboratory.

3.2.2.2 Homogenization

Some studies choose to 'homogenize' peat samples by creating a slurry by blending to control peat properties such as moisture content or aggregate size (more applicable to mineral soils). We decided that these techniques would greatly disturb the samples and give results less representative of *in situ* conditions. Therefore, samples did not undergo any form of homogenization other than removal of any stick material that obstructed the peat core from fitting into the tubes.

3.2.2.3 Substrate additions

We added glucose to peat from Site DP to test if the temperature response was co-limited by substrate supply. We added 0.27 g of glucose powder (D-GLUCOSE, Ajax Chemicals UNIVAR 783-500G) to 20 ml distilled water to form a glucose solution (Numa, 2020; Numa *et al.*, 2021). Considering the peat cores were similar in size and the objective of this experiment was to flood the system with more glucose than would be needed by methanogen communities, we simply added enough glucose solution to submerge each individual core.

3.2.3 Incubation

To capture production values from a wide temperature range, we incubated our samples in a temperature gradient block (Figure 3.5a). The temperature gradient block was fundamental for this experiment as it provided 18 evenly spaced cells at temperatures ranging from ~8.5–51°C. Each cell could accommodate three Hungate tubes, so we could incubate multiple replicates at each temperature during the same period. The 18 cells were spaced evenly within the aluminium body of the temperature block (168 cm × 13 cm × 23 cm) with a water bath (Julabo F10-UC/3) containing anti-freeze connected at one end of the temperature block and a heating component (Shinko ECS series controller & GEWISS GW 44 217 junction box) situated at the other end. These mechanisms drove the gradient in temperature along the block. Approximately two to three hours after turning the bath and heater on, the block temperatures stabilized at 7–10°C in cell 1 and linearly increased by ~2.5°C between each cell, up to 50–52°C in cell 18. These values were measured using temperature data loggers (Maxim iButton®

devices). Each cell has a volume of ~230 cm^3 initially designed to incubate small intact peat cores, using 2.5×10 cm alloy corers and a steel lid with rubber O-ring seals. A septum plugs a hole in the centre of the lid to cease exposure to ambient airflow. The cells can also host Hungate tubes by removing the aluminium lids and fixing a detachable foam mat with holes above each cell to hold the tubes in place during incubation. In addition to the field sampling advantages of Hungate tubes, the space in each cell of the temperature block holds three tubes per cell Figure 3.5b. A detachable polystyrene lid designed to fit over the top of the Hungate tubes limited the exposure of samples within each cell to fluctuations in ambient air temperature.

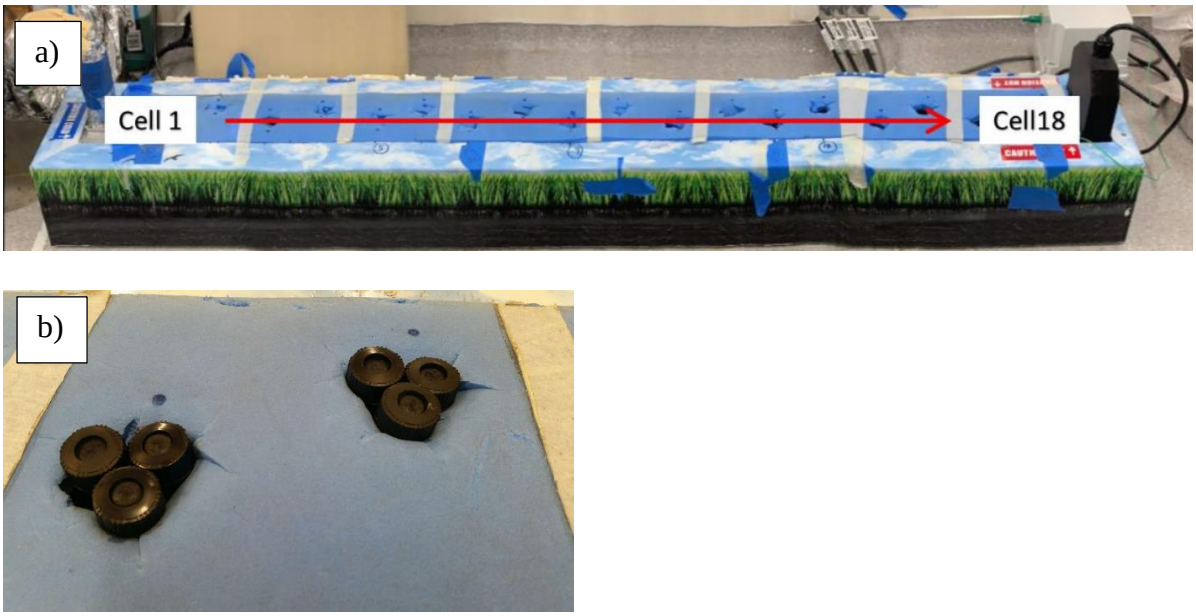

Figure 3.5 Temperature gradient block with (a) the lid removed to show cell (1–18) placement, photograph sourced from Numa *et al.* (2021), and (b) triplicates of Hungate tubes in two cells

In addition to the temperature gradient block, we tested samples in different incubators using more than three replicates at a given temperature to compare against temperature block results. These included a –20°C freezer, fridges set at 4°C, 5°C, 10°C, and 14°C, a temperature-controlled room at 19°C, as well as water baths and ovens that could be set anywhere above ambient temperature. All samples from the temperature block and other incubators were in dark conditions for the majority of their incubation but sometimes samples from the other incubators were exposed to light when taking a headspace sample. To assess the stability of temperatures over several hours in each incubator including the temperature block, we used temperature data loggers (Maxim iButton® devices).

3.2.3.1 Incubation length

We placed peat samples into incubators within hours of returning to the lab and took the first headspace samples approximately 24 hours after flushing. The rapid turnaround time was intended to best represent *in situ* conditions (Hopple *et al.*, 2020). We continued headspace sampling daily (approximately every 24 hours) for the duration of the incubation. Other studies have tended to have long incubations of two weeks or more (Blazewicz *et al.*, 2012; Treat *et al.*, 2015). We used the linear regression of the increase in CH_4 headspace concentration each day in the calculation of production rates. Here, we tested for optimal incubation length by running an initial two-week experiment, tracking headspace concentration daily. From these preliminary incubations, gas headspace concentrations increased linearly each day (Figure 3.6) for four days, after which production rates began to plateau or decrease for the majority of samples incubated between temperatures 8.5–51°C. This information helped us determine that the length of our incubations would only need to be 4 days in duration to get clear measurements of the production rates and have enough replicates for a robust average.

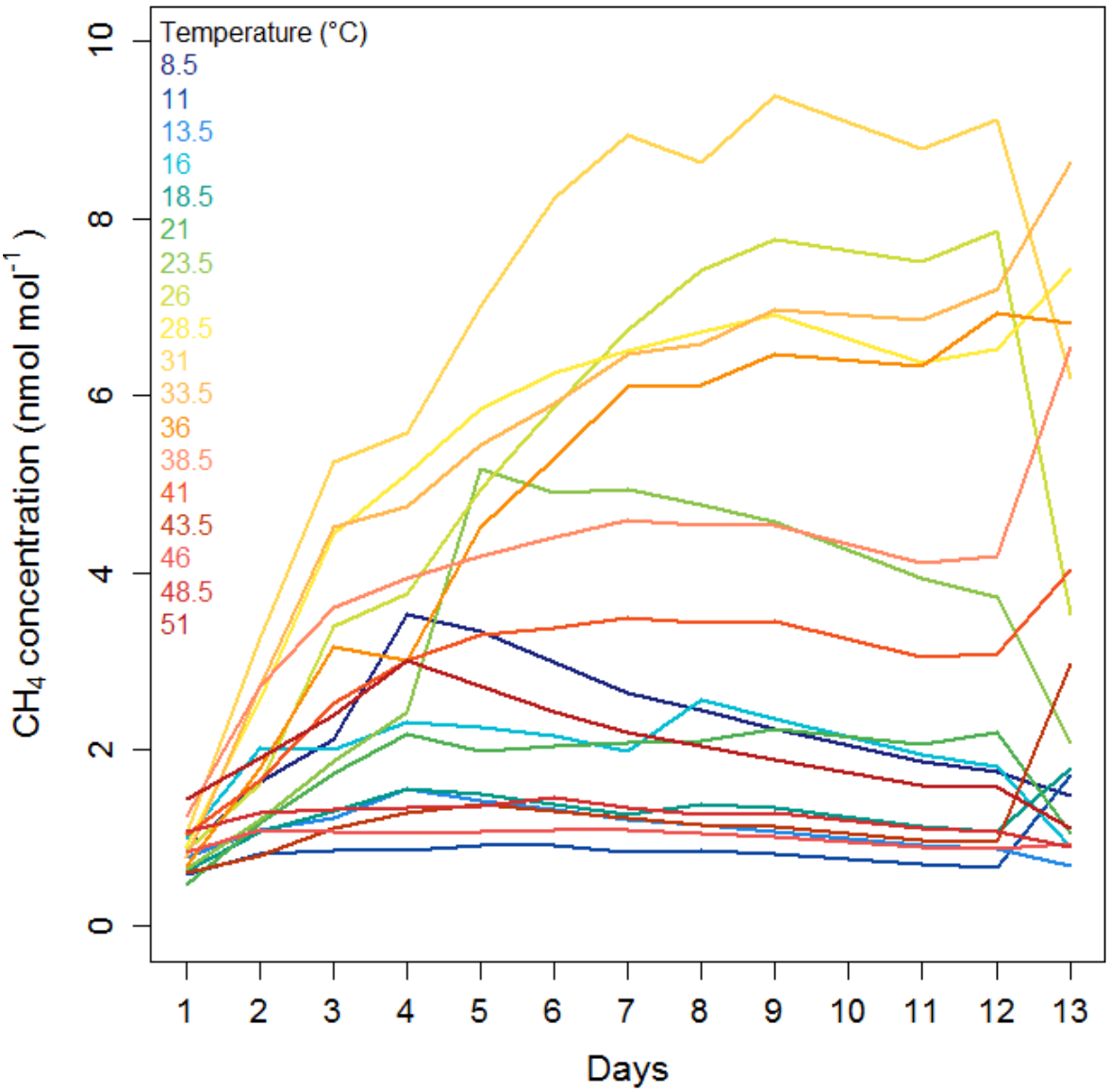

Figure 3.6 The change in CH_4 concentration (nmol mol^{-1}) for peat samples incubated for 13 days between temperatures 8.5–51°C (indicated by line colour).

3.2.3.2 Pre-incubation

There is much debate on the necessity of pre-incubating peat samples before beginning an incubation experiment. One common method in the literature is to have long pre-incubation periods to settle the methanogen populations after disturbance (Blazewicz *et al.*, 2012; Treat *et al.*, 2014). Another interesting method in Kolton *et al.* (2019) involved pre-incubating samples in a temperature gradient block. Despite these considerations, we chose to have no pre-incubation period so samples represented *in situ* conditions as closely as possible, similar to methods outlined by Hopple *et al.* (2020). Figure 3.7 illustrates how after four days of incubation between 8.5–51°C, there is a decrease or plateau in production rate. This could be indicative of another process occurring, such as CH_4 consumption or substrate depletion

(Bergman *et al.*, 1998), meaning valuable production information may be lost before measurements begin. We also found no significant difference between production rates from samples pre-incubated for up to five days compared to samples placed immediately into the temperature block ($p = 0.241$), as long as samples were flushed before entering the temperature block.

3.2.4 Headspace sampling

Using 1 ml insulin syringes, we took headspace samples through the septa of the Hungate tubes. The syringe was plunged three times to stimulate gas mixing and prevent sampling of gas accumulated at the top of the Hungate tube. We noted the time of sampling as the number of hours since flushing the sample and included this value in the equation for calculating production. We backfilled tubes with N_2 gas to maintain a constant pressure and volume and accounted for this in the flux calculation.

Each 1 ml sample for CH_4 was stored in a 3.7 ml exetainer vial, previously evacuated using a vacuum pressure set to 80 kPa, and filled with 5 ml inert N_2 gas providing overpressure of 1.3 ml. The length of time spent evacuating vials (2–5 minutes) did not show any significant difference in measured headspace concentrations ($p = 0.13$). To account for residual CH_4 contaminating exetainer vials after flushing, we averaged the residual CH_4 concentration found in a set of ten empty vials treated the same as a sample vial and subtracted this value from all results. We stored exetainer vials holding headspace samples in a refrigerator at 4°C for up to three weeks before analysis. To test whether exetainer storage time impacted the quality of results we processed the same set of samples two weeks apart. We found there was no significant difference ($p = 0.6$) in CH_4 concentration detected in the vials measured on both dates, providing confidence that there were no issues with storing samples in exetainers for extended periods.

Exetainer vial storage was not required for CO_2 samples as the infra-red gas analyser (IRGA) was located within the same room as the incubating samples. This meant there was minimal travel time between extracting the 1 ml headspace sample from each tube and analysing the sample on the IRGA. To reduce gas loss between the time of drawing the headspace sample and processing it on the IRGA (≤10 minutes), the needle of the syringe was inserted into a rubber bung. In order to make comparisons between CH_4 and CO_2 results, we accounted for the dilution factor associated with injecting 1 ml CH_4 samples in exetainers before analysis. After evacuating, 5 ml of N_2 gas and the 1 ml sample were added to the exetainer. Therefore,

the peak areas detected during analysis were representative of a diluted CH_4 sample, so to account for this we multiplied the peak area for each sample by 6 (5+1).

3.2.5 Sample analysis

After storing the gaseous headspace samples in exetainers, we processed samples using a quantum cascade laser (QCL) as part of the EC system installed at Site DP. Kroon *et al.* (2007) detail the instrumentation and methodology associated with QCL systems. Wecking *et al.* (2020) provide a detailed description of the set-up of a QCL for manual injections (Figure 3.7). We based our methods on techniques developed in Wecking *et al.* (2020), adapted to suit headspace samples taken from the laboratory, as opposed to those taken from in-field static chambers (Wecking *et al.*, 2020). The required equipment included a QCL, desktop monitor, mouse, and keyboard to connect to QCL computer, N_2 bottle, regulator, and connective tubing to control the carrier gas, as well as samples stored in exetainer vials and syringes for extracting samples from vials and sampling through the QCL injection port.

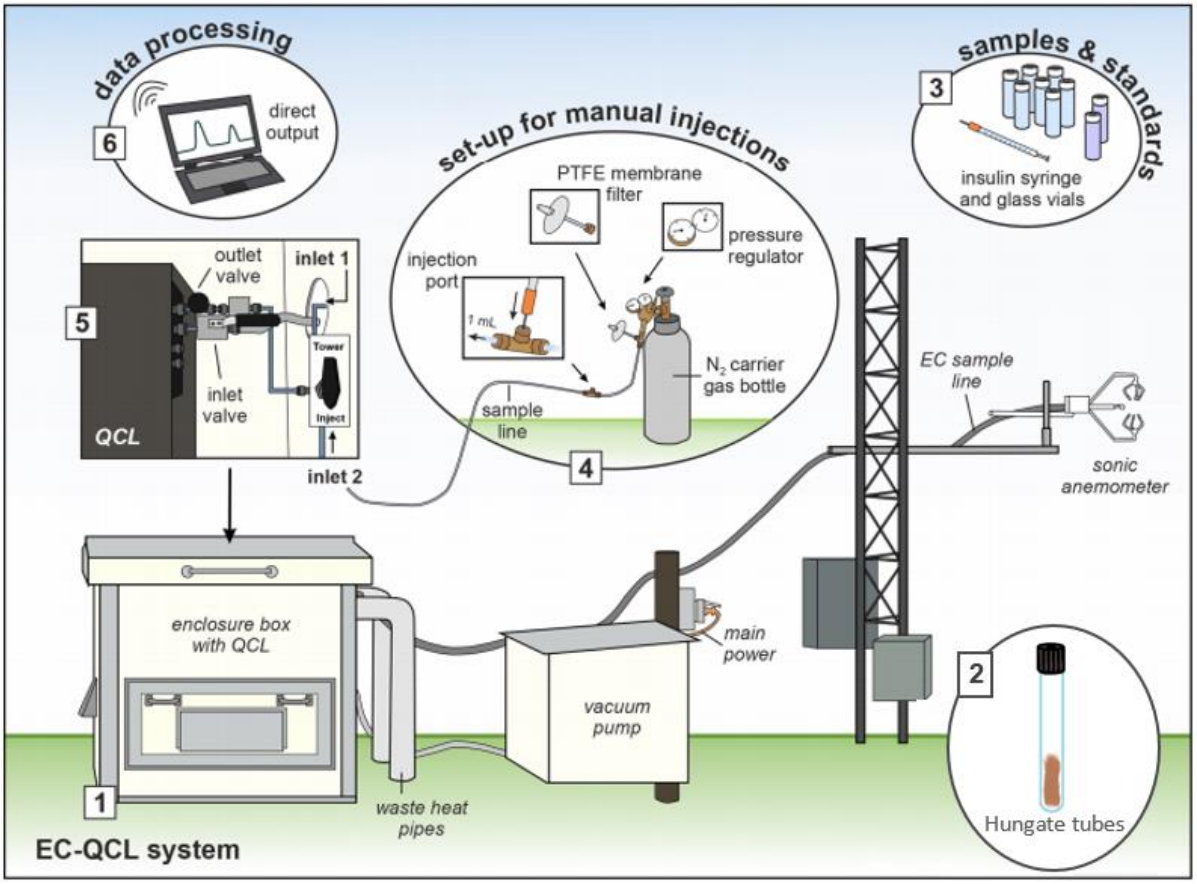

Figure 3.7 Schematic diagram of the set-up of a field-based QCL for EC measurements and manual injections adapted from Wecking *et al.* (2020). (1) The main components of the QCL EC system; (2) the Hungate tubes where the peat sample is stored and CH_4 headspace samples are taken through the septa; (3) dated glass vials containing headspace sample. The set-up for manual injection (4) adjusts the QCL air inlet

(5) to draw air via the injection tube (inlet 2) as opposed to drawing ambient air through the EC sample line (inlet 1). Samples and standards are received by the QCL via the injection port and produced immediate data output (6) (Wecking *et al.*, 2020).

As noted above, for CO_2 samples, we extracted another 1 ml from the headspace of each Hungate tube and immediately processed this on the lab-based infrared gas-analyser (IRGA). The same principles involved in IRGA set-up and associated peak identification apply to the QCL injection mode at Site DP. This includes a gas-processing unit, IRGA (LI-COR, LI-7000, CO_2/H_2O Analyser), attached to pressure regulated zero-grade oxygen-free N_2 bottle. Flow rate from N_2 bottle was approximately 37.5 l min^{-1}. We injected samples via a septum and peak outputs were processed via MATLAB.

We ran associated gas standards through both the QCL and the IRGA to ensure our results were accurate and to generate a standard curve for each run of samples. For the QCL, we made all standards using 5000 ppm CH_4 diluted with oxygen-free N_2 gas and overfilled each bottle with 25 ml overhead pressure. The three standard bottles consisted of 'high', 'low', and 'very low' methane. We processed standards through the QCL in 0.1 ml increments from 0.1 ml to 1 ml to create a standard curve. We generally injected a set of standards in between sets of incubation samples, while also logging the time for specific samples and standards. This made for easier peak identification during data processing. CO_2 standards consisted of 1% CO_2 and were processed through the IRGA in 0.2 ml increments using the highest and lowest sample peak sizes to decide the range of standards used. Standards ranged between 0.04 ml and 20 ml; however, on average we only required 0.1–1 ml samples to create a standard curve.

After the incubation period, we removed peat core samples from the Hungate tubes, dried them for ~24 hours in the oven at 105°C, and weighed them to obtain the dry weight of each sample. We then used this value for calculating the production rate from each sample.

3.2.6 Data processing

We used MATLAB to calculate peak area and produce a set of all peaks in graph form with an associated Excel file output showing the characteristics of each detectable peak (Figure 3.8). The MATLAB code accounted for noise by identifying peaks that were larger than one standard deviation from the running mean. This was particularly helpful for QCL data where the N_2 carrier gas was only controlled by a gas tank regulator and was prone to changing pressure. This was unlike the IRGA set-up, which had a gas tank regulator and two other flow controllers along with the connective tubing before reaching the IRGA.

The Excel output provided the peak area for each sample run. We matched these with the associated samples run at that time, as indicated by notes taken in the field and separation of incubation samples and standards. The production rate for a given sample was calculated as the slope of the linear regression using the daily headspace concentration over time for the four-day incubation period. This was then divided by the dry weight of the sample, resulting in production rates in units of nmol CH_4 hr^{-1} g^{-1} dry peat.

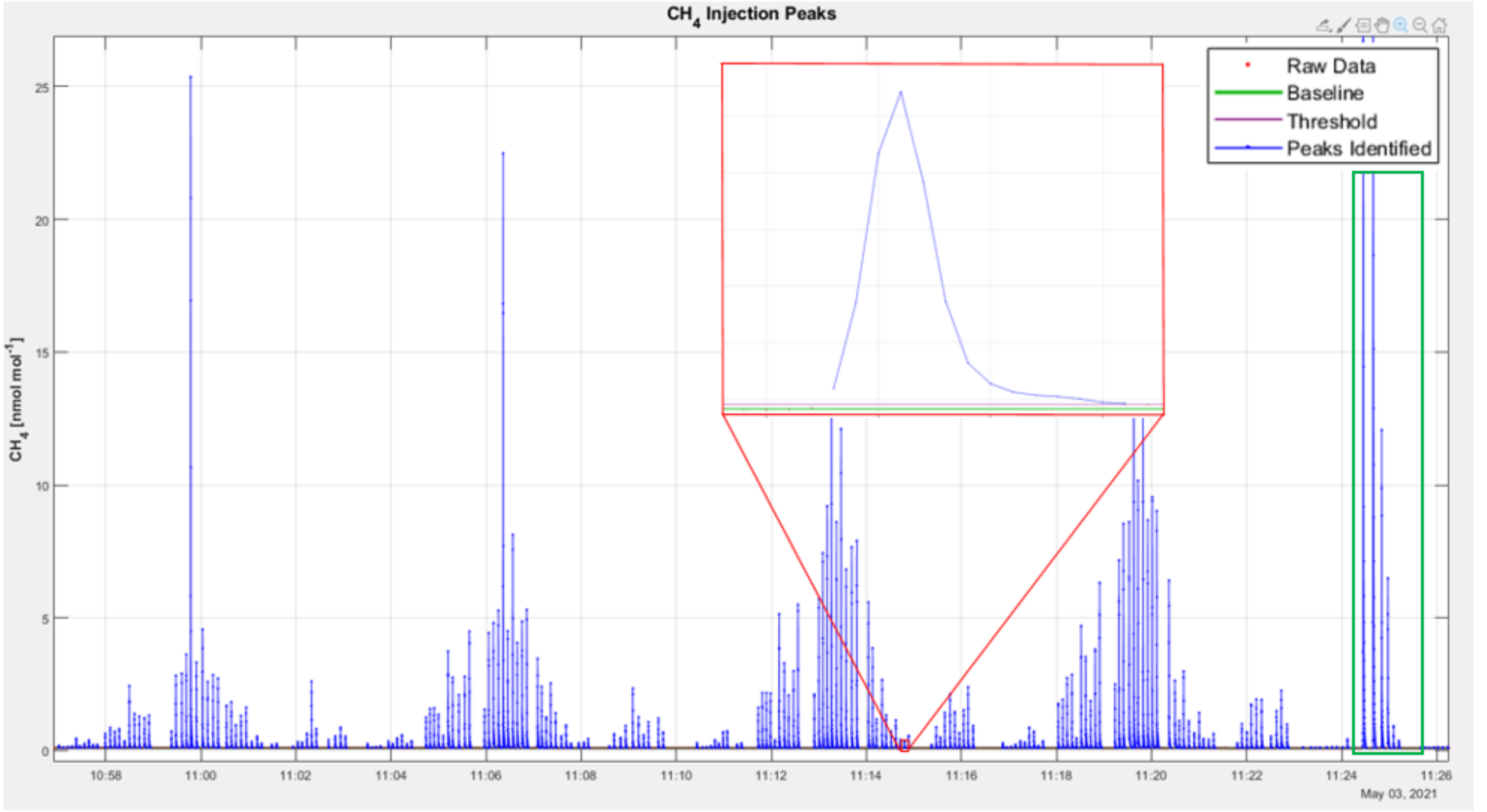

Figure 3.8 Raw data from the QCL MATLAB output showing peaks of CH_4 generated from three replicates of 18 peat cores across a temperature gradient over four incubation days. An example of standards that span this range of samples and bracket sample sets are outlined in green (total range of standard peaks not shown). Inset image (red outline) to show close-up of a single peak.

3.2.6.1 Curve fitting

We used MMRT (Equation 3-1) to fit temperature response curves for both CH_4 and anaerobic CO_2 production.

$$\ln(k) = \ln\left(\frac{k_B T}{h}\right) - \frac{\Delta H^{\ddagger}_{T_0}}{RT} - \frac{\Delta C_p^{\ddagger}(T - T_0)}{RT} + \frac{\Delta S^{\ddagger}_{T_0}}{R} + \frac{\Delta C_p^{\ddagger}(\ln T - \ln T_0)}{R} \quad (3\text{-}1)$$

Where k is the rate, k_B is Boltzmann's constant, T is the temperature (K), h is Planck's constant, R is the universal gas constant, $\Delta H^{\ddagger}_{T_0}$ (‡ superscript denotes transition state) is the change in enthalpy (J mol^{-1}) between the reactant state and the transition state, $\Delta S^{\ddagger}_{T_0}$ is the change in entropy (J mol^{-1} K^{-1}), both at reference temperature T_0 (309 K, 36ºC), $\Delta C_p^{\ddagger}$ is the change heat capacity (J mol^{-1} K^{-1}). For T_0, we used the mid-point temperature from a given set of incubations.

We used a standard non-linear least squares estimator to fit MMRT to the rate data (R v4.0.2). For each temperature block incubation run, we standardized the rate data by scaling the rates from 0–1. This allowed us to compare the shape of the resulting curves without regard for the magnitude of the rates. Given the relatively flat, but non-zero, response to high and low temperatures for CH_4 production, we used only data between 16–48°C, when fitting curves. The nature of the measured CH_4 production at these tail ends of the temperature response may be indicative of something other than the biologically mediated reaction represented by MMRT (Hobbs *et al.*, 2013). The first derivative of each fitted curve was used to determine T_{opt}, while the second derivative was used to calculate T_{inf}.

Pair-wise comparisons between temperature response parameters T_{opt}, T_{inf}, ΔC_p, ΔH, and ΔS were tested using Tukey's Honest Significant Difference (HSD) test. The comparisons tested for significant differences (critical value used for alpha = 0.05) in production between the different vegetation types.

Chapter 4

Characterising the temperature dependence of CH_4 production in New Zealand peatlands

4.1 Abstract

Understanding the temperature response of microbial processes in peatlands is important in determining consequences for peatland carbon dynamics and the production of CH_4 as the climate warms. We currently have a limited understanding of the microbial temperature responses in peatlands, particularly for Southern Hemisphere systems. To improve our understanding, we measured the response of anaerobic CH_4 and CO_2 production across a large temperature range of 8.5–51°C, from two New Zealand peatland systems, including an intact bog and a drained peat pasture. Peat was incubated anaerobically for four days in a temperature gradient block with 18 discrete temperatures. We applied macromolecular rate theory (MMRT) to the CH_4 and CO_2 production response to derive the temperature optimum (T_{opt}) and the inflection point (T_{inf}) for each gas. The T_{opt} for CH_4 production ranged from 30.1–32.8°C and T_{inf} values ranged from 23.3–25.6°C, in comparison to the anaerobic CO_2 T_{opt} of 35.4–44.0°C and T_{inf} of 25–32.2°C. The temperature response did not significantly differ among sites, and the production rates of CO_2 had much higher magnitudes than CH_4 production. Additionally, there was a rapid increase in the ratio of CO_2:CH_4 after warming above the methanogenic T_{opt}, which may have implications for climate change and for the rewetting of drained peatlands.

4.2 Introduction

Methane (CH_4) accounts for 15–25% of the global greenhouse gas (GHG) budget (Etminan *et al.*, 2016), of which natural wetlands, including peatlands, contribute ~30% to global CH_4 emissions, making wetlands the largest natural source to the atmosphere (Saunois *et al.*, 2020). Additionally, peatlands represent one-third of the terrestrial carbon (C) pool, making them a major global C stock (Keller & Bridgham, 2007; Hopple *et al.*, 2020). Much of this C exists beneath the water table, where oxygen is limited and anaerobic microbial decomposition dominates (Keller & Bridgham, 2007; Conrad, 2020). Peatland C storage has resulted in a net cooling effect on global climate over millennia (Frolking & Roulet, 2007), however, the peatland C cycle is sensitive to temperature changes (Hopple *et al.*, 2020). If significant

amounts of this stored carbon were transferred to the atmosphere as carbon-based GHGs (C-GHGs), including CH_4 and CO_2, this would initiate an important positive feedback to climate change (Eville, 1991; Davidson & Janssens, 2006; Portner *et al.*, 2010).

Peatland microbial communities, hydrology, temperature, and substrate availability are among the major factors that control the production and flux of CH_4 from peat. Changes in these factors have the potential to amplify the drivers of climate change by stimulating the return of stored soil C to the atmosphere as CH_4 (Dunfield *et al.*, 1993; Metje & Frenzel, 2005, 2007; Tveit *et al.*, 2015; Zalman *et al.*, 2018; Hopple *et al.*, 2020). The consensus of previous studies is that climate change will likely result in warming-induced acceleration of organic matter decomposition and subsequent stimulation of CH_4 emissions (Davidson & Janssens, 2006; Weedon *et al.*, 2013; Goodrich *et al.*, 2015). Despite these predictions, the response of peatland CH_4 production to rising temperatures is poorly understood (Kolton *et al.*, 2019).

Understanding the temperature dependence of microbially-mediated organic matter decomposition and C-GHG flux dynamics in wetlands is critical for predicting ecosystem responses to climate change (Schimel & Holland, 2005; Ma *et al.*, 2017). However, many existing models use oversimplified temperature response functions for CH_4 production, in part because few studies have measured this response in peatlands with sufficient detail (Kolton et al. 2019). Experiments quantifying the temperature dependence of anaerobic soil respiration have produced variable results, possibly due to differences in experimental methods including using a limited number of incubation temperatures, failing to adequately capture the curvature (Dunfield *et al.*, 1993; Kolton *et al.*, 2019; Hopple *et al.*, 2020; Numa *et al.*, 2021). There is a wide range of mathematical models proposed to describe biochemical responses to changing temperature in soil. Many studies base these models on the Arrhenius and Q_{10} functions (Lloyd & Taylor, 1994; Davidson & Janssens, 2006; Sierra *et al.*, 2015). However, the Arrhenius model does not include an inflection point (T_{inf}) and relative temperature sensitivity is not constant with increasing temperatures as often assumed when using Q_{10}. Macromolecular rate theory (MMRT) represents the temperature response by using the thermodynamic properties of biological macromolecules, specifically enzymes, to describe the temperature-dependence of reaction rates (Hobbs *et al.*, 2013; Schipper *et al.*, 2014). Temperature optima (T_{opt}) and T_{inf} are two important metrics derived from the MMRT equation. T_{opt} describes the temperature of maximum production rate, while the T_{inf} describes the temperature where an increase in rate is maximal relative to temperature (Schipper *et al.*, 2019). Fitting MMRT to soil or peat

incubation data requires a large range of temperatures for the exploration of nonlinear curve response fitting (Portner *et al.*, 2010; Hopple *et al.*, 2020).

The majority of studies focusing on the temperature response of peatland CH_4 production originate from Northern Hemisphere systems, while Southern Hemisphere peatlands are relatively underrepresented. Despite their climatological and hydrological differences, Northern and Southern Hemisphere bogs are similar in terms of CH_4 flux dynamics (Goodrich *et al.*, 2015). However, Goodrich *et al*. (2015) found annual total CH_4 fluxes from a New Zealand peat bog were notably higher than analogous Northern Hemisphere systems. Globally, around 65 Mha of peatlands have been altered from their natural state and ≥90% of New Zealand wetlands have been drained (Scott, 1996; Ausseil *et al.*, 2015; Dymond *et al.*, 2021).

The aim of this study was to quantify the temperature response of anaerobic organic matter decomposition to CH_4 and CO_2 in New Zealand peatland systems and to characterize this response using MMRT. This requires refining the methodologies for anaerobic incubation studies used in international literature to suit New Zealand peat soils. We explored differences in rates and temperature response among different vegetation communities that exist in the intact bog and the agricultural drained peatland.

4.3 Site description and methods

4.3.1 Site description

Two research sites located within the Waikato Region, Te Ika-a-Māui (North Island), Aotearoa New Zealand were investigated during this study. In order to capture the full range of New Zealand peat conditions, we chose to compare an intact site (Kopuatai 37°25.11′S, 175°33.19′E) to a drained farm site. The intact peat site, Kopuatai peat dome, is a large ombrotrophic restiad peat bog located in the Hauraki Plains. Kopuatai began forming 13,500 years ago with a present-day extent of ~90 km^2 (9,665 ha), the dome is the largest remaining undisturbed raised peat bog in New Zealand (Newnham *et al.*, 1995; Goodrich *et al.*, 2017). The peat is highly acidic (pH ~4) and nutrient-poor with depth ranges from 1–14 m (Newnham *et al.*, 1995). Distinctive vegetation zones exist throughout Kopuatai, mostly dominated by species of the Restionaceae vascular plant family. Jointed wire rush (*Empodisma robustum*) is the main peat-forming plant and the most abundant species within the bog. *E. robustum* communities are widely distributed and are most dominant towards the centre of the bog. Greater jointed rush (*Sporadanthus ferrugineus*) is also locally dominant as well as sedge

species (*Machaerina spp.*) (Agnew *et al.*, 1993; Wagstaff & Clarkson, 2012). Woody shrubs including manuka (*Leptospermum scoparium*) are predominantly found towards the fringes of the bog, where conditions are more mesotrophic due to changes in land use and development (Pronger *et al.*, 2014), but are found in stunted forms throughout the bog. In addition to comparing CH_4 and CO_2 production from intact and drained sites, we sampled multiple sites within Kopuatai to explore spatial variability related to vegetation type. Mean annual precipitation (1981–2010) for Kopuatai, measured at an official climate station 11 km to the east of the study site was 123.2 cm, and mean annual air temperature was 13.7°C (NIWA, 2019).

The drained peat site is a dairy pasture ~2.5 km away from the remnant ombrotrophic peat bog Moanatuatua (37°55.50′S, 175°22.20′E), located ~50 km southwest of Kopuatai. Peat accumulation began ~13,000 years ago in a depression formed by an ancient path of the Waikato River upon an impermeable layer of volcanic ash deposits (Campbell, 1964). Once estimated to cover 75 km^2 of land, this remnant bog is now reduced to 1.1 km^2 due to extensive draining and land use change (Clarkson *et al.*, 2004). The surrounding drained land includes the sampling site for this study, converted to dairy pasture in 1975, with the drainage history and current management practices outlined in Campbell *et al.* (2021). The site is characterised by closely spaced (~30 m apart) shallow surface drains and the site is classified as "deep-drained" (WTD ≥30 cm) according to IPCC (2014), with a mean WTD of 65.7 cm during the study year. The site is rotationally grazed throughout the year, and ryegrass (*Lolium perenne*) and white clover (*Trifolium repens*) are the dominant pasture species. Sampling locations for both Kopuatai and the drained peatland were close to eddy covariance (EC) instruments providing ancillary data (Campbell *et al.*, 2014; Goodrich *et al.*, 2017). Mean annual precipitation (1981–2010) for the drained peatland, measured at a nearby site was 116.7 cm, and mean annual air temperature was 13.8°C (NIWA, 2019).

Site names are denoted as 'Site' followed by letter description of peatland type (I for intact Kopuatai peatland, D for drained peatland) and of the vegetation dominating the site (E for *E. robustum*), M for manuka (*L. scoparium*), S for sedge of (*Machaerina spp.*), P for pasture) (e.g., Site DP).

4.3.2 Peat sample collection

An important objective of this study was to develop the methodology for sampling and processing peat in order to measure C-GHG production. Methods involved collecting, processing, and incubating peat samples, extracting gas headspace samples, processing samples on an infrared gas analyser (IRGA) for CO_2 and a quantum cascade laser (QCL) for CH_4, and assessing the outputs using MATLAB and R. More detailed methodologies are provided in Chapter 3.

The surface layers of the intact peat at Kopuatai bog (≤50 cm depth) were sampled using a 9.2 cm diameter stainless steel cylindrical corer with a removable handle and serrated bottom edge that cuts into the peat while avoiding compression. After coring the peat, the intact core was sliced into ~0.5×2 cm sub cores with a serrated bread knife which proved to be the most effective method for cutting peat without compressing it (Hopple *et al.*, 2020). The sub-sampled peat was then inserted into 15 ml Hungate tubes, sealed with lids, and transported back to the lab (see Figure 3.3 Chapter 3 Methods section).

Samples were collected from the peat layer between –5 to –20 cm depth, within the hypothesized zone of maximum production for CH_4 production (Goodrich *et al.*, 2015). At the drained peat site, we took samples from –30–35 cm depth. This layer is situated above the water table in both winter (av. WTD –50 cm) and summer (av. WTD –100 cm), but still within the capillary zone, where the peat draws up water in the profile to extend the zone of saturation above the water table (Campbell *et al.*, 2021). We extracted peat samples at the drained site by digging an open pit to take samples from target depths rather than coring. To limit oxygen exposure, we used a syringe with a sawed-off and sharpened bottom to extract peat from the side of the pit and plunged the samples into Hungate tubes.

4.3.3 Sample preparation and incubation

We prepared the peat samples for incubation by flushing the Hungate tubes containing the peat samples with nitrogen (N_2) gas to remove any existing oxygen (Yavitt *et al.*, 2006; Kolton *et al.*, 2019; Hopple *et al.*, 2020). We performed this process in the laboratory using a multi-hose needle manifold with an inflow and outflow needle inserted into each tube. The manifold system was attached to an N_2 gas cylinder that purged samples with gas immediately on returning from the field. Hungate tubes were flushed for approximately 3 minutes to remove

any detectable CH_4 and CO_2. Samples were not homogenized in this study to avoid greatly disturbing the microbial communities (Hopple *et al.*, 2020).

We incubated our samples in a temperature gradient block with 18 pre-set temperatures between ~8.5–51°C, which linearly increased by ~2.5°C between each cell. One end of the block was cooled with a water bath (Julabo F10-UC/3) containing anti-freeze and the other end was heated with a heating component (Shinko ECS series controller & GEWISS GW 44 217 junction box). We incubated three sample tubes per cell as replicates for each incubation temperature. A detachable polystyrene lid designed to fit over the top of the Hungate tubes limited the exposure of samples to fluctuations in ambient air temperature and all samples from the temperature block were in dark conditions for the duration of the incubation. The stability of temperatures over several hours in the temperature block was assessed using temperature data loggers (Maxim iButton® devices).

After returning from the field, peat samples were immediately placed into incubators, the headspace samples were taken approximately 24 hours after flushing, and approximately every 24 hours for the duration of the incubation. This rapid turnaround time was intended to best represent *in situ* conditions (Hopple *et al.*, 2020). Headspace CH_4 concentrations tended to increase more or less linearly for four days, after which the concentrations levelled off or began to decline for most samples (Figure 3.6). We therefore used the first four days of incubation to calculate linear regressions of concentration increase over time (i.e., nmol CH_4 hr^{-1}). We then divided by dry sample weight to get production in nmol CH_4 hr^{-1} g^{-1}. Peat samples were dried for ~24 hours in the oven at 105°C and weighed to obtain the dry weight.

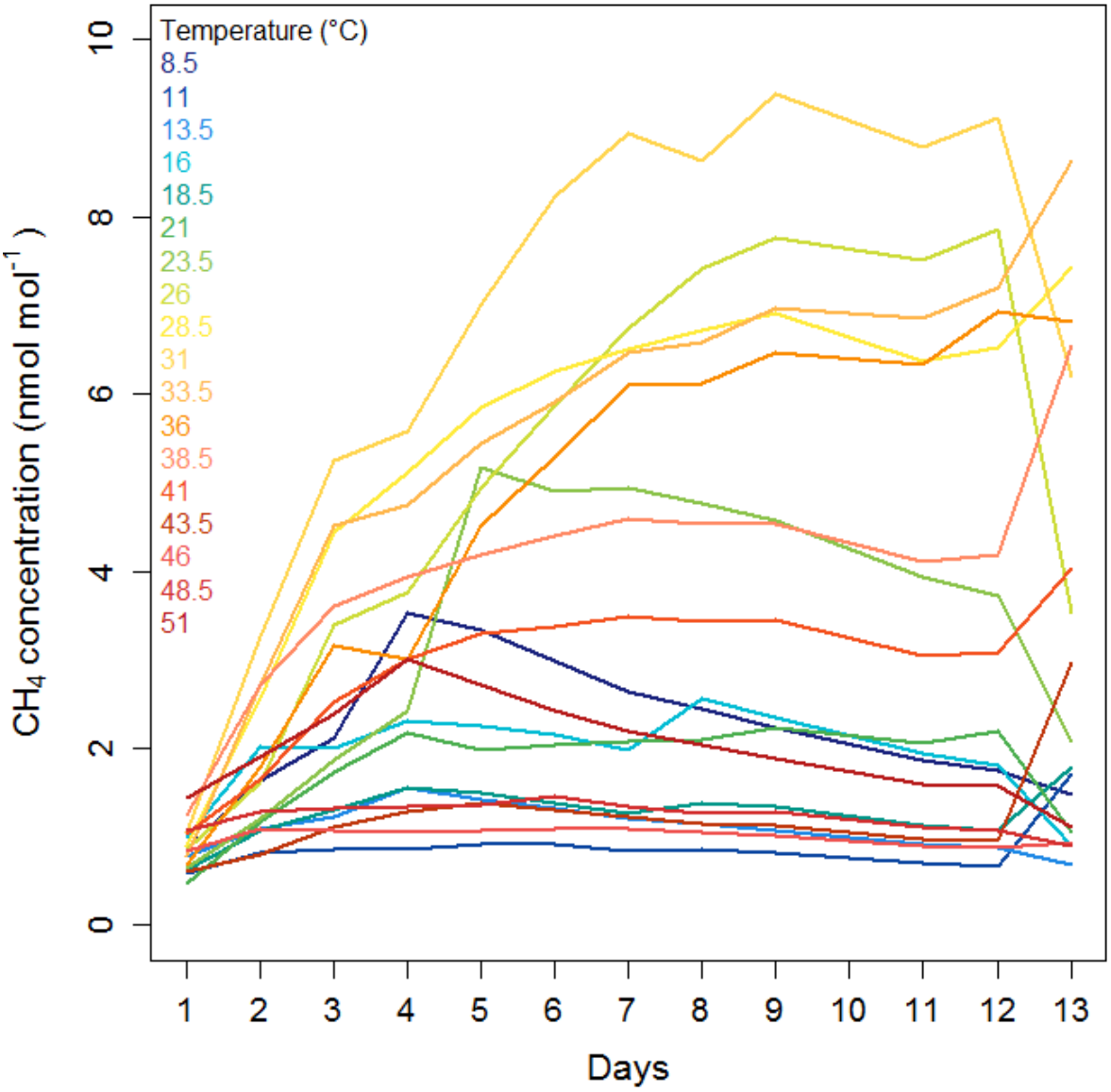

Figure 4.1 The change in CH_4 concentration (nmol mol^{-1}) for peat samples incubated for 13 days between temperatures 8.5–51°C (indicated by line colour).

4.3.4 Headspace sampling

We took headspace samples through the septa of the Hungate tube using 1 ml insulin syringes. The syringe was plunged three times to stimulate gas mixing and prevent sampling of gas accumulated at the top of the Hungate tube. We backfilled tubes with N_2 gas to maintain constant pressure, accounting for this dilution in subsequent calculations. Each 1 ml sample for CH_4 was stored in a 3.7 ml exetainer vial, previously evacuated, and filled with 5 ml inert N_2 gas. To account for residual CH_4 contaminating exetainer vials after flushing, we averaged the residual CH_4 concentration found in a set of ten blank vials treated the same as sample vials

and subtracted this value from all results. Exetainers were stored at 4°C for up to three weeks before processing, however, storage time did not distort results as we found there was no significant difference ($p = 0.6$) in CH_4 concentration detected in duplicate samples processed two weeks apart.

For anaerobic CO_2 production, headspace samples were immediately processed on the IRGA. To reduce gas loss between drawing the headspace sample and processing it on the IRGA (≤10 minutes), the needle of the syringe was inserted into a rubber bung.

4.3.5 Sample processing and analysis

We processed gas samples for CH_4 analysis using a continuous-wave quantum cascade laser absorption spectrometer (QCL, Aerodyne Research Inc. Billerica, MA, USA). We based our methods on techniques developed by Wecking *et al.* (2020), adapted to suit headspace samples taken in the laboratory. The equipment set-up included a septum in between a regulated N_2 tank and the QCL. Samples were extracted from exetainers using 1 ml syringes and injected into the QCL via the septum. The time-series data containing the concentration peaks were processed in MATLAB. For CO_2 samples, we processed the sample on the lab-based infrared gas-analyser (IRGA). The system and associated peak identification were set up much like the QCL injection-mode. A septum was attached in between a gas-processing unit, IRGA (LI-COR, LI-7000, CO_2/H_2O Analyser), and a pressure-regulated zero grade oxygen-free N_2 bottle. We ran associated gas standards through both the QCL and the IRGA to ensure our results were accurate and provide a baseline to measure against sample peak areas.

4.3.6 Data analysis

We used MMRT to fit temperature response curves for both CH_4 and anaerobic CO_2 production (Hobbs *et al.*, 2013).

$$\ln(k) = \ln\left(\frac{k_B T}{h}\right) - \frac{\Delta \mathrm{H}^{\ddagger}_{T_0}}{RT} - \frac{\Delta \mathrm{C}^{\ddagger}_{\mathrm{p}}(T - T_0)}{RT} + \frac{\Delta \mathrm{S}^{\ddagger}_{T_0}}{R} + \frac{\Delta \mathrm{C}^{\ddagger}_{\mathrm{p}}(\ln T - \ln T_0)}{R} \quad (4\text{-}1)$$

Where k is the rate, k_B is Boltzmann's constant, T is the temperature (K), h is Planck's constant, R is the universal gas constant, $\Delta H^{\ddagger}_{T_0}$ (‡ superscript denotes transition state) is the change in enthalpy (J mol^{-1}) between the reactant state and the transition state, $\Delta S^{\ddagger}_{T_0}$ is the change in entropy (J mol^{-1} K^{-1}), both at reference temperature T_0 (309 K, 36°C), $\Delta C_p^{\ddagger}$ is the change heat capacity (J mol^{-1} K^{-1}). For T_0, we used the mid-point temperature from a given set of incubations.

We used a standard non-linear least squares estimator to fit MMRT to the rate data (R v4.0.2 – R code found in Appendix B). For each temperature block incubation run, we standardized the rate data by scaling the rates from 0–1. This allowed us to compare the shapes of the resulting curves without regard for the magnitudes of the rates. Given the relatively flat, but non-zero, response to high and low temperatures for CH_4 production, we used only data between 16–48°C, when fitting curves. The nature of the measured CH_4 production at these tail ends of the temperature range may be indicative of something other than the biologically mediated reaction represented by MMRT (Hobbs *et al.*, 2013). Finally, the first derivative of each fitted curve was used to determine T_{opt}, while the second derivative was used to calculate T_{inf}.

Pair-wise comparisons between temperature response parameters T_{opt}, T_{inf}, ΔC_p, ΔH, and ΔS were tested using Tukey's Honest Significant Difference (HSD) test. The comparisons tested for significant differences (critical value used for alpha = 0.05) in production between the different vegetation types.

4.4 Results

4.4.1 Climate and hydrological conditions

Sampling commenced on 29 October 2020 and finished on 13 May 2021. This period (outlined between the red lines in Figure 4.2 Time series of daily mean air and soil temperatures (blue and red lines, respectively) for Kopuatai (a) and the drained peat site (b), and daily mean water table depth (WTD, blue lines) and daily total rainfall (black bars) for Kopuatai (c) and the drained peat site (d), between 1 July 2020 to 30 June 2021. Note the sampling period (29 October 2020-13 May 2021) within vertical red lines experienced the lowest water table depths and the highest temperatures for the year. During the sampling period, mean daily soil temperature ranged between 10.4–17.1°C for Kopuatai at –10 cm depth, compared to 13.6–25.1°C for the drained peat site at –20 cm. The relationship between soil and air temperature

followed a similar pattern. However, a striking difference between the two sites is that air temperature generally exceeded peat temperature at Kopuatai, whereas the opposite was true for the drained site. Daily mean air temperature at the drained peat site ranged between 6.2–22.3°C across the study period and very rarely exceeded the soil temperature (Figure 4.2a: Kopuatai; Figure 4.2c: drained peat site). Air temperature at Kopuatai ranged between 5.5–21.7°C, similar to the drained peat site temperatures. However, peat temperature was generally lower than the air temperature. Increases in daily mean WTD were associated with rainfall events. Daily mean WTD ranged between –5.25 to –2.51 cm beneath the peat surface at Kopuatai and between –33.8 to –109.3 cm below the peat surface at the drained peat site (Figure 4.2b: Kopuatai; Figure 4.2d: drained peat site).

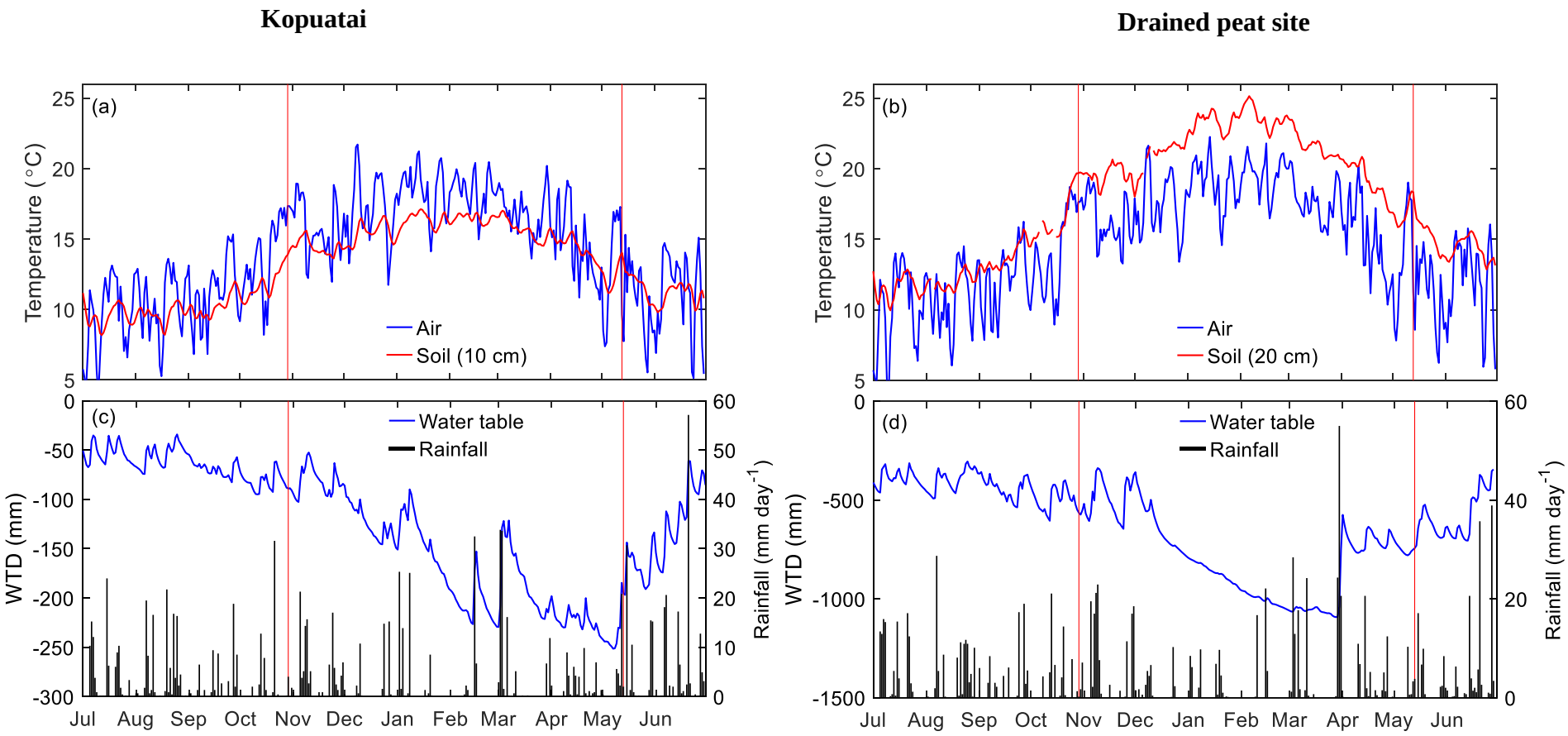

Figure 4.2 Time series of daily mean air and soil temperatures (blue and red lines, respectively) for Kopuatai (a) and the drained peat site (b), and daily mean water table depth (WTD, blue lines) and daily total rainfall (black bars) for Kopuatai (c) and the drained peat site (d), between 1 July 2020 to 30 June 2021. Note the sampling period (29 October 2020-13 May 2021) within vertical red lines and the differences in WTD scales in (c) and (d).

4.4.2 Depth profiles of CH_4 and CO_2

We collected soil samples from both the intact and drained sites from varying depths down to 50 cm and 100 cm, respectively, and incubated these anaerobically at 19°C. We did this to characterise the two ecosystems and to compare the differences in the magnitude of anaerobic CH_4 and CO_2 production at each site. The magnitude of C-GHG production was very different between the two sites, particularly for CH_4 production. There was a negative relationship between anaerobic CO_2 production and depth for both intact and drained sites (Figure 4.3b and d), with the highest CO_2 production rates at the surface. On the other hand, CH_4 production peaked at 30 cm and 80 cm for the intact (Figure 4.3a) and drained (Figure 4.3c) sites, respectively.

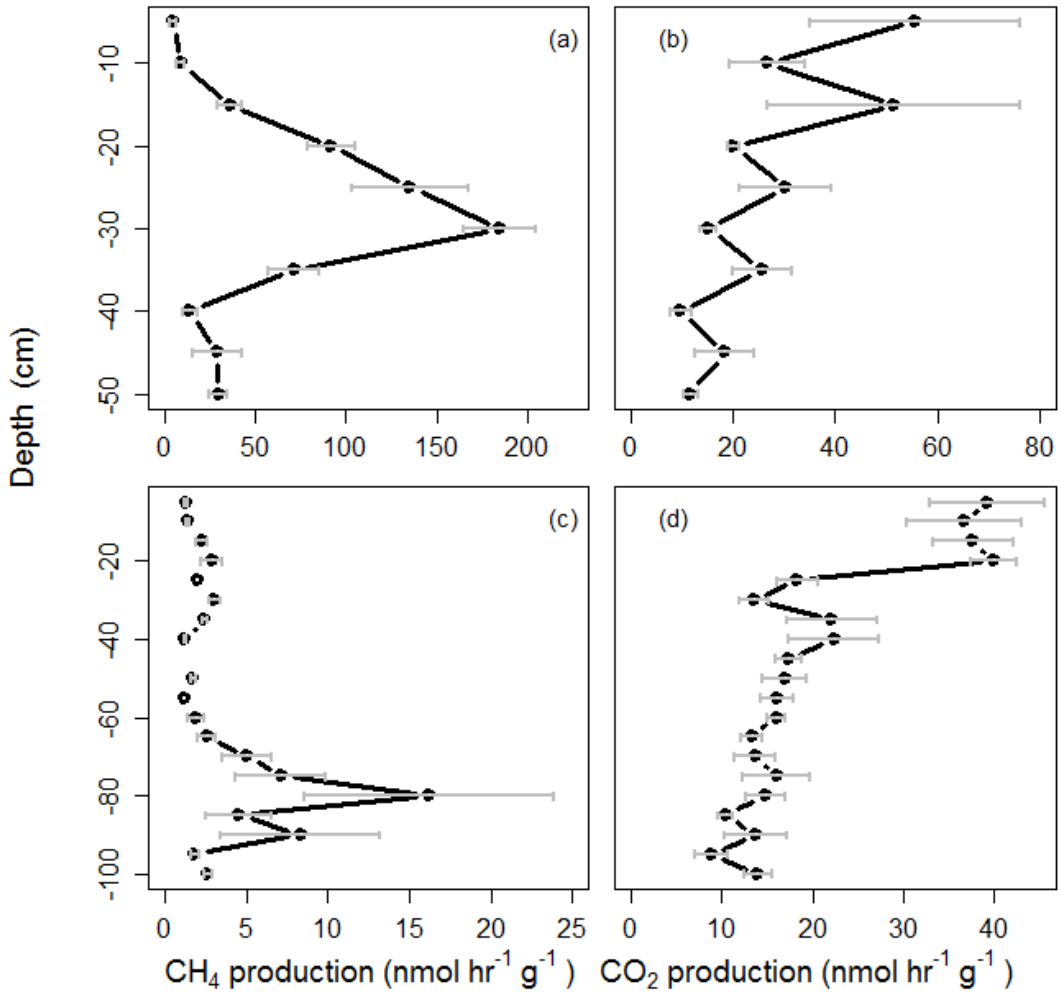

Figure 4.3 Gas production versus depth profiles for Kopuatai (sampled at Site IE) for (a) CH_4 and (b) anaerobic CO_2, and for the drained site (Site DP) for (c) CH_4 and (d) anaerobic CO_2. Bars represent ±1 standard deviation. Note differences in depth scales for Kopuatai (top panels) and the drained site (bottom panels) and note differences in production rate (x-axis) scales in every panel.

4.4.3 Temperature dependence of CH_4 production

All samples from the intact peatland incubated in the temperature gradient block were collected between 5 and 20 cm depth unless specified otherwise. This peat depth was based on ecosystem-scale data of maximum CH_4 flux from Goodrich *et al*. (2015). The temperature response of peatland CH_4 production was captured from three different vegetation types that are characteristic of intact peatlands in New Zealand (*E. robustum*-Site IE, manuka-Site IM, and sedge-Site IS) and one drained peat site with pasture (Site DP). Peat soil from DP was sampled between 5–20 cm depth. For each site, the production rates increased rapidly with temperature before reaching an optimum value (T_{opt}), after which production declined equally rapidly (Figure 4.4). Triplicates for each of the 18 set temperatures were averaged to account for variability and at least three sets of incubations were undertaken for each site to account for variability within the sites.

The CH_4 temperature responses of different vegetation types found in the intact site and the drained site all have similar curvature. Site IE samples had the highest production rates, while there was surprisingly little difference in rates among samples from Sites IS, IM, and DP. The sudden peak and collapse in CH_4 production rates between 17 and 45°C (most obvious in Site IE) shows that CH_4 production is tightly constrained within these temperatures.

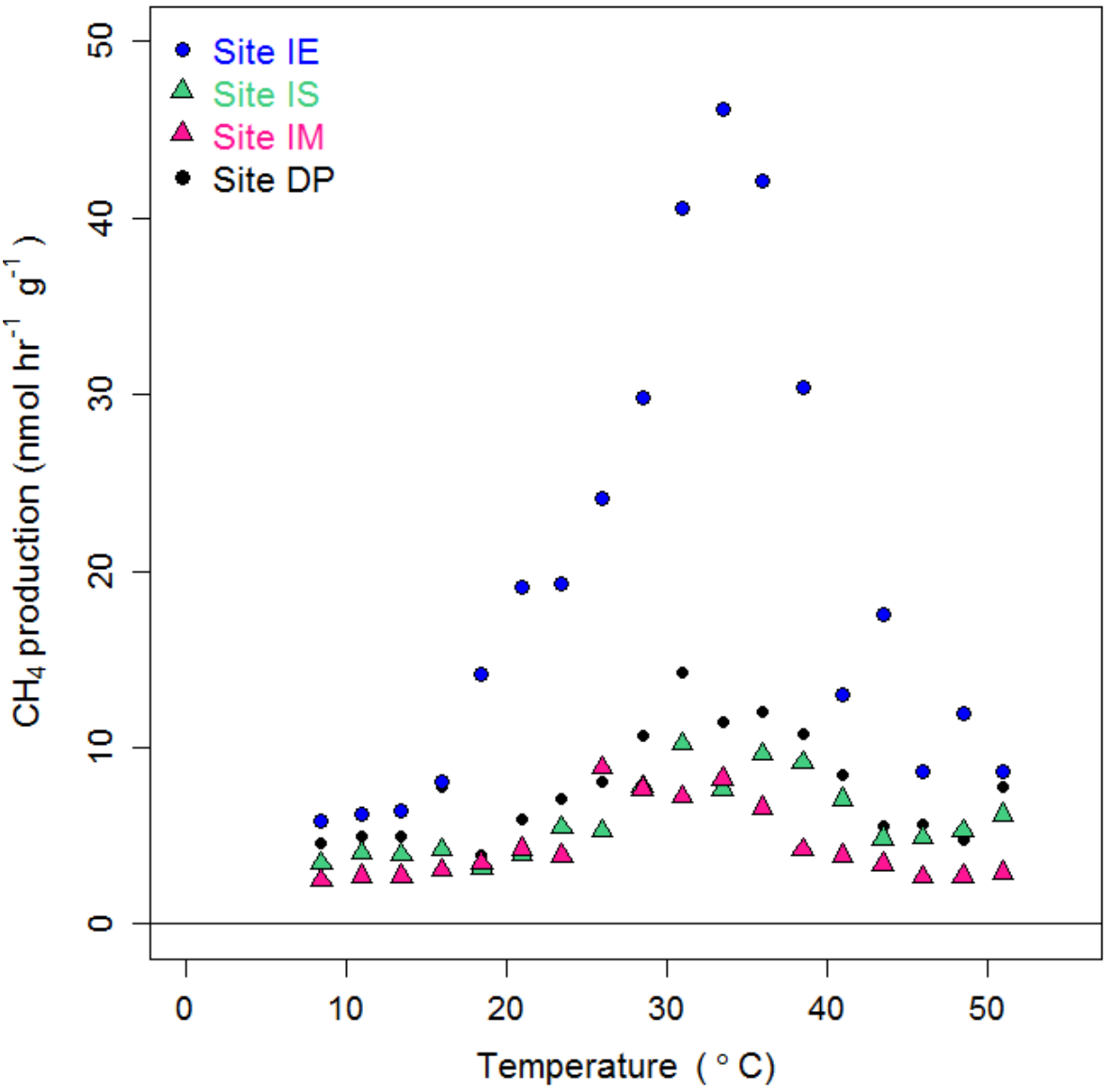

Figure 4.4 Temperature response of CH_4 production from incubations comparing peat from a drained site (DP) to production from three sites within an intact peatland (IE, IS, IM). Results averaged from 3+ site sampling dates at each site and averages of triplicates per run.

The mean and standard deviation of CH_4 production rate for the data shown in Figure 4.4 is represented in Figure 4.5. For each site, the average of three replicates per temperature is plotted for the three or more incubations performed on each peat type. There is a positive relationship between CH_4 production and standard deviation, and the points diverge as temperature increases. The highest production rates tend to have the highest standard deviation, suggesting that variation increases as the CH_4 production rate increases.

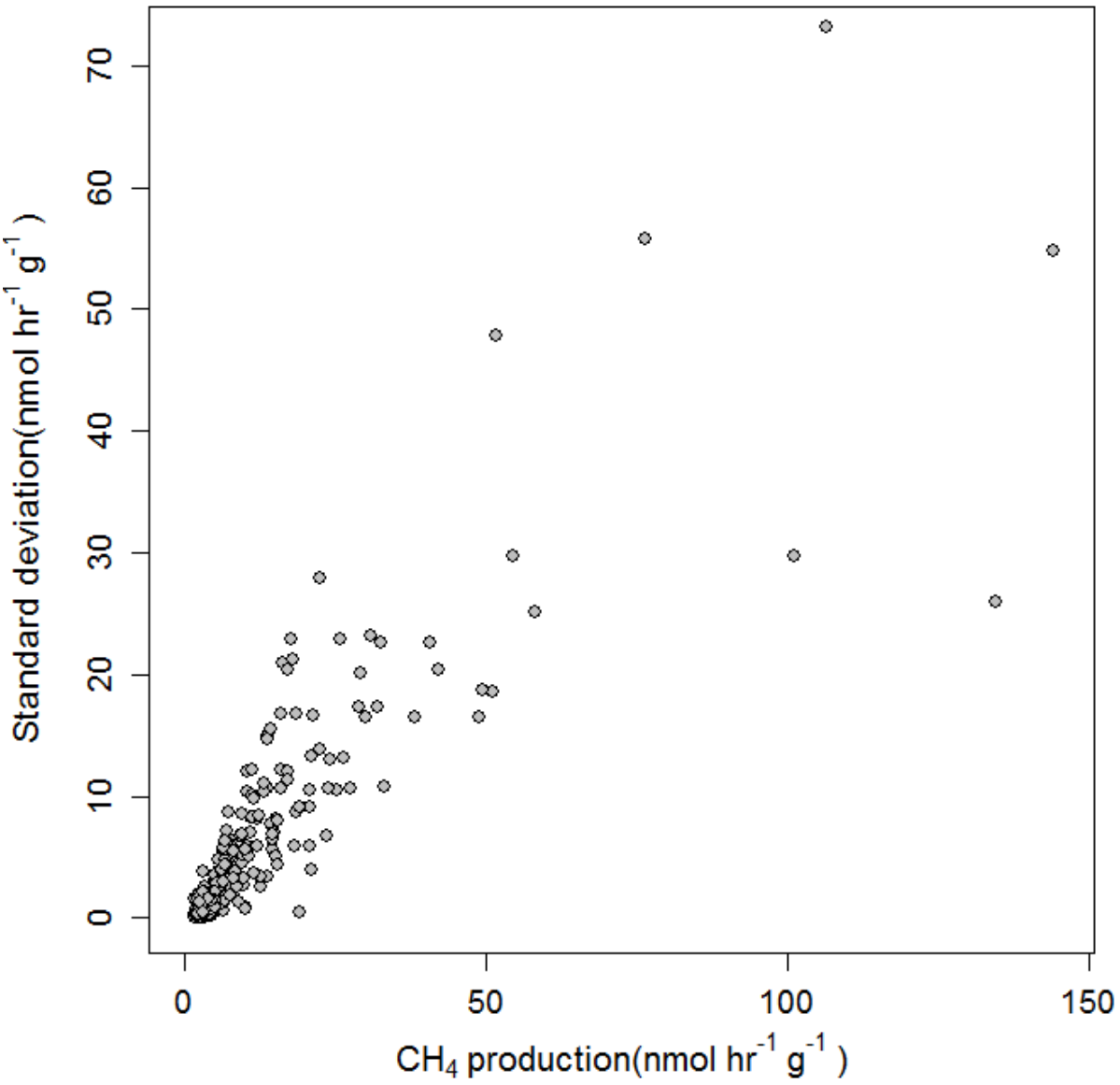

Figure 4.5 Variation in CH_4 production rates, shown as the mean production rate of three replicates for each incubation on the temperature block (averaged in Figure 4.5) versus the standard deviation of those three replicates for each site and all of the runs conducted.

To fit MMRT to the CH_4 production rate results from each site, production rates were standardized between zero and one to capture the shapes of the temperature response curves, irrespective of differences in magnitude across sampling sites and dates (Figure 4.6). Throughout the sampling period, we sampled peat from each site and incubated these samples in the temperature block, at least three times. The data plotted for each site include these three sets of 18 incubation temperatures and each point represents the average of three replicates at each of those temperatures. The curve was fitted using points between 16°C and 48°C and all points outside of this range were excluded from the fit (grey points). This was because lower

and upper values distorted the overall fit by flattening the curve and failing to capture the steepness of the peak (see Appendix Figure A1 for failed MMRT fits for temperatures fitted between 8.5–51°C).

All four sites exhibited curvature that could be fitted using MMRT and we were able to derive T_{opt} and T_{inf} from the MMRT equation. Each site had large negative changes in heat capacities (ΔC_p), ranging between –13312 to –17776 J mol^{-1} K^{-1} (

Table 4.1) indicative of the steep curvature illustrated in Figures 4.6 & 4.7. All the T_{opt} and T_{inf} values were within 2.7°C and 2.3°C of each other, respectively. Site IE samples had the lowest T_{opt} (30.1°C) and T_{inf} (23°C), while Site DP had the highest (T_{opt} 32.8, T_{inf} 25.6). A Tukey's HSD test revealed there were no significant differences between any of the parameters from the different peat types, or if there were differences, they were smaller than our data were able to detect (Appendix Table A1). This suggests the temperature response of CH_4 production is similar among the sites. MMRT was best fit to Site DP (RMSE = 0.59), while Site IM had the worst fit (RMSE = 0.85) (Table 4.2).

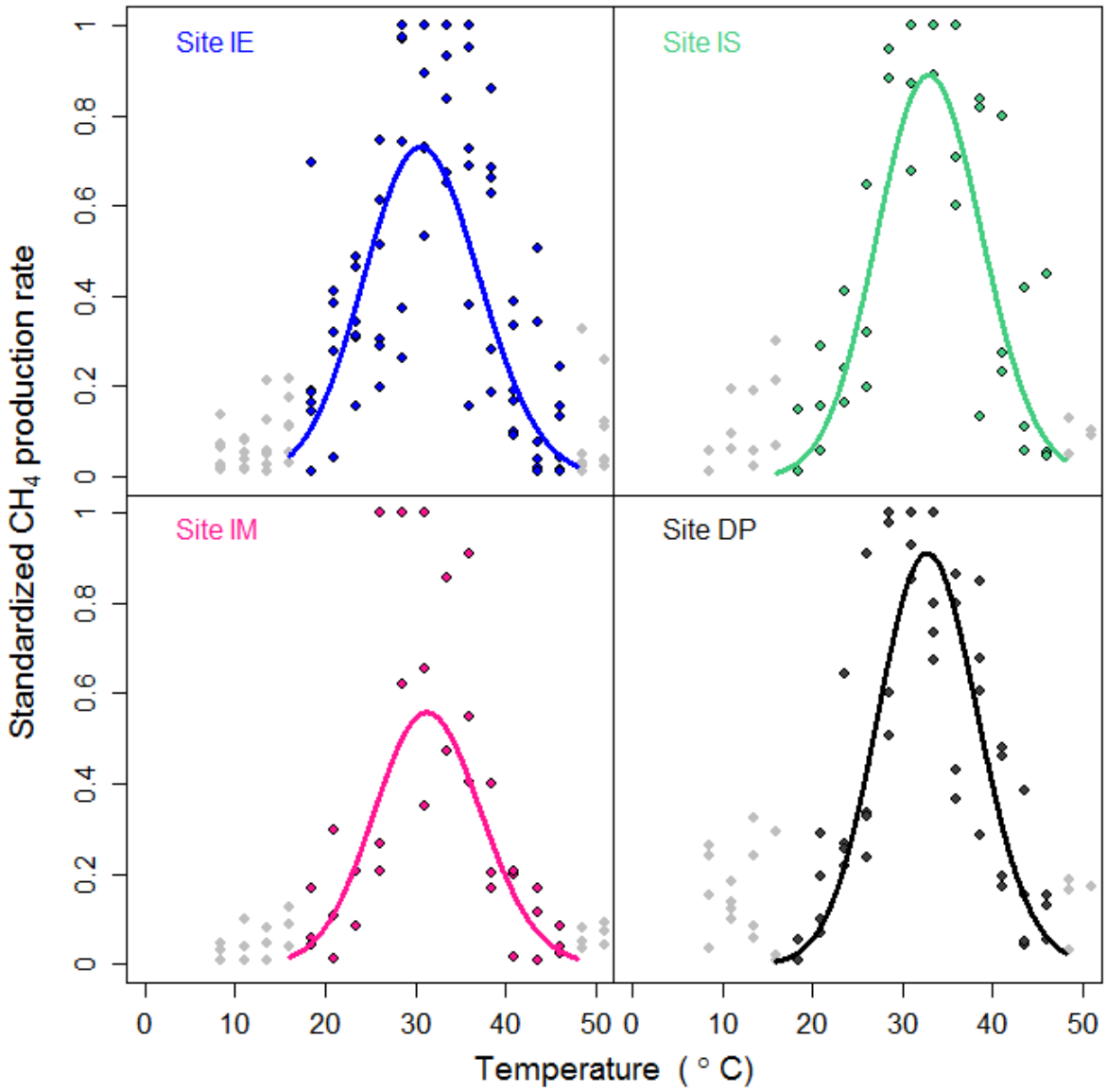

Figure 4.6 The fit of the MMRT equation to CH_4 production rates vs. temperature for a drained site (DP) and from three sites within an intact peatland (IE, IS, IM). Curve fit between temperatures 16–48°C.

The T_{opt} at each site were similar (Table 4.1), as was the general shape of each curve. Figure 4.7 shows the alignment of the MMRT curves fit to each site. Using Tukey's HSD test, we found that even these two sites with highest and lowest T_{opt} were not significantly different from each other (–2, 7.33 = 95% CI). Similarly, none of the T_{inf} from each site were significantly different. Each curve is noticeably narrow and steep, which represents how constrained the highest CH_4 production rates are between 16–48°C. Sites IS and DP appeared to be the most tightly constrained (ΔC_p –9379, 18043 = 95% CI), however, none of the ΔC_p values were significantly different among sites.

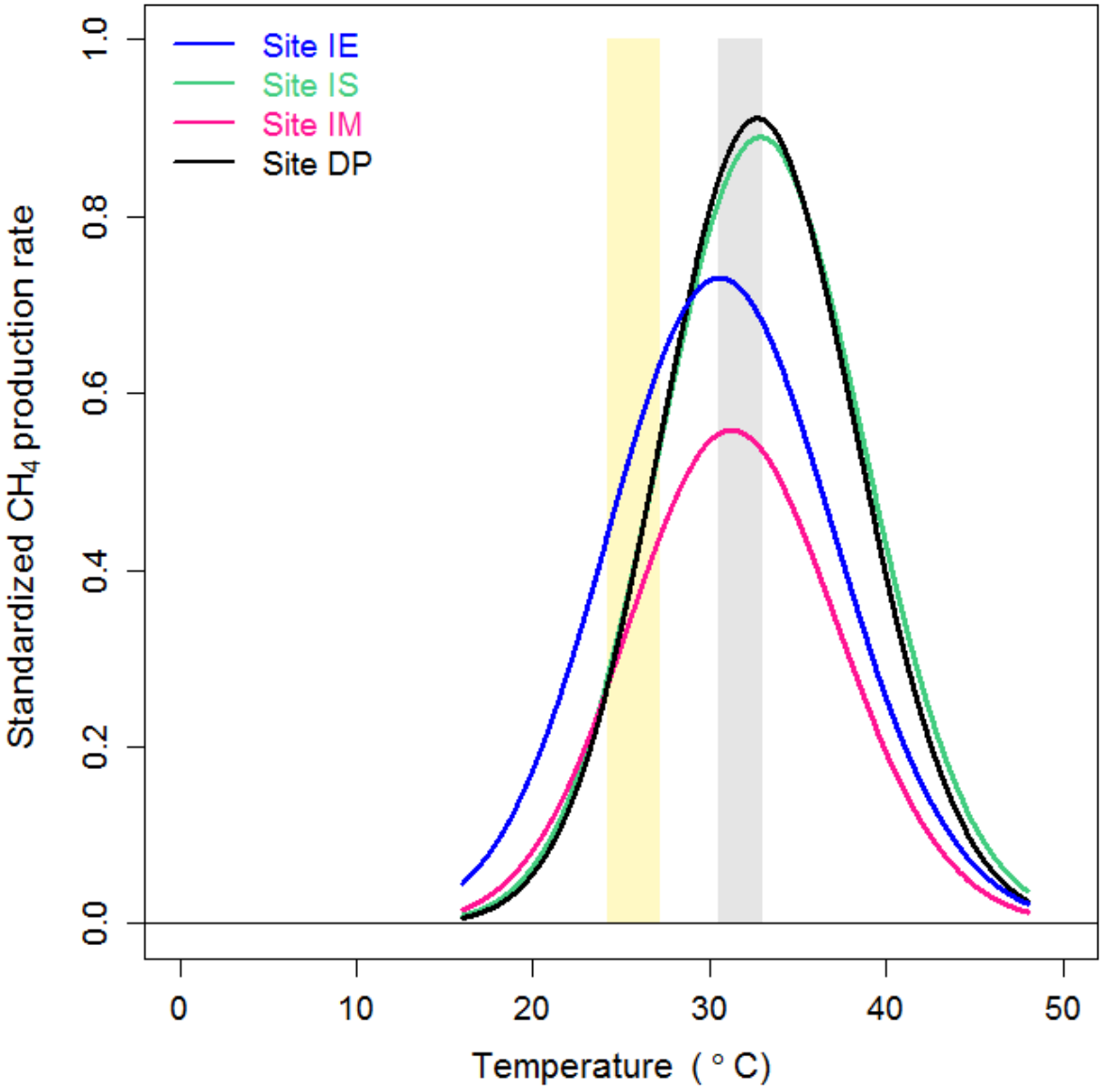

Figure 4.7 Comparison of the temperature response of CH_4 production rates vs. temperature for a drained site (DP) and three sites at an intact peatland (IE, IS, IM). Curves were fit between temperatures 16–48°C and the ranges for the T_{opt} and T_{inf} points across sites are represented by the grey and yellow bands, respectively.

Table 4.1 Fitted parameters from MMRT for CH_4 production (Eq. 4-1), and the derived metrics T_{opt} and T_{inf} associated with each fit for the four sampling locations.

Sampling location	T_{opt}°C	T_{inf}°C	$\Delta C_p^{\ddagger}$ J mol^{-1} K^{-1}	$\Delta H_{T_0}^{\ddagger}$ J mol^{-1} K^{-1}	$\Delta S_{T_0}^{\ddagger}$ J mol^{-1} K^{-1}
Site IE	30.1	23.3	–17776	–3575	–259
Site IM	30.4	23.7	–16979	7473	–227
Site IS	32.5	24.8	–13312	3416	–137
Site DP	32.8	25.6	–17644	34213	–135

Figure 4.8 shows CH_4 production results alongside data from other studies focussed on the temperature response of CH_4 production from peatlands that also incubated samples across a large temperature range (0–70°C). Values from other publications presented in Figure 4.8 were extracted using DataThief III version 1.6 (www.datathief.org). All the responses followed a similar pattern to our data when standardized between zero and one. All the datasets exhibit a very similar response, including a sharp increase to maximum production values ranging between ~25–35°C, before production rapidly decreased at higher temperatures. The decline in production after the maximum production value is more tightly constrained than the sharp increase before this point.

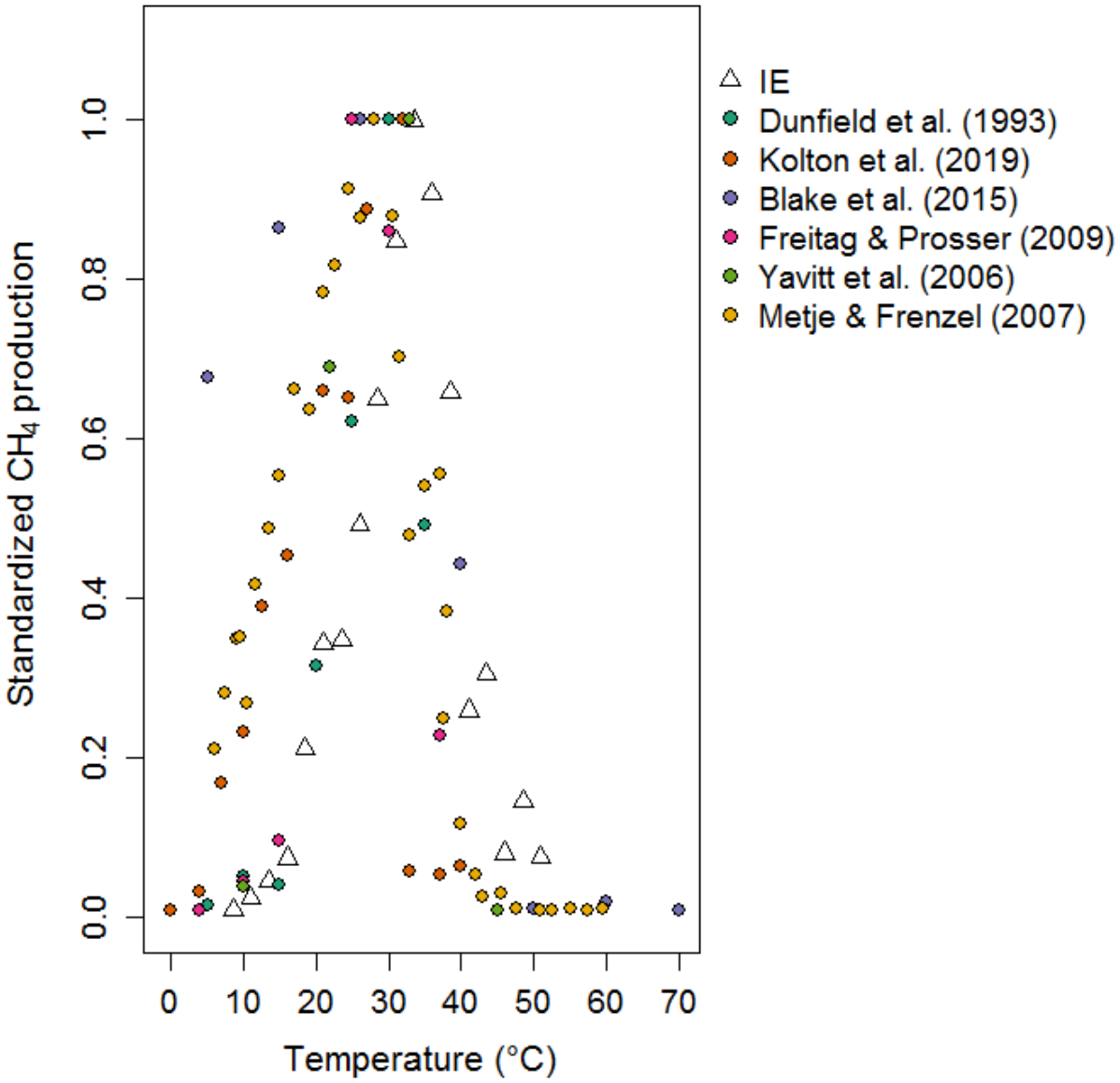

Figure 4.8 Site IE results plotted (triangles) alongside CH_4 production data from peatlands found in the literature where studies included at least four temperatures with a ≥35°C temperature range.

4.4.4 Temperature dependence of anaerobic CO_2 production

CO_2 production rates sharply increased with temperature until reaching an optimum, similar to CH_4 production. However, the response differed to CH_4 in that CO_2 production was an order of magnitude higher on a molar basis and that the decline after T_{opt} was less steep compared to CH_4. Figure 4.9 illustrates the anaerobic CO_2 production rates at each site across a temperature range of 8.5 to 51°C.

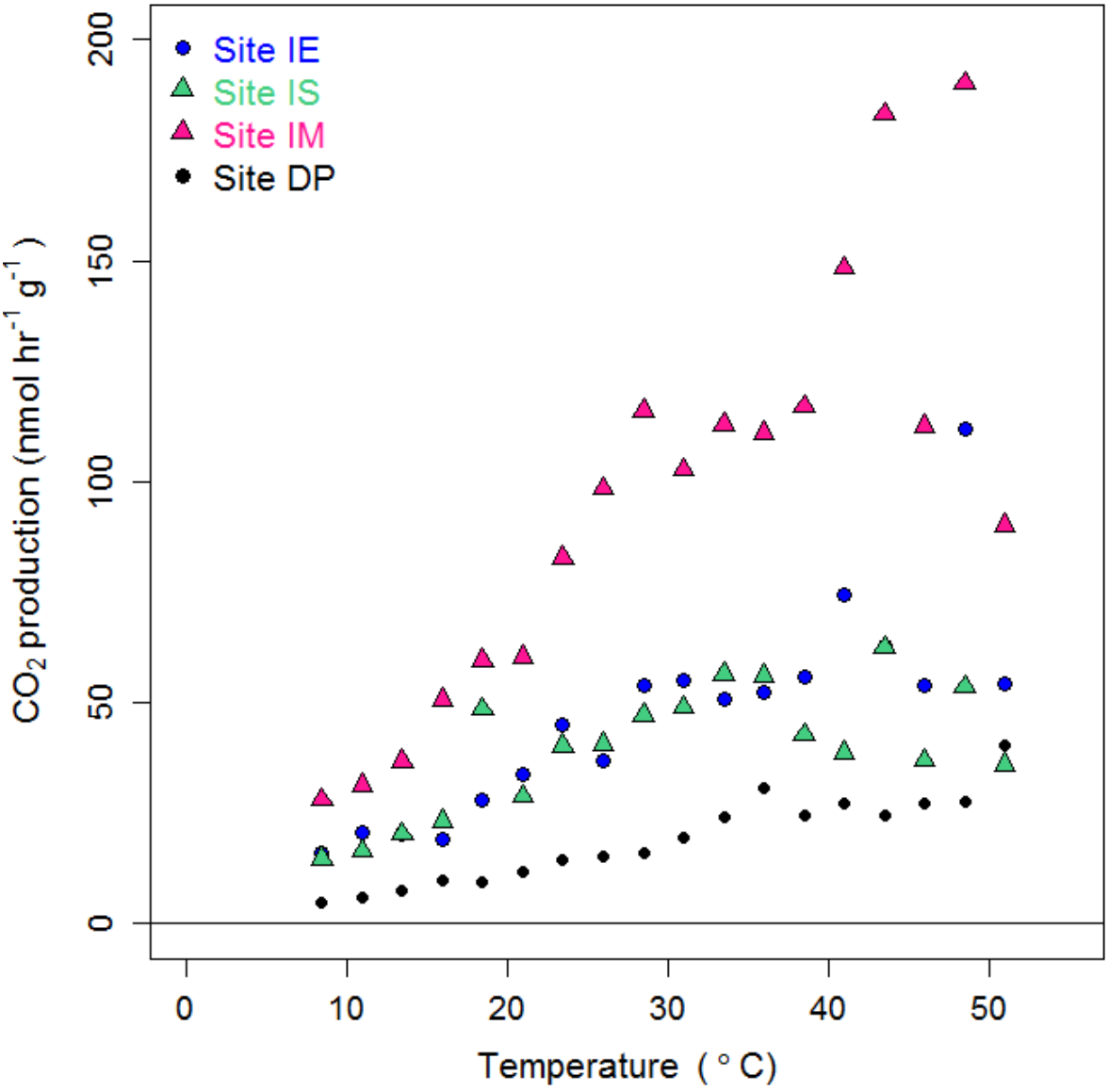

Figure 4.9 Temperature response of anaerobic CO_2 production rates from incubations comparing peat from a drained site (DP) to production from three sites within an intact peatland (IE, IS, IM). Results averaged from 3+ site sampling dates at each site and averages of triplicates per run.

The magnitude of the CO_2 production differed across sites. Site DP had a maximum mean CO_2 production rate of ≤50 nmol hr^{-1} g^{-1}, compared to Site IM, which reached nearly 200 nmol hr^{-1} g^{-1}. Site DP had the lowest production rates across all temperatures, similar to CH_4 production results (maximum CH_4 production rate ≤15 nmol hr^{-1} g^{-1}). At each site, CO_2 production rates increased sharply until ~35–40°C, after which the relationship became unclear. This was unlike the rapid decline in rates associated with CH_4 production at these temperatures.

In order to explain the possible reasons Site DP showed a seemingly linear response, we wanted to explore the impact of adding labile substrates (Appendix Figure A2a), as well as sampling peat from beneath the water table (–100 cm) (Appendix Figure A2b). Results from these tests suggested that production rates for samples collected beneath the water table had no obvious response to temperature and production rates from peat with glucose additions showed a similar response to control samples without added glucose. The rates for Site DP samples collected beneath the water table were relatively high (up to 10 times higher) in comparison to samples collected at 30–35 cm.

MMRT was fitted to the average of triplicates of more than three separate incubations for each site (coloured points, Figure 4.10), as described for Figure 4.6. Unlike for CH_4, where we used a threshold of 16–48°C, we did not exclude any temperatures from the CO_2 fit. CO_2 production was standardized for curve fitting, so the magnitude of the MMRT curves are not reflective of each site. The success of the fit varied among sites, but Site IE had the least successful fit (RMSE = 0.66) in comparison to the IS, IM, and DP sites (RMSE = 0.5, 0.37, 0.43, respectively) (Table 4.2). The T_{opt} values for each site were similar but not as constrained as T_{opt} values for CH_4 production (Table 4.23). Site IS had the lowest T_{opt} for CO_2 production at 35.4°C, followed by Site IM (37.1°C). Topt for Sites IE (40.5°C) and DP (44°C) were higher. Overall, none of the T_{opt} and T_{inf} values were significantly different and were all within 8.6°C and 7.3°C of each other, respectively.

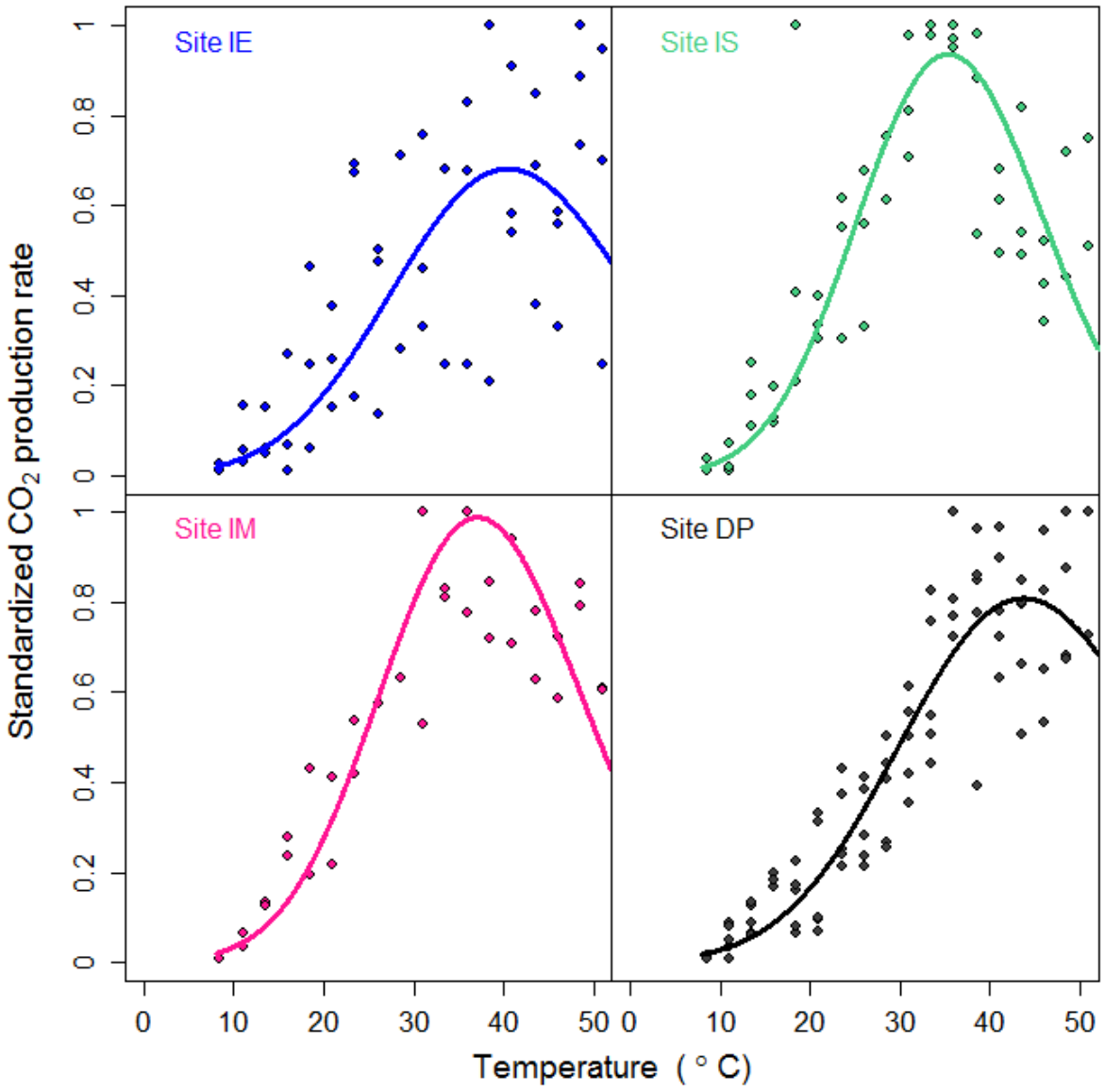

Figure 4.10 The fit of the MMRT equation to anaerobic CO_2 production rates vs. temperature for a drained site (DP) and from three sites within an intact peatland (IE, IS, IM). Curves fit between temperatures 8.5–51°C.

Figure 4.11 shows comparison of MMRT curve alignment and curve characteristics for anaerobic CO_2 production. The T_{opt} values at each site differed (range 8.6°C) more than the T_{opt} values derived from CH_4 production (range 2.7°C). The T_{inf} values for anaerobic CO_2 had a range of 7.2°C between sites. The T_{inf} for Site DP was 32.2°C, 13.3°C lower than T_{opt}, in comparison to Site IM, which had a T_{inf} of 25.9°C, 10.4°C lower than T_{opt}. Despite the differences in T_{opt}, Site IS and IE had similar T_{inf} values of 11.2 and 11.8°C, respectively. The shapes of each curve also showed more variation among sites in comparison to the CH_4 results. Sites DP and IE appear to have wider, shallower curves than IM and IS sites.

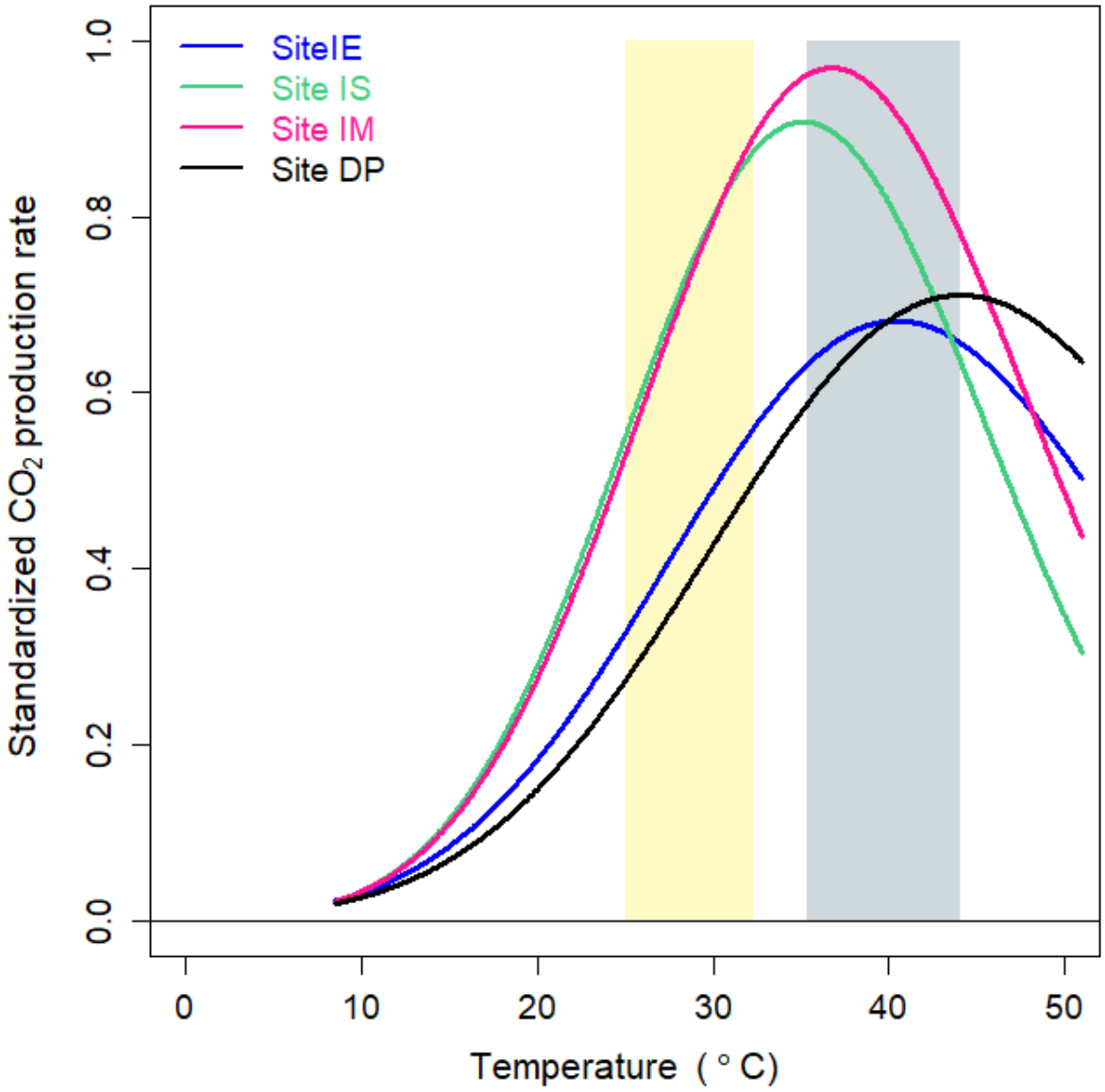

Figure 4.11 Comparison of the fitted temperature response of anaerobic CO_2 production rates vs. temperature for a drained site (DP) and three sites at an intact peatland (IE, IS, IM). Curves were fit between temperatures 8.5–51°C and the ranges for the T_{opt} and T_{inf} points across sites are represented by the grey and yellow bands, respectively.

Table 4.2 Root mean square error (RMSE) for the MMRT functions fitted to anaerobic CH_4 and CO_2 production shown in Figures 4.7 and 4.11.

	CH_4	CO_2
Site IE	0.817	0.660
Site IS	0.718	0.500
Site IM	0.852	0.368
Site DP	0.586	0.433

Table 4.2 Fitted parameters from MMRT for anaerobic CO_2 production (Eq. 4-1), and the derived metrics T_{opt} and T_{inf} associated with each fit for the four sampling locations.

Vegetation	T_{opt}°C	T_{inf}°C	$\Delta C_P^{\ddagger}$ J mol^{-1} K^{-1}	$\Delta H_{T_0}^{\ddagger}$ J mol^{-1} K^{-1}	$\Delta S_{T_0}^{\ddagger}$ J mol^{-1} K^{-1}
Site IE	40.5	27.2	–6576	43794	–106
Site IM	37.1	25.9	–3317	35437	–133
Site IS	35.4	25	–1967	20976	–184
Site DP	44.0	32.2	–2946	43925	–108

4.4.5 Ratio of CO_2:CH_4 production

To assess the partitioning of carbon between CO_2 and CH_4 production under anaerobic conditions, we simultaneously extracted headspace samples for CH_4 and CO_2 from the Hungate tubes during incubation runs. The molar ratio CO_2:CH_4 was plotted against temperature (Figure 4.12). CO_2:CH_4 was generally constant up to ~30°C, apart from Site IE, which showed a decline. The magnitude of this production ratio was highest for Site IM, followed by IS, and finally, DP and IE were approximately the same. This relationship implies that the system became less methanogenic and more dominated by CO_2 above 30–40°C.

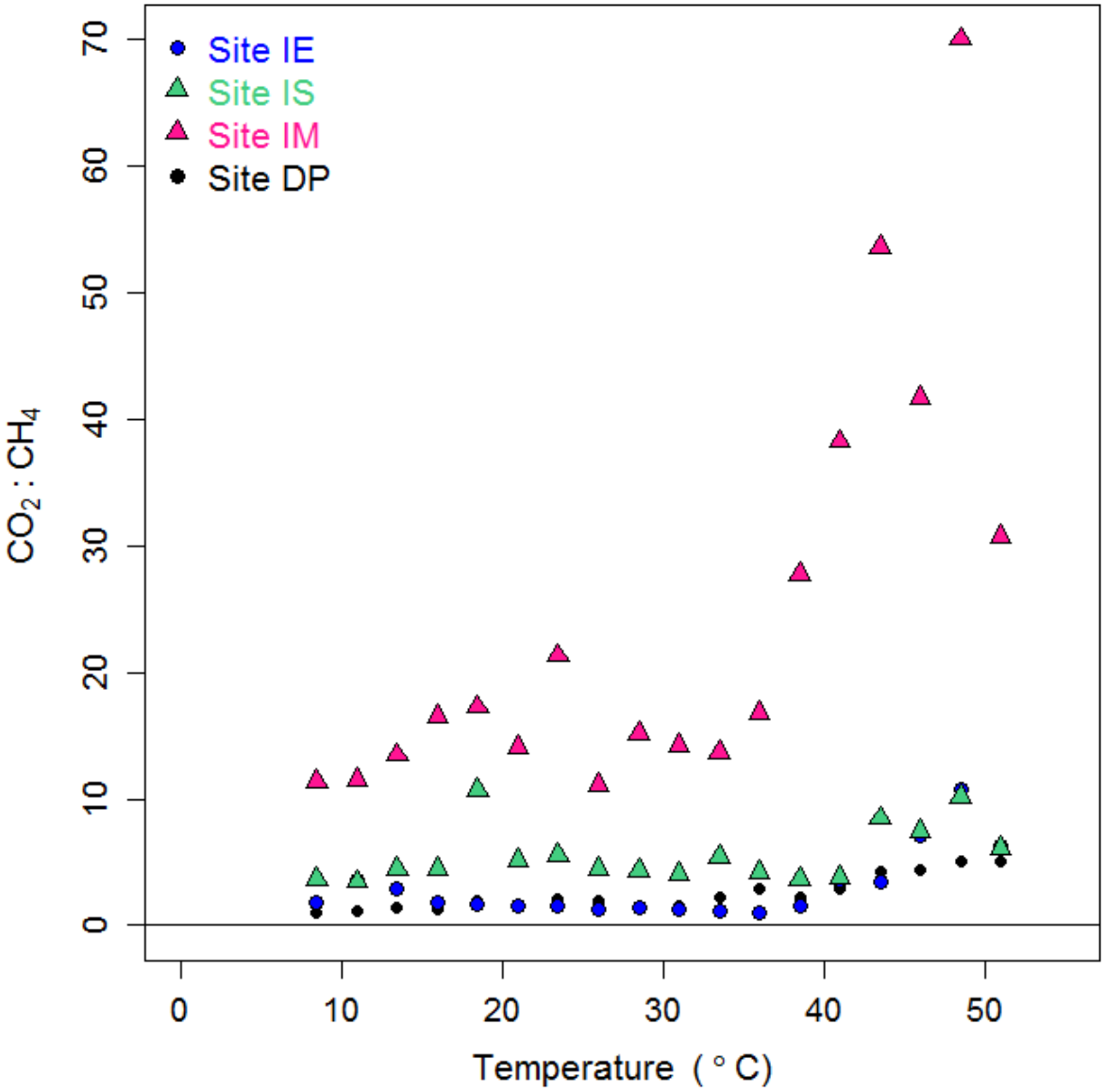

Figure 4.12 Temperature dependence of the anaerobic CO_2:CH_4 production ratio from intact and drained peatlands sites.

4.5 Discussion

4.5.1 Temperature dependence of CH_4 production

Methane production in two New Zealand peatlands were found to have a very constrained temperature response. This is consistent with other studies, demonstrating that CH_4 production rates from peatlands should increase with climate warming to a point (Dunfield *et al.*, 1993; Yavitt *et al.*, 2006; Metje & Frenzel, 2007; Freitag & Prosser, 2009; Blake *et al.*, 2015; Kolton *et al.*, 2019). It is important to understand the response of anaerobic CH_4 production rates across

a wide temperature range for projecting GHG emissions in a changing climate because limiting incubation temperatures below 30°C does not allow for the determination of temperature optima (T_{opt}) or inflection point (T_{inf}) (Schipper *et al.*, 2014).

The curvature of the temperature response was similar for all four sites in this study. Each site had low CH_4 production below 10°C, rapidly increasing in rate until reaching a temperature optima (T_{opt}) at 30.1–32.8°C, before rapidly declining and producing low levels of CH_4 again above 40°C. The temperature response for CH_4 production found in this study was consistent with previous publications from Northern Hemisphere peatlands (Dunfield *et al.*, 1993; Kolton *et al.*, 2019; Hopple *et al.*, 2020). Most temperature response studies agree CH_4 production rates increase exponentially with temperature; however, few studies have incubated soils at temperatures high enough to see the point of decrease in production rates (Bergman *et al.*, 1998; Hargreaves & Fowler, 1998; Treat *et al.*, 2014; Hanson *et al.*, 2016; Wilson *et al.*, 2016a; Hopple *et al.*, 2020). For the studies that have observed the response of CH_4 production from peatlands across a temperature range of ≥35°C, T_{opt} values were within the range 25–35°C (Figure 4.9) (Dunfield *et al.*, 1993; Yavitt *et al.*, 2006; Metje & Frenzel, 2007; Freitag & Prosser, 2009; Blake *et al.*, 2015; Kolton *et al.*, 2019). This is consistent with the T_{opt} values found at each of our sites, which ranged between 30.1–32.8°C and were not significantly different from each other. Because no other studies have used MMRT to describe CH_4 or CO_2 production rates, we are approximating T_{opt} based on the published rates.

Kolton *et al.* (2019) found that the maximum potential CH_4 production rates at 4°C comprised only 1 to 10% of the rates determined at 25 to 30°C. Using the same methodology as Kolton *et al.* (2019), we found this was consistent with our results, which also suggested that at the lowest temperature in this study (8.5°C) the methane production rate comprised 16–42% of the mean rate determined at 26 to 36°C across the four sites. Considering the similarity in T_{opt} and T_{inf} across sites, the process of methanogenesis seems to be relatively conservative, and based on the overlapping 95% confidence intervals (Appendix Table A.3), we found there were no significant differences among sites. On the other hand, the variability in CH_4 production rates within sites is reflected in the relatively large 95% confidence intervals on the temperature response metrics (Appendix Table A1) despite the convergence of the standardized responses. Using chemical analysis of soil and pore water samples and understanding differences in vegetation characteristics would help provide a better basis for explaining the connection between vegetation type and CH_4 production.

Our results suggest that the temperature range for highest methanogen activity at our sites was between ~15–45°C for Site IE, which was wider than IM, DP, and IS sites (~20–43°C). T_{opt} values within 20–30°C are considered to be a mesophilic response, which was expected because the study sites all represent a temperate peatland (Tveit *et al.*, 2015; Kolton *et al.*, 2019). On the other hand, while comparing other studies that have quantified CH_4 production across a large temperature range (Figure 4.9), Blake *et al.* (2015) and Metje and Frenzel (2007) also found a T_{opt} at ~30°C despite sampling from permafrost soil. The other Northern Hemisphere sites that have quantified CH_4 production across a large temperature range (Figure 4.9), were located in Northern U.S.A., Canada, and the U.K., and are also temperate but may be subject to extreme seasonal changes, unlike the year-round growing season experienced at Kopuatai (Goodrich *et al.*, 2017). Despite these latitudinal differences and bearing in mind these data were standardized for visual comparison purposes, the response of CH_4 to temperature was very similar when comparing our results to these Northern Hemisphere sites, particularly the T_{opt} range (~25–35°C). Yavitt *et al.* (2006) found that methanogens from three peatland types all had temperature optima close to 35°C, and suggested this response is typical of methanogenesis even in soils that experience prolonged cold temperatures. The low production below 10–15°C found for Site IE was also found for Yavitt *et al.* (2006) and Dunfield *et al.* (1993), in comparison to the production from the other sites in Figure 4.9, which had relatively high production. These results suggest that multiple peat systems throughout the Northern Hemisphere show similar CH_4 rates to our study sites, which could have implications in terms of modelling this response across multiple ecosystems. On the other hand, methanogen populations sampled from a slurry, rice paddy soils, and lake sediments showed similar T_{opt} values (33–37°C, 32–41°C, and 34°C respectively) (Schulz *et al.*, 1997; Yao & Conrad, 2000; Hamilton, 2010; Elsgaard *et al.*, 2016). Considering the lack of variability in the response among these ecosystems, it is not surprising that our sites, located within the same region, show a high degree of similarity. This information points towards the idea of a 'global' methanogenic temperature response.

Despite differences in vegetation, the microbial response was relatively conserved across all sites in this study. This suggests that, in this case, environmental conditions across sites are not sufficiently different to support a different response or that the intrinsic genetic response of microbes is unchanging despite changing environmental conditions. The mesophilic temperature optima found at each of our sites suggests the microbial communities within these environments must all be mesophilic and that psychrophilic or thermophilic microbial

populations did not exist or were inactive during our experiments. T_{opt} values within this range are fairly consistent with results across research into peatland temperature response, however, some non-peatland environments, for example, flooded soils, can also produce CH_4 at elevated temperatures up to about 50°C (Yao & Conrad, 2000; Deng *et al.*, 2019). Temperature affects both the rate and pathway of CH_4 production by changing the activity and abundance of individual microorganisms, however, Glissman *et al.* (2004) found that changes in temperature primarily affected the activity rather than the structure of the methanogen community. The phylogenetic composition of methanogenic archaea changes as temperatures rise above 30°C and further shifts as temperatures rise above 40°C (Glissman *et al.*, 2004). Not only do archaeal communities shift around these temperatures, but bacterial communities involved in upstream processes leading to methanogenesis have also been shown to undergo structural changes between 35–45°C (Glissman *et al.*, 2004). This is an important consideration in determining the overall CH_4 production rate (Hamilton, 2010). In addition, Deng *et al.* (2019) suggested that changes in temperature elicit thermodynamic changes in microbial activities, which is an important consideration when choosing equations to model this response.

Consistent with our results, previous studies have also found low or no CH_4 production at temperatures below 10°C and above 40°C. Dunfield *et al.* (1993) also found that low temperatures produced very low rates of CH_4 production and that this may be an effect of hydrogen-producing bacteria, also perhaps in addition to an effect on the methanogens themselves (Dunfield *et al.*, 1993). In our results, there was no evidence of microbial populations adapted to low temperatures being present as the optima were in the range of 20–30°C; however, it is not known which microorganisms are responsible for the observed responses at our study sites.

At the other end of the temperature response, we observed a rapid decline in CH_4 production rate above the T_{opt} for all sites. The thermal response tended to decline sharply from the optimum range to what has been described as the "maximum tolerable temperature" (Hamilton, 2010; Deng *et al.*, 2019). Hamilton (2010) suggested that maximum tolerable temperatures are often referred to as temperatures at which an organism can no longer function, however, the T_{opt} are generally well below these tolerances. The rapid decline in production rate is consistent with results from previous studies across a large temperature range, which link the decrease to a decline in microbial diversity (Dunfield *et al.*, 1993; Kolton *et al.*, 2019). At high temperatures (≥30°C), Hamilton (2010) suggests differences in temperature optima affect competitive dynamics between species, and often diversity drops above 35°C. Moderate

temperature increases can produce unexpectedly large reductions or shifts in microbial composition and diversity, with unknown biochemical complications (Hamilton, 2010). In this study, we did not perform DNA or RNA sequencing to determine the microbial populations present. However, some studies have used these techniques to explain this commonly observed rapid decline in production post-T_{opt}. Kolton *et al.* (2019) used assays to conclude that microbial diversity slowly declined with increasing temperature and, after 30°C, no DNA sequences associated with methanogens were detected. Moreover, Deng *et al.* (2019) also found methane production rates increased between 10–30°C, but at 45°C, CH_4 production was negligible, and bacterial and archaeal ribosomal RNA decreased with incubation time, indicating inactivation or death of methanogens. This suggests that at these elevated temperatures, the microbial communities reach a threshold where they can no longer cope with further warming. Alongside this, the exposure to these elevated temperatures for extended incubation periods could be contributing to the low production rates and microbial diversity in these studies (Deng *et al.*, 2019; Kolton *et al.*, 2019). These results may not be relevant for our study considering our short incubation lengths. Alternatively, declines in CH_4 production after the T_{opt} could be a function of the change in the heat capacity between the enzyme-substrate and the enzyme-transition state complexes as predicted by MMRT (Hobbs *et al.*, 2013; Prentice *et al.*, 2020).

During our incubations, methane concentration increased linearly each day, implying the production rate was constant for the duration of the incubation (four days), however, after this time, production rates declined. This decline may be indicative of another process (e.g., CH_4 consumption) or some sort of methodological issue (e.g., gas leaking from Hungate tubes). Either way, incubation duration should be factored into temperature response studies, as it may be a confounding variable. Bergman *et al.* (1998) found that, after a three-week incubation, CH_4 production rates decreased with increased incubation temperature and suggested that samples conditioned at higher temperatures became more substrate-depleted than those at low temperatures. Overall, the negative relationship between temperature increase and microbial diversity evident from the literature has potential implications for climate warming. The exposure of peatland ecosystems to climate change perturbations may lead to microbial diversity loss and a shift in species composition and functional diversity, which may impact overall ecosystem function (Kolton *et al.*, 2019). As demonstrated in Kolton *et al.* (2019) and Deng *et al.* (2019), the use of genetic sequencing could help identify specific microbial populations present in the peat at each of our sites. This would better inform us on whether

differences in magnitude between sites are due to larger community sizes or that microbial activity is increased.

Methane production is usually the result of a mixture of acetoclastic and hydrogenotrophic methanogenesis. Deng *et al.* (2019) suggested that temperature changes cause a shift between pathways for methanogenesis. Contribution from the latter pathway has been found to increase gradually with increasing temperature, supposedly caused by a gradual shift in thermodynamics favouring H_2 production by fermenting bacteria (Glissman *et al.*, 2004; Deng *et al.*, 2019). Previous studies on lake sediments and rice paddies have found the relative contribution of hydrogenotrophic methanogenesis decreased with decreasing temperature and these soils produce CH_4 exclusively via hydrogenotrophic methanogenesis above 40°C (Schulz *et al.*, 1997). The sharp decline in production after 30–35°C for sites in our study suggests that thermophilic methanogens were not present (Glissman *et al.*, 2004; Conrad, 2020). On the other hand, acetogenic bacteria are stimulated at low temperatures, while hydrogenotrophic methanogenesis is suppressed. A possible explanation for acetogenic bacteria being more active than methanogenic archaea at low temperatures could be based on different membrane structures. Bacteria membrane structures (ether lipids) are more flexible than archaean membrane structures (ester lipids) at low temperatures (Conrad, 2020). Another reason acetoclastic methanogenesis may be favoured at low temperatures could be the thermodynamics of H_2 production. The production of H_2 becomes less exergonic as temperature decreases, producing less H_2 (Conrad, 2020). The low production rates at low temperatures recorded in our study suggest there may be no psychrophilic acetogenic microbial populations present. Deng *et al.* (2019) found over 70% of CH_4 was produced via the acetoclastic pathway between 10–30°C, however, hydrogenotrophic methanogens were dominant (82%) at 45°C, leading to an accumulation of acetate. The percentage of hydrogenotrophic was 23% at low and moderate temperatures, close to the theoretical 33% constrained by the stoichiometry of conversion processes. Meanwhile, there was a lack of acetoclastic methanogens at 45°C, consistent with the decrease in pH and accumulation of acetate at this temperature (Deng *et al.*, 2019). Consistent with these results, Kolton *et al.* (2019) failed to sequence any acetoclastic methanogens across a temperature range of 4–40°C. Hydrogenotrophic methanogens may also be outcompeted by functional guilds that can consume H_2 at 3–10 times the rate of methanogens under low temperatures (Bergman *et al.*, 1998; Kolton *et al.*, 2019).

Variability in CH_4 production showed a positive relationship with increased production rate. The highest production occurred between 30–40°C for each site, suggesting these temperatures exhibit the most variability. Higher temperatures cause increased microbial enzyme activities and fermentation of associated by-products. Methane production depends on the quality and the amount of bioavailable C substrate as methanogens utilize some of these fermentation products (e.g. acetate, hydrogen, and methyl compounds) (Inglett *et al.*, 2012). Constraining an accurate response within this temperature range is important because this temperature range contains the T_{opt}, a valuable parameter for understanding temperature response curvature and use in modelling. As found from a number of studies, variability in CH_4 production rates tends to be the rule rather than the exception (Zalman *et al.*, 2018), while the reason for greater variability at high temperatures is poorly understood. Increased variability in CH_4 production with increasing temperatures was found by Hopple *et al.* (2020), Kolton *et al.* (2019) and, Dunfield *et al.* (1993) based on the spread of plotted points or the length of standard error bars. More data are needed to constrain the temperature dependence of anaerobic respiration in wetland soils using lab incubations to interrogate differences in temperature ranges and incubation times.

Optimum temperature for soil microorganisms is generally much higher than temperatures found *in situ* (Deng *et al.*, 2019). This was apparent at our sites as T_{opt} values in our study did not correlate with maximal CH_4 fluxes measured at the ecosystem scale (Goodrich *et al.*, 2015). The CH_4 production rates at environmental temperatures observed between 8–18°C (typical environmental temperatures *in situ*, Goodrich *et al.* 2015) were only 13–46% of the peak production rate at T_{opt} (Figure 4.5). The *in situ* temperatures observed at Kopuatai during the sampling period were similar (10.4–17.1°C) to those of Goodrich *et al.* (2015). The misalignment in maximum CH_4 production detected at the ecosystem scale compared to the soil community scale may relate to scaling discrepancies. For example, Prentice *et al.* (2020) found T_{inf} for enzymes (37°C) aligned with the community T_{opt} of soil production. The T_{inf} of microbial communities in soil may therefore align with the T_{opt} of environmental temperatures that includes a host of other processes including respiration rates from all other organisms at this scale. However, it is difficult to extrapolate due to a host of other processes and spatial heterogeneity (Bridgham *et al.*, 2013; Kolton *et al.*, 2019) The higher end of the *in situ* temperatures ~18°C was ~5–9°C below T_{inf} points at the Kopuatai sites (23.3–24.8°C). Maximum *in situ* temperatures for Site DP (drained site) during the sampling period (25.1°C) was ~7°C lower than T_{inf} (32.2°C). The CH_4 production rates at the environmental temperatures

observed at Site DP (13.6–25.1°C) comprised 53% of the peak production rate at T_{opt} (Figure 4.5).

As demonstrated in Figure 4.2, peat temperature is generally lower than the air temperature at Kopuatai, while the opposite is true for the drained site. This is interesting considering the drained site has an almost identical climate and similar CH_4 production temperature responses, yet production at *in situ* temperature is likely to be higher (and shifted to the right in the production versus temperature curve) in comparison to Kopuatai sites.

4.5.2 Temperature dependence of anaerobic CO_2 production

Studies on the temperature response of anaerobic CO_2 production from peat soils are surprisingly limited (Tfaily *et al.*, 2014; Treat *et al.*, 2015; Tveit *et al.*, 2015; Wilson *et al.*, 2016b; Kolton *et al.*, 2019; Schädel *et al.*, 2020). These studies have been mainly focused on CH_4 production despite anaerobic CO_2 often being the dominant gaseous end-product (Updegraff *et al.*, 1998).

From the few existing published studies, the temperature response of anaerobic CO_2 production appears to have been variable and inconclusive (Yao & Conrad, 2000; Metje & Frenzel, 2005, 2007; Sjögersten *et al.*, 2018; Kolton *et al.*, 2019). The majority of previous studies observed exponential increases in CO_2 production over the given range of incubation temperatures (Waddington *et al.*, 2001; Glissman *et al.*, 2004; Treat *et al.*, 2014; Hanson *et al.*, 2016; Wilson *et al.*, 2016b; Deng *et al.*, 2019; Hopple *et al.*, 2020; Liu *et al.*, 2021). However, few of these studies incubated samples at temperatures above 30°C, and most had very few measurement temperatures (≤4), therefore, were not be representative of the full curvature of the response. Waddington *et al.* (2001), Treat *et al.* (2014), and Hopple *et al.* (2020) found CO_2 production rates were exponential but did not incubate any higher than 20°C. Glissman *et al.* (2004), Sjögersten *et al.* (2018), Liu *et al.* (2021) also found the same exponential response but did not incubate at temperatures higher than 30–35°C.

Studies that incubated peat above 30°C found there was a decline in rates after a T_{opt}. Yao and Conrad (2000) observed CO_2 production at all temperatures between 4.7–49.5°C and found rates were highest between 25–40°C. This temperature range is fairly consistent with the highest production rates found in our study, however, some of our sites demonstrate the highest production values at temperatures exceeding 40°C. McKenzie *et al.* (1998) and Waddington *et*

al. (2001) linked these warmer soil temperatures to better conditions for decomposing microorganisms and increased chemical reaction rates that result in higher production rates. Metje and Frenzel (2005) also observed anaerobic CO_2 production across a wide temperature range (0–60°C) and found that, after an initial decline at 35°C, CO_2 production rates increased again at 40°C and continued increasing until 47°C. Metje and Frenzel (2007) confirmed this relationship in another study and observed the initial decline at 30°C, followed by an increase in production until 58°C. These results are relevant to the CO_2 production responses found in our results, given the relationship becomes unclear above ~30–35°C. Yao and Conrad (2000) also found that maximum anaerobic CO_2 production differed 1) between field locations in the Philippines and Italy and 2) during their 16-day incubation period. With the exception of one site, CO_2 production reached a T_{opt} at 35–40°C between incubation days 0–2, but between days 2–4 production at those temperatures was much lower. The multiple T_{opt} detected throughout the duration of the incubation during the Yao and Conrad (2000) experiments were suggested to be caused by the presence of multiple microbial communities activated at different temperatures. The initial T_{opt} found between 0–2 days are similar to the T_{opt} we observed across four days. Deng *et al.* (2019) observed a T_{opt} at 45°C for the first ~58 days of their incubation, however, this changed to 30°C for the remaining 40 days of the incubation. Bergman *et al.* (1998) suggested that longer incubations may suffer from the depletion of substrate. To understand whether differences in CO_2 curves are meaningful and to constrain the CO_2 temperature response, we would need more incubation runs.

While most studies observed maximum potential rates of CO_2 at temperatures around 30°C, followed by a decline in rate, an exception to this was Kolton *et al.* (2019). They found separate production optima throughout the duration of their four-week incubation. Most similar to our results was the T_{opt} at 33°C found after 0.4 days of their incubation, although T_{opt} at 4–7°C and 20–23°C were also found during the incubation (Kolton *et al.*, 2019). They attribute the low T_{opt} to faster utilization of other TEAs under warmer conditions during the week-long pre-incubation period and that multiple microbial communities are active within this temperature range. At our sites, no clear T_{opt} was detected at 20–23°C suggesting that perhaps these communities did not exist, or if they did exist, the T_{opt} was not clearly defined during the four-day incubation. Our choice of the experimental temperature range (8.5–51°C) precludes detection of T_{opt} in the range of 4-7°C. Our results did not show a rapid decline in production rate after T_{opt}, but perhaps this could be attributed to the length of the incubation period. Had incubations been longer, there may have been a decrease in production rates at certain

temperatures, causing the change in T_{opt} observed in the Kolton study. Their reported CO_2 production rates were highly variable across the temperature range, with no coherent pattern in temperature response. Their study included one incubation run with three replicates per temperature, highlighting the difficulty in obtaining clear data for building these relationships. Kolton *et al.* (2019) provided figures in their Supplementary Material outlining the change in response rate over time for each temperature increment across the temperature gradient. The response rate at each temperature notably changed over time, suggesting that response rates averaged over a few weeks could produce a different result to response rates averaged over a few days. Yao and Conrad (2000) observed that after 16 days there was low production suggesting substrate had been exhausted, similar to the exhaustion of TEAs theorized by Kolton *et al.* (2019). Our results were based on peat samples incubated over four days, which is a relatively short incubation period for sampling anaerobic gas production from peat, considering the length of incubations undertaken in previous publications. Longer incubations would be required to find out whether the temperature response shifts through time or whether production ceases at a certain point.

Kolton *et al.* (2019) observed the two detectable temperature optima reflected environmental temperatures found *in situ* during winter and summer. *In situ* temperatures at our sites did not reach the T_{opt} described by our temperature response curves. Maximum soil temperatures for Site DP at the sampling depth (–20 cm) were ~25°C, which was ~7°C below the T_{inf} of 32°C. At Kopuatai, maximum temperatures at the sampling depth (–10 cm) were around 15°C, which was well below the T_{inf} at any of the Kopuatai sites (25–32.2°C). Waddington *et al.* (2001) found that drained sites were characterized by stronger temperature fluctuations and microbial populations may adapt to these changing conditions and warmer temperatures.

The temperature responses and magnitude differed for CH_4 and CO_2 production. Methane production rates had sharper declines after the T_{opt}, whereas the decline after the T_{opt} for CO_2 was less constrained and highly variable. Furthermore, the maximum CO_2 production rates were much higher. For example, the highest rates from Site IM were ~200 nmol hr^{-1} g^{-1}, whereas CH_4 production peaked at ~10 nmol hr^{-1} g^{-1}. This was not the case for Glissman *et al.* (2004), who observed CH_4 had twice the production rate of CO_2. Anaerobic CO_2 is an important by-product and reactant in the processes of acetoclastic and hydrogenotrophic methanogenesis, respectively. Alongside these two processes, anaerobic CO_2 can be produced via other interactions in the soil profile including upstream fermentation reactions before undergoing methanogenesis and contact with oxygen in the soil profile (Keller & Bridgham,

2007; Bridgham *et al.*, 2013). Metje and Frenzel (2007) found that CO_2 production rates were strongly correlated with CH_4 production rates, and that CO_2 production mainly originated from acetoclastic methanogenesis. However, we would need additional measurements to explore the specific pathway for CO_2 production from our sites.

In terms of magnitude, Site IM had the largest anaerobic CO_2 production rates compared to the other sites, while Site DP had the lowest. This result may seem surprising considering ecosystem respiration rates measured at Site DP using EC techniques were very high compared to Kopuatai (Goodrich *et al.*, 2017; Campbell *et al.*, 2021). However, this signal is dominated by aerobic decomposition following drainage. Inglett *et al.* (2012) found that rates of anaerobic CO_2 production were just 7% of production rates found under aerobic conditions, which could explain why anaerobic CO_2 was so low for Site DP despite large overall net CO_2 fluxes at the ecosystem scale. Waddington *et al.* (2001) also compared a native (intact) site to two drained sites of varying times since initial drainage and found the CO_2 production was highest for the native site and lower for the drained sites, although production did not differ based on time since drainage. Waddington *et al.* (2001) explained that the fibric surface layer in the intact peat provides a substantial supply of labile carbon in comparison to the drained sites.

The CO_2 production temperature response curvature differed among all our sites, as indicated by the differences in T_{opt} and the shape of the curvature evident in Figures 4.10–4.12. This could be due to differences in initial decomposition steps releasing CO_2. However, to improve interpretation, we would need to take more incubation runs to resolve the variability among samples. In particular, we briefly explored additional incubation experiments to understand why we did not observe a clear T_{opt} from Site DP. We hypothesized that the lack of T_{opt} was a result of microbial processes in the soil being substrate– or hydro–limited (too wet or too dry), but our results suggested this was not the case. Sampling peat from beneath the water table (–100 cm), resulted in a relatively flat temperature response with relatively high production rates. Interestingly, this was also similar to results we obtained after attempting a kill control by autoclaving samples before incubation (Appendix A). Anaerobic CO_2 production rates were very high and variable (results not shown), possibly because of surviving microbial populations feeding on new labile substrate in the form of dead microbial biomass.

On the other hand, adding glucose to the drained peat sampled from ~300 mm depth, resulted in the same temperature response curve as non-glucose amended control soils, but with increased production across all temperatures. The stimulatory effect on CO_2 production with

higher concentrations of glucose may imply that the microbial community was substrate limited (Bergman *et al.*, 1998), but we did not see a subsequent change in curvature of the temperature response as described by Numa *et al.* (2021). The temperature response measured in our incubations is the net result of the biological process (enzyme-mediate rate) and physical processes (diffusion of substrates and resulting products). We expected that the added substrate would result in our measured temperature response being dominated by the biological compenent, as shown in aerobic CO_2 respiration studies (Schipper et al., 2019; Numa et al., 2021), where curvature becomes dictated more by MMRT than by Arrhenius. However, the complexity of pathways contributing to anaerobic CO_2 production may require a more nuanced approach to determine the nature of this behavior in saturated peatland environments, especially those degraded by drainage.

In order to understand the mechanisms controlling the temperature response of anaerobic CO_2 production, we require more data from wetland soils interrogating a wide range of temperatures. Additionally, soil heterogeneity, a lack of CO_2 production measurements, and a lack of standard techniques for quantifying rates have led to uncertainties in the temperature response of anaerobic CO_2 production (Kolton *et al.*, 2019). We also suggest the need to isolate particular reactions to understand the various pathways of anaerobic CO_2 production.

4.5.3 Anaerobic CO_2:CH_4 production ratio

All four of our sites exhibit a similar pattern of decline in the CO_2:CH_4 production ratio with increasing temperature until reaching the T_{opt} of methanogenesis (~35°C), followed by a sudden and rapid increase due to continued high rates of CO_2 production. This initial decline with temperature was expected, as previous studies have found that peat systems become increasingly more methanogenic with increasing temperature (Inglett *et al.*, 2012; Wilson *et al.*, 2016b; Hopple *et al.*, 2020). However, these studies also omit temperatures above the T_{opt} of methanogenesis (≥30°C), failing to capture the critical point where CH_4 production crashes. Kolton *et al.* (2019) captured both anaerobic CH_4 and CO_2 production above 30°C and suggested the system became increasingly methanogenic after the CO_2 T_{opt} (4–7°C). However, as discussed in Section 4.5.2, their anaerobic CO_2 production data were highly variable and based on only one round of incubations. Hopple *et al.* (2020) and Inglett *et al.* (2012) suggested that CO_2:CH_4 ratios are strongly controlled by the disproportionate increase in methanogenesis at higher temperatures, rather than decreasing CO_2 rates. Our results show that much more

work is needed to determine the trajectory of this ratio with warming, and any reduction in CO_2:CH_4 production may be punctuated by a sharp reversal above the CH_4 production T_{opt}.

The low concentrations of alternative TEAs in peatlands (Keller & Bridgham, 2007), suggests that methanogenesis is likely to dominate anaerobic C mineralization in these systems and produce equimolar CO_2:CH_4 (Conrad, 2020). Contrary to this, high CO_2:CH_4 ratios are a common finding in anaerobic C mineralization studies, particularly during laboratory incubations. Therefore, the high magnitude of CO_2 production in comparison to CH_4 in our results was expected, although the reasons for this are poorly understood (Segers & Kengen, 1998; Yavitt & Seidman-Zager, 2006; Keller & Bridgham, 2007; Bridgham & Ye, 2013). Yavitt and Seidman-Zager (2006) found the CO_2:CH_4 production ratio ranged from 5:1 to 40:1, with an average of 12:1, in peat soils and was larger in samples from drier, forested sites than wet sedge sites. We found that CO_2:CH_4 production ratios were within the range given by Yavitt and Seidman-Zager (2006) for IS, IE, and DP sites which ranged from 1:1 to 11:1. However, the ratio for Site IM ranged from 11:1 to 70:1, far exceeding the other sites in their study. The CO_2:CH_4 production rate was 1:1 for the lower temperatures of Site DP and around the CH_4 production T_{opt} for Site IE. Wilson *et al.* (2017) suggested that environments that lack alternative TEAs generally conform to the predicted 1:1 ratio, however, our results fail to demonstrate this. Wilson *et al.* (2017) attributed the non-stoichiometric production of CO_2 to the hydrogenation of unsaturated OM. The apparent CO_2:CH_4 imbalance was explained in other studies by aromatic compounds inhibiting methanogenesis (Ye *et al.*, 2012; Bridgham & Ye, 2013), build-up of fermentation by-products and the accumulation of acetate (Bridgham *et al.*, 2013), anaerobic oxidation of CH_4 (Smemo & Yavitt, 2011; Blazewicz *et al.*, 2012), and microbial growth elevating CO_2 production (Conrad, 2020; Liu *et al.*, 2021). Kolton *et al.* (2019) suggested that an increased abundance of CO_2-producing bacteria compared to CH_4-producing archaea could be responsible for the majority of anaerobic organic matter decomposition. However, these explanations cannot sustain increased CO_2 production without subsequent CH_4 generation, as they do not represent terminal electron sinks for the additional electrons produced when CO_2 is produced without concomitant CH_4 (Wilson *et al.*, 2017).

The observed increase in the CO_2:CH_4 ratio with increasing temperature, driven by the strong curvature of CH_4 production temperature dependence, may have important implications for temperature-driven carbon loss from wetlands (Keller & Bridgham, 2007) and for future positive feedbacks to global warming (Yvon-Durocher *et al.*, 2014). If systems become more methanogenic, this is important given the greater global warming potential of CH_4 compared

to CO_2 (28–34 times that of CO_2 over a 100-year time frame) (Myhre *et al.*, 2013). We need to determine the net effect of warming to understand how potential increases in carbon sequestration due to increasing plant biomass production may be offset by the climate forcing of projected temperature-driven increases in CH_4 production (Hopple *et al.*, 2020; Duffy *et al.*, 2021). Günther *et al.* (2020) suggested that metrics such as GWP fail to account for temporal forcing dynamics. While CH_4 has an increased radiative forcing compared to CO_2, the long-term persistence of CO_2 in the atmosphere may be more impactful based on accumulation and time-dependent climatic effects. Both GWP and temporal forcing dynamics of both gases are important considerations in the conversation around the rewetting of drained peat. Günther *et al.* (2020) suggested rewetting peatlands is a viable method for decreasing carbon emissions, despite the reestablishment of CH_4 emissions. The observed long-term effects of CO_2 emissions from drained peat outweighed the CH_4 emissions associated with rewetting drained peat (Günther *et al.*, 2020) Despite the continued anaerobic production of CO_2 at higher temperatures observed at our sites, in contrast to the rapid decline in methanogenesis, the contribution of anaerobic CO_2 production to total ecosystem CO_2 respiration is generally small. However, our results suggest that if soil temperatures were to exceed the methanogenic T_{opt} (30.1-32.8°C), CO_2 production would dominate anaerobic carbon emissions from both intact and drained peat. This process will likely compound with current trajectories for CO_2 emissions from drained or rewetted peat. Waddington *et al.* (2001) suggest that beginning restoration of drained peatlands through rewetting is crucial to prevent increases in peat temperature and subsequent CO_2 production. Currently, environmental peat temperatures sit below the T_{inf} for each site, however, soil temperatures are consistently lower at Kopuatai compared to the drained site, despite similar air temperatures. This is likely caused by increased litter quantities at Kopuatai preventing solar radiation from reaching the peat surface (Goodrich *et al.*, 2017). This negative feedback is another crucial addition to the conversation on rewetting drained peatlands as it implies that revegetating drained peatlands with intact peatland vegetation will reduce production rates at *in situ* temperatures.

4.5.4 Utility of MMRT in describing temperature dependence

Our data present the full curvature of the CH_4 production response to a wide temperature range. This is an important step in understanding how temperature constrains biological processes associated with the production of CH_4 from these peat systems and what implications this might have for climate change. Alster *et al.* (2020) and Mukhtar *et al.* (2019) recommended

temperature response experiments be designed to cover as many discrete temperatures as possible, across a biologically relevant temperature range that includes T_{opt}. In addition to collecting adequate data representing biological response rates, another method for understanding this relationship is modelling. Derived from thermodynamic first principles, MMRT was a useful representation of our data because it fit well and allowed us to derive biologically relevant metrics. Understanding how temperature fundamentally controls biological reactions across communities, organisms, and processes is important for interpreting microbial responses to climate change (Davidson & Janssens, 2006; Schipper *et al.*, 2014; Alster *et al.*, 2020). Microbial temperature response traits including temperature optimum (T_{opt}), change in heat capacity (ΔC_p), and the inflection point temperature (T_{inf}), provide insights into the organismal response to temperature changes.

To date, the only other study to apply MMRT to CH_4 production was Schipper *et al.* (2014), who used an illustrative example from Yao and Conrad (2000), producing T_{opt} between 30–35°C. The lack of results on CH_4 temperature responses modelled using MMRT means we cannot directly compare our findings to other studies. However, multiple peat systems throughout the Northern Hemisphere show a similar temperature response to our results from Southern Hemisphere sites (Figure 4.8). This suggests that multiple peat systems, including permafrost peat, could be modelled using MMRT if methods were standardized.

Several mathematical equations have been developed to simulate the intrinsic temperature response of microbial processes in soils, including the Arrhenius function, exponential function, and the MMRT model (Mukhtar *et al.*, 2019). However, Alster *et al.* (2020) suggested Arrhenius and Q_{10} functions give misleading metrics of soil biological temperature sensitivity. The Arrhenius model and Q_{10} functions are often used to model temperature response due to their relative simplicity and familiarity (Updegraff *et al.*, 1998), although, neither account for a decline in rates above a T_{opt} (Schipper et al. 2014). For those studies that did not take temperature measurements across a range large enough to derive a T_{opt}, the researcher generally observed a highly significant, positive, exponential response in production rate with temperature, which could sufficiently be modelled using Q_{10} and Arrhenius functions. However, Q_{10} values can overestimate rates at low temperatures and show extreme variation in the literature with values ranging between 1 and 28 (Dalal *et al.*, 2007). MacDonald *et al.* (1998) found an exponential increase in CH_4 production rates between temperatures 5–30°C with Q_{10} of 2.5–3.5. This exponential pattern was also captured in our study below the T_{opt}, however CH_4 and CO_2 production data measured from both the intact sites and the drained site showed

a subsequent decline in rates. Therefore, Arrhenius or Q_{10} functions would be incapable of describing the full curvature of the response between temperatures 8.5–51°C.

Parameters estimated by MMRT have the potential to improve our understanding of theoretically dependent, enzyme-catalyzed reactions with temperature. MMRT is an important tool for representing and recognizing how enzymes and organisms adapt to temperature in soil systems and for making predictions of microbial temperature responses to climate change (Alster *et al.*, 2020), in contrast to the status quo (i.e. Q_{10}). MMRT is most often used to predict rate responses for aerobic CO_2 at the enzyme scale, although recent publications have investigated this response at the soil ecosystem to global scales (Numa *et al.*, 2021). Our study highlights the ability of MMRT to predict the temperature-rate response for anaerobic peat C-GHG production and adds to the growing dataset of responses at the soil community scale.

On the other hand, there are pitfalls and disadvantages to using MMRT, including that it uses three parameters, which could lead to overfitting. In comparison, Arrhenius has two parameters, Q_{10} has one single slope parameter, and more complex models may require more parameters (Alster *et al.*, 2020). Our data clearly show an inflecting temperature response that requires extra parameters to allow the curve to reflect that, furthermore, other studies find a similar result for CH_4 production (Robinson *et al.*, 2017; Alster *et al.*, 2018; Alster *et al.*, 2020). MMRT also requires a large set of temperatures across a wide temperature range and temperatures above the T_{opt} are particularly important (Alster *et al.*, 2020). However, Alster *et al.* (2020) suggest interactions between high temperatures and soil moisture may confound temperature response results and recommends controlling for these variables where possible.

4.5.5 Method review and applicability to other systems

The handling of peat samples during field and laboratory work may have caused a disturbance to microbial activity. Peat samples were exposed to oxygen during removal in the field, which may have caused an increased C-GHG loss as aerobic CO_2. Wilson *et al.* (2016b) suggests that results from manipulation studies often see a large initial change in headspace gas concentrations, which is lessened over time when ecosystems are pushed rapidly from equilibrium. Despite the physical disturbance of taking cores and digging soil pits, we observed consistent temperature response results for CH_4 production, suggesting microbial communities were generally still functioning predictably. However, the CO_2 production response to temperature was more difficult to interpret. It is possible that the processes and microbial

communities responsible for the observed CO_2 production were more affected by removal from *in situ* conditions.

The time between field sampling and flushing the sample containers to maintain anaerobic conditions should be kept to a minimum (Bridgham & Ye, 2013; Hopple *et al.*, 2020). Ideally, the sample should be flushed with oxygen-free gas immediately upon extraction from the soil or peat; however, this was not practical in our experiment. For example, it was not feasible in our case to carry the N_2 gas tank on the 4 km round-trip walk into the peatland for flushing in the field. Flushing in the field or transporting the core back to the lab and cutting in an oxygen-free glove box may have been more effective methods of maintaining anaerobic conditions as observed by Hopple *et al.* (2020). However, an oxygen-free glove box was also not available in this study. On the other hand, a benefit of flushing in the lab was that multiple sample tubes could be flushed at once using a gas manifold, saving considerable time given the large number of sample tubes we collected. Flushing after a few hours may also have removed any excess gas that may have accumulated in the tube after disturbance during removal from *in situ* conditions. Keller and Bridgham (2007) found that a consistent linear production of CH_4 throughout the course of their incubations suggested their samples were effectively anaerobic. Across the four-day incubation in this experiment, the production of CH_4 and anaerobic CO_2 were linear, suggesting our samples were also effectively anaerobic.

Despite homogenization of samples being a relatively common preparation technique for organic soils, we chose not to homogenize peat to avoid as much microbial disturbance as possible. Homogenizing our samples may have reduced the observed variability, as we found there was large variation in the production results among triplicates, particularly when CH_4 production was high (Figure 4.6). However, similar amounts of variation were also detected in studies that did homogenize their soils (Dunfield *et al.*, 1993; Kolton *et al.*, 2019). This suggests that the variation in production is less a function of methodology and more a function of the inherent variability in methanogenic activity.

Storage time for samples between collection and analysis was kept to a minimum to best represent *in situ* conditions based on methods in Hopple *et al.* (2020). Other studies typically store peat on ice or at 4°C, however low temperatures can slow CH_4 production or cause loss of methanogenic activity due to the build-up of acetate (Yavitt & Seidman-Zager, 2006; Conrad, 2020). We did our best to avoid this in our study, however, there may be an initial increase in production rates associated with disturbance and solubility of CH_4 from peat (Wilson *et al.*,

2016b), which could have impacted our results. Accounting for changes in CH_4 solubility with temperature may reduce uncertainty in future incubation analysis.

We used four-day incubations for generating temperature response curves after testing longer incubation times. The first four days of incubations at each temperature produced linear increases in headspace gas concentrations, for which we used linear regressions to calculate slopes and determine production rates. After four days, however, we observed variable responses in headspace concentrations over time, including levelling off and even declines in concentration. Long incubations may disrupt the natural processes in bog soils that we were interested in observing. This includes restricting natural flows of water, gas, and substrate into and out of the system (Belyea & Baird, 2006). Longer incubations may also suffer from the depletion of substrate over time. Bergman *et al.* (1998) suggested that during their three-week incubation period, substrate was likely depleted at increasing rates with increasing temperatures. Yao and Conrad (2000) found that CH_4 production between 4–16 days was much lower than production in the first four days with no clear T_{opt}, suggesting substrate had been exhausted. Duc *et al.* (2010) also suggested a drawback of longer incubation periods is that other processes, including CH_4 consumption, may occur, leading to an underestimation of production rates. For this reason, Duc *et al.* (2010) calculated headspace concentration change over the first two days after beginning incubation. The linear increase in headspace concentration over time in Kolton *et al.* (2019) differed in slope with each subsequent measurement. This is in contrast to results from Glissman *et al.* (2004), who found both CH_4 and CO_2 production were constant from Day 8 to 73 of incubation at any temperature. Tveit *et al.* (2015) also found that CH_4 headspace concentration increased linearly over 25–150 days. Alongside substrate depletion and CH_4 consumption, production rate decline may be indicative of a methodological issue (e.g., gas leaking from Hungate tubes). Without further analysis into CH_4 consuming processes or methodological inconsistencies, it remains unclear what may have caused the declines in headspace concentrations we observed over long incubation periods.

Given that there are so few examples of temperature response curves with sufficient detail, it is difficult to relate the results described in this study for two New Zealand ombrotrophic peatland systems to either Northern Hemisphere systems or other Southern Hemisphere systems. Hopple *et al.* (2020) suggested that anaerobic C cycling and CH_4 emissions differ significantly among southern habitats. Zalman *et al.* (2018) also suggested that even seemingly similar peatlands within the same geographical region can differ in CH_4 dynamics. In contrast, our results show that the temperature response of CH_4 production of a drained peatland used

for agriculture was similar to an intact peatland, despite the sites having very different hydrological and biogeochemical profiles. Zalman *et al.* (2018) suggest that caution should be used when extrapolating a relationship from one site and that using one peatland to represent all peatlands is inappropriate, even among outwardly very similar peatlands (Zalman *et al.*, 2018). However, we compared our results to a diverse set of CH_4 production temperature responses from the literature, which, despite the highly variable magnitudes, all demonstrated similar temperature-rate curve characteristics. Therefore, we suggest that that CH_4 production has a conserved temperature response regardless of the environment.

4.6 Conclusion

Methane production from intact and drained New Zealand peatlands demonstrated a consistent temperature response, despite differences in gross magnitudes, hydrology, and vegetation among sites. T_{opt} ranged between 30.1 and 32.8°C, while T_{inf} ranged between 23.3 and 25.6°C. The temperature range over which CH_4 production peaked was relatively constrained, with both sharply increasing and decreasing tails on the response curves. The temperature response of CH_4 production was also similar to that of Northern Hemisphere peatlands, where a similar temperature range was examined. Our data show that production rates were most variable near the T_{opt} (30–40°C), and in order to better constrain this parameter, future studies should consider doing more replicates at each site to produce a better average.

In terms of anaerobic CO_2 production, temperature response metrics did not significantly differ among sites, however, T_{opt} and T_{inf} parameters were slightly higher than for CH_4 production. The anaerobic CO_2 T_{opt} ranged between 35.4 and 44.0°C, while T_{inf} ranged between 25 and 32.2°C.

Unlike the rapid decline in CH_4 production rates above T_{opt}, the relationship between CO_2 production and temperature became more variable, but the temperature range encompassing the highest rates of production for anaerobic CO_2 was notably larger than observed for CH_4. This led to a consistent temperature dependence in the CO_2:CH_4 ratio among sites, whereby the systems seemed to become more methanogenic with temperature until ~30°C, the methanogenic T_{opt}, above which the ratio rapidly increased. As observed in previous studies, the CO_2:CH_4 ratio was consistently ≥1 at all temperatures across all sites due to higher magnitudes of CO_2 production, although the various contributions to anaerobic CO_2 production are not well understood. Further research into the microbial communities present in these

systems may provide insight into the pathways and sources of anaerobic CH_4 and CO_2 production. The relationship between anaerobic CH_4 and CO_2 production with temperature outlined in this study provides valuable new data on the full temperature response of anaerobic decomposition in peatlands. These relationships are important in understanding carbon dynamics and C-GHG production from peatlands in a warming climate, as well as for the rewetting of drained peatlands.

Chapter 5
Conclusion

5.1 Findings

Studies on the temperature response of CH_4 production from peatlands are limited, particularly where carried out over a large temperature range. Currently, the most supported conclusion is that CH_4 production increases with increasing temperature, however, few studies incubate peat across a range wide enough temperature range to see a decline in production rates at higher temperatures. In this study, we measured CH_4 production rates from intact and drained New Zealand peatlands at 18 discrete temperatures across a temperature range of 8.5–51°C.

We observed that the temperature response of CH_4 production did not differ significantly across drained and intact sites. Additionally, examination of peat from different vegetation zones within the intact site revealed that the temperature response of CH_4 production did not significantly differ across vegetation types. The temperature range of CH_4 production was relatively constrained, with MMRT-derived metrics of T_{opt} between 30.1–32.8°C and T_{inf} between 23.3–25.6°C. The response was conserved across all sites and showed similarities to the temperature responses of Northern Hemisphere peatlands across similar temperature ranges. Production rates were most variable near the T_{opt} (30–40°C). Variability in CH_4 production is a common result as found in previous studies (Zalman *et al.*, 2018). Constraining the relationship between CH_4 production and temperature has been challenging considering the variability and sensitivity of methanogen communities (Inglett *et al.*, 2012; Zalman *et al.*, 2018). The temperature response of CH_4 production can be attributed to microbial species and their temperature ranges and the pathways of methanogenesis. Environmental temperature ranges and substrate quality as a function of vegetation inputs in turn determine the pathways for methanogenesis in the peat. It also remains unclear how the temperature response parameters T_{opt} and T_{inf} represent in relation to *in situ* temperatures, as there was no obvious correlation between environmental temperatures and these metrics.

Despite differences in the shape of the responses for anaerobic CO_2 production, sites did not significantly differ in terms of temperature metrics derived from MMRT. T_{opt} and T_{inf} parameters for anaerobic CO_2 were slightly higher than CH_4 production with anaerobic CO_2 T_{opt} between 35.4–44°C and T_{inf} between 25–32.2°C. Studies on the temperature response of anaerobic CO_2 from peatlands are limited (Waddington *et al.*, 2001; Treat *et al.*, 2014; Tveit *et*

al., 2015; Hanson *et al.*, 2016; Wilson *et al.*, 2016b; Hopple *et al.*, 2020), particularly over a large temperature range (Yao & Conrad, 2000; Glissman *et al.*, 2004; Metje & Frenzel, 2005; Yavitt *et al.*, 2006; Metje & Frenzel, 2007; Sjögersten *et al.*, 2018; Deng *et al.*, 2019; Kolton *et al.*, 2019; Liu *et al.*, 2021). Therefore, it was difficult to compare our results and understand the drivers of each site response. In terms of a comparison between CH_4 and CO_2 production versus temperature curvature, the rapid decline in CH_4 production above T_{opt} was not clearly observed for anaerobic CO_2 production. After this point, the relationship between CO_2 production and temperature became unclear. The temperature range of activity for anaerobic CO_2 was larger than observed for CH_4. The rapid decline in CH_4 production rates after the T_{opt} and the large negative ΔC_p suggested that CH_4 was a more temperature sensitive process, relative to anaerobic CO_2 production. Another point of difference between CH_4 and CO_2 production was the much larger magnitude of CO_2 production rates, which was expected, based on other publications, however, the cause of this is still debated.

Few studies have incubated peat above 30–35°C, but for those that have, there is an obvious decline in rate above this temperature (Svensson, 1984; Dunfield *et al.*, 1993; Yao & Conrad, 2000; Yavitt *et al.*, 2006; Metje & Frenzel, 2007; Freitag & Prosser, 2009; Blake *et al.*, 2015; Sjögersten *et al.*, 2018; Deng *et al.*, 2019; Kolton *et al.*, 2019). Frequently used models that describe the relationship between soil decomposition and temperature, including Arrhenius and Q_{10} functions, fail to capture this decline in rates and tend to overestimate rates at lower temperatures. However, MMRT successfully fit the temperature responses of CH_4 and anaerobic CO_2 production for all sites, including Sites DP and IE, despite these sites failing to exhibit an obvious decline in production rates for anaerobic CO_2. After previous success using MMRT to model enzymatic rates and aerobic CO_2, these results are a valuable test of the ability of MMRT to model anaerobic C-GHG production at the soil community scale. The previous use of MMRT for modelling CH_4 production was limited to a rice paddy soil (Schipper *et al.*, 2014) and we are not aware of it being used to model CH_4 production rates from any peatlands. Our results add to the growing applications for MMRT in modelling soil carbon dynamics. Understanding the temperature responses of soil biological processes is crucial in determining consequences for soil carbon dynamics with climate change (Alster *et al.*, 2020). The similarity in the responses we detected between our results and multiple Northern Hemisphere peat systems implies that MMRT could also be used in other peat systems.

The CO_2:CH_4 production ratio followed a similar pattern with temperature at each site. Initially, the change in CH_4 production rate dominated the decline (Site IE) or plateauing (Sites IM, IS, DP) of the ratio until the methanogenic T_{opt} was exceeded. Thereafter, the rapid reduction in

CH_4 production combined with the continuously high CO_2 production rates causes the ratio to rapidly increase. The decline in the ratio towards the methanogenic T_{opt} observed for Site IE has been observed in previous studies, which suggests peat systems become relatively more methanogenic with increasing temperature. However, these studies did not incubate above methanogenic T_{opt}, consequently failing to capture the rapid increase in the ratio controlled both by the crash in CH_4 production and high production rates of CO_2 at this temperature. Also observed in previous studies is that the CO_2:CH_4 ratio was consistently ≥1 at all temperatures across all sites in this study. This was most obvious for Site IM ratios, which ranged from 11:1 to 70:1. Previous studies have debated the cause of the apparent CO_2:CH_4 imbalance and the source of CO_2 is unknown. This is often the case for anaerobic incubations (Keller & Bridgham, 2007); however, this could be due to methodological discrepancies in the handling of the peat.

In terms of methodology, our technique produced consistent results. Anaerobic CH_4 and CO_2 responses with temperature were detected and production rates remained relatively constant for the duration of our incubation period, suggesting the techniques used in this experiment provided results representative of methanogen communities (Keller & Bridgham, 2007). Throughout the four-day incubations in this experiment, we did not detect multiple T_{opt} or a decline in overall production rates. These types of observations are evident in studies with longer incubations and are attributed to shifts in microbial diversity over time (Deng *et al.*, 2019; Kolton *et al.*, 2019), CH_4 consumption, or issues with methodology.

5.2 Implications for rewetting drained peatlands

The relationship between anaerobic CH_4 and CO_2 production with temperature outlined in this study provides new data on the temperature response of methanogenesis in anaerobic peatlands. This relationship is important in understanding carbon dynamics and C-GHG production from peatlands under climate warming scenarios and for the rewetting of drained peatlands.

The rapid increase in the CO_2:CH_4 ratio at the methanogenic T_{opt} may encourage the temperature-driven CO_2 loss from wetlands (Keller & Bridgham, 2007) and cause positive feedbacks to climate warming scenarios. Rewetting peatlands is a feasible option to decrease carbon emissions because, despite the revival of CH_4 emissions, the long-term effects of CO_2 emissions from drained peat exceed the impact of CH_4 emissions associated with rewetting drained peat (Günther *et al.*, 2020). Our results suggest that if soil temperatures were to exceed the methanogenic T_{opt} (30.1–32.8°C), CO_2 production would increasingly dominate C-GHG emissions from both intact and drained peatlands. This process will likely compound current

trajectories for CO_2 emissions from anaerobic zones in drained or rewetted peat. Beginning restoration of drained peatlands through rewetting is crucial to mitigate increases in peat temperature and subsequent CO_2 production. Additionally, determining the net effect of warming will help us understand how potential increases in carbon sequestration due to increasing plant biomass production may be offset by the climate forcing of projected temperature-driven increases in anaerobic CH_4 and CO_2 production (Hopple *et al.*, 2020; Duffy *et al.*, 2021).

5.3 Future work

Until now, there have been no studies on the production of anaerobic CH_4 and CO_2 from Southern Hemisphere peatlands across a wide temperature gradient. This data paucity exacerbates uncertainties associated with estimation of global C-GHG output from peatlands. This study provides results indicating that the temperature response of CH_4 production for a drained and intact New Zealand peatland is tightly constrained and relatively conserved with temperature. Previous studies focussed on the temperature response of CH_4 production revealed a similar response across different peatland types (Dunfield *et al.*, 1993; Yavitt *et al.*, 2006; Metje & Frenzel, 2007; Freitag & Prosser, 2009; Blake *et al.*, 2015; Kolton *et al.*, 2019). Therefore, we suggest collecting samples from a variety of global peatland systems and incubating samples across ≥18 independent temperatures using the same methodology described in this study. More than 18 independent temperatures within the temperature range given in this study would provide more production rates and allow increased accuracy of curve fits. It would also be beneficial to undertake more replicates to improve accuracy and get better averages. The 95% CIs around derived parameters were large suggesting we would need more replicates in order to detect any potential differences in the populations used in this study. Overall, these considerations could help determine whether the relationship between temperature and CH_4 production is conserved across a wider distribution of peatland systems. Furthermore, research into the microbial communities present in these anaerobic peat systems might provide an insight into the sources of C-GHG production. Conducting microbial assays and DNA sequencing could better inform us of the microbial populations present at a given temperature and whether this changes over a temperature gradient.

For consistency, it would be beneficial for studies to use the same methodology when quantifying the temperature response of anaerobic C-GHG. Our suggestions would be to limit the peat disturbance during sampling where possible, avoid homogenizing peat, and avoid

performing long pre-incubation or incubation periods unless the objective is to observe a time-dependent temperature response. A faster turnaround time from the time of sampling peat until incubation likely better represents *in situ* conditions (Hopple *et al.*, 2020). Studies like this will ensure more accurate and reliable data are collected and available for climate projections focused on C cycling and Earth system models.

It would also be worthwhile further investigating the response of anaerobic CO_2 to temperature to improve our understanding of this relationship and how it relates to CH_4 production. Alongside increasing the number of independent incubation temperatures, it would be useful to assess CO_2 production across a larger temperature range. Unlike CH_4 production, the full curvature of the anaerobic CO_2 response was not captured across the temperature range in this study (i.e., did not observe a decline in rates for Site IE and DP). Quantifying the anaerobic CO_2 response after amending peat with substrate additions could be useful in understanding why the shape of the curvature differed among the four sites in this study (Numa *et al.*, 2021). Additionally, investigating how CO_2 is produced under anaerobic conditions would inform us of the sources and pathways of C in these soils and whether exposure to oxygen during sampling is destabilizing C from peat cores.

In terms of patterns of CH_4 production with depth, Figure 4.4 suggests that the highest production rates are at –30 cm at the intact wetland site, contrary to the depth of maximum production deduced at the ecosystem scale (Goodrich *et al.*, 2015). Collecting peat samples at different depths within the profile and recreating CH_4 temperature response curves for these samples would provide insight into how the magnitude of CH_4 production changes with depth.

5.4 Recommendations

Overall, the thermal optima and temperature response of microbial processes is a topic that deserves greater attention (Hamilton, 2010). While the future work section outlined suggestions for repeating studies similar to this one, the following recommendations outline the next steps needed to improve our understanding of the relationship between anaerobic CH_4 and CO_2 production and temperature incubations:

- Collecting more replicates at each site (≥3) and increasing the number of replicates at each temperature (≥3) would allow more accurate means and reduce variability in production rates. Additionally, peat should be incubated at as many different temperatures (≥18) as necessary to produce accurate curve fits.

- To capture the full curvature of the responses, incubations should extend to temperatures above 30°C, as these data will capture the decline in CH_4 production rates after T_{opt}.
- MMRT should be used to fit models describing the temperature response of anaerobic production processes. Other models e.g., Arrhenius and Q_{10} are incapable of simulating temperature response dynamics.
- During sampling, aim to reduce exposure of the peat sample to air and keep the time between sampling and incubation to a minimum and avoid pre-incubating samples where possible.
- Aim for short incubation durations (≤4 days) for assessing C-GHG production, unless specifically assessing the changes in production rates with temperature over time.

References

Agnew, A., Rapson, G., Sykes, M., & Bastow Wilson, J. (1993). The functional ecology of *Empodisma minus* (Hook, f.) Johnson & Cutler in New Zealand ombrotrophic mires. *New Phytologist, 124*(4), 703-710.

Alster, C. J., von Fischer, J. C., Allison, S. D., & Treseder, K. K. (2020). Embracing a new paradigm for temperature sensitivity of soil microbes. *Global Change Biology, 26*(6), 3221-3229.

Alster, C. J., Weller, Z. D., & von Fischer, J. C. (2018). A meta‐analysis of temperature sensitivity as a microbial trait. *Global Change Biology, 24*(9), 4211-4224.

Ausseil, A.-G., Jamali, H., Clarkson, B., & Golubiewski, N. (2015). Soil carbon stocks in wetlands of New Zealand and impact of land conversion since European settlement. *Wetlands Ecology and Management, 23*(5), 947-961.

Baird, A. J., Beckwith, C. W., Waldron, S., & Waddington, J. (2004). Ebullition of methane‐containing gas bubbles from near‐surface *Sphagnum* peat. *Geophysical Research Letters, 31*(21).

Bartlett, D. S., Bartlett, K. B., Hartman, J. M., Harriss, R. C., Sebacher, D. I., Pelletier‐Travis, R., Dow, D. D., & Brannon, D. P. (1989). Methane emissions from the Florida Everglades: Patterns of variability in a regional wetland ecosystem. *Global Biogeochemical Cycles, 3*(4), 363-374.

Basiliko, N., Stewart, H., Roulet, N. T., & Moore, T. R. (2012). Do root exudates enhance peat decomposition? *Geomicrobiology Journal, 29*(4), 374-378.

Bellisario, L., Bubier, J., Moore, T., & Chanton, J. (1999). Controls on CH_4 emissions from a northern peatland. *Global Biogeochemical Cycles, 13*(1), 81-91.

Belyea, L. R., & Baird, A. J. (2006). Beyond "the limits to peat bog growth": Cross‐scale feedback in peatland development. *Ecological Monographs, 76*(3), 299-322.

Bergman, I., Klarqvist, M., & Nilsson, M. (2000). Seasonal variation in rates of methane production from peat of various botanical origins: effects of temperature and substrate quality. *FEMS Microbiology Ecology, 33*(3), 181-189.

Bergman, I., Svensson, B. H., & Nilsson, M. (1998). Regulation of methane production in a Swedish acid mire by pH, temperature and substrate. *Soil Biology and Biochemistry, 30*(6), 729-741.

Blake, L. I., Tveit, A., Øvreås, L., Head, I. M., & Gray, N. D. (2015). Response of methanogens in Arctic sediments to temperature and methanogenic substrate availability. *PLoS One, 10*(6), e0129733.

Blazewicz, S. J., Petersen, D. G., Waldrop, M. P., & Firestone, M. K. (2012). Anaerobic oxidation of methane in tropical and boreal soils: ecological significance in terrestrial methane cycling. *Journal of Geophysical Research: Biogeosciences, 117*(G2).

Bosatta, E., & Ågren, G. I. (1999). Soil organic matter quality interpreted thermodynamically. *Soil Biology & Biochemistry, 31*(13), 1889-1891.

Bridgham, S. D., Cadillo‐Quiroz, H., Keller, J. K., & Zhuang, Q. (2013). Methane emissions from wetlands: biogeochemical, microbial, and modeling perspectives from local to global scales. *Global Change Biology, 19*(5), 1325-1346.

Bridgham, S. D., & Ye, R. (2013). Organic matter mineralization and decomposition. *Methods in Biogeochemistry of Wetlands, 10*, 385-406.

Broder, T., Blodau, C., Biester, H., & Knorr, K.-H. (2012). Peat decomposition records in three pristine ombrotrophic bogs in southern Patagonia. *Biogeosciences, 9*(4), 1479-1491.

Brown, M. G., Humphreys, E. R., Moore, T. R., Roulet, N. T., & Lafleur, P. M. (2014). Evidence for a nonmonotonic relationship between ecosystem‐scale peatland methane emissions and water table depth. *Journal of Geophysical Research: Biogeosciences, 119*(5), 826-835.

Campbell, D. I., Glover-Clark, G. L., Goodrich, J. P., Morcom, C. P., Schipper, L. A., & Wall, A. M. (2021). Large differences in CO_2 emissions from two dairy farms on a drained peatland driven by contrasting respiration rates during seasonal dry conditions. *Science of The Total Environment, 760*, 143410.

Campbell, D. I., Smith, J., Goodrich, J. P., Wall, A. M., & Schipper, L. A. (2014). Year-round growing conditions explains large CO_2 sink strength in a New Zealand raised peat bog. *Agricultural and Forest Meteorology, 192*, 59-68.

Casado, M. R., Corstanje, R., Bellamy, P., & Marchant, B. (2013). Issues of sampling design in wetlands. *Methods in Biogeochemistry of Wetlands, 10*, 1-19.

Castro, M. S., Steudler, P. A., Melillo, J. M., Aber, J. D., & Bowden, R. D. (1995). Factors controlling atmospheric methane consumption by temperate forest soils. *Global Biogeochemical Cycles, 9*(1), 1-10.

Chapin, F. S., Woodwell, G. M., Randerson, J. T., Rastetter, E. B., Lovett, G. M., Baldocchi, D. D., Clark, D. A., Harmon, M. E., Schimel, D. S., & Valentini, R. (2006). Reconciling carbon-cycle concepts, terminology, and methods. *Ecosystems, 9*(7), 1041-1050.

Charman, D. J. (2002). *Peatlands and environmental change*. Chichester: Chichester : Wiley.

Chin, K.-J., Lukow, T., & Conrad, R. (1999). Effect of temperature on structure and function of the methanogenic archaeal community in an anoxic rice field soil. *Applied and Environmental Microbiology, 65*(6), 2341-2349.

Clarkson, B. R., Schipper, L. A., & Lehmann, A. (2004). Vegetation and peat characteristics in the development of lowland restiad peat bogs, North Island, New Zealand. *Wetlands, 24*(1), 133-151.

Clymo, R. (1984). The limits to peat bog growth. *Philosophical Transactions of the Royal Society of London. B, Biological Sciences, 303*(1117), 605-654.

Conrad, R. (2020). Importance of hydrogenotrophic, aceticlastic and methylotrophic methanogenesis for methane production in terrestrial, aquatic and other anoxic environments: A mini review. *Pedosphere, 30*(1), 25-39.

Dalal, R. C., Allen, D. E., Livesley, S. J., & Richards, G. (2007). Magnitude and biophysical regulators of methane emission and consumption in the Australian agricultural, forest, and submerged landscapes: a review. *Plant and Soil, 309*(1-2), 43-76.

Davidson, E. A., & Janssens, I. A. (2006). Temperature sensitivity of soil carbon decomposition and feedbacks to climate change. *Nature, 440*(7081), 165-173.

Deng, Y., Liu, P., & Conrad, R. (2019). Effect of temperature on the microbial community responsible for methane production in alkaline NamCo wetland soil. *Soil Biology and Biochemistry, 132*, 69-79.

Deverel, S. J., Ingrum, T., & Leighton, D. (2016). Present-day oxidative subsidence of organic soils and mitigation in the Sacramento-San Joaquin Delta, California, USA. *Hydrogeology Journal, 24*(3), 569-586.

Dinsmore, K. J., Billett, M. F., Skiba, U. M., Rees, R. M., Drewer, J., & Helfter, C. (2010). Role of the aquatic pathway in the carbon and greenhouse gas budgets of a peatland catchment. *Global Change Biology, 16*(10), 2750-2762.

Dinsmore, K. J., Skiba, U. M., Billett, M. F., Rees, R. M., & Drewer, J. (2009). Spatial and temporal variability in CH4 and N2O fluxes from a Scottish ombrotrophic peatland: Implications for modelling and up-scaling. *Soil Biology and Biochemistry, 41*(6), 1315-1323.

Dlugokencky, E. J., Nisbet, E. G., Fisher, R., & Lowry, D. (2011). Global atmospheric methane: budget, changes and dangers. *Philosophical Transactions of the Royal Society A: Mathematical, Physical and Engineering Sciences, 369*(1943), 2058-2072.

Duc, N. T., Crill, P., & Bastviken, D. (2010). Implications of temperature and sediment characteristics on methane formation and oxidation in lake sediments. *Biogeochemistry, 100*(1), 185-196.

Duffy, K. A., Schwalm, C. R., Arcus, V. L., Koch, G. W., Liang, L. L., & Schipper, L. A. (2021). How close are we to the temperature tipping point of the terrestrial biosphere? *Science Advances, 7*(3), eaay1052.

Dunfield, P., Knowles, R., Dumont, R., & Moore, T. (1993). Methane production and consumption in temperate and subarctic peat soils: Response to temperature and pH. *Soil Biology & Biochemistry, 25*(3), 321-326.

Dymond, J. R., Sabetizade, M., Newsome, P. F., Harmsworth, G. R., & Ausseil, A.-G. (2021). Revised extent of wetlands in New Zealand. *New Zealand Journal of Ecology, 45*(2), 3444.

Elsgaard, L., Olsen, A. B., & Petersen, S. O. (2016). Temperature response of methane production in liquid manures and co-digestates. *Science of the Total Environment, 539*, 78-84.

Etminan, M., Myhre, G., Highwood, E., & Shine, K. (2016). Radiative forcing of carbon dioxide, methane, and nitrous oxide: A significant revision of the methane radiative forcing. *Geophysical Research Letters, 43*(24), 12,614-12,623.

Eville, G. (1991). Northern Peatlands: Role in the Carbon Cycle and Probable Responses to Climatic Warming. *Ecol Appl, 1*(2), 182-195.

Fang, C., & Moncrieff, J. (2001). The dependence of soil CO_2 efflux on temperature. *Soil Biology and Biochemistry, 33*(2), 155-165.

Fiore, A. M., Jacob, D. J., Field, B. D., Streets, D. G., Fernandes, S. D., & Jang, C. (2002). Linking ozone pollution and climate change: The case for controlling methane. *Geophysical Research Letters, 29*(19), 25-1-25-4.

Fisher, M., & Reddy, K. (2013). Soil pore water sampling methods. *Methods in Biogeochemistry of Wetlands, 10*, 55-70.

Freitag, T. E., & Prosser, J. I. (2009). Correlation of methane production and functional gene transcriptional activity in a peat soil. *Applied and Environmental Microbiology, 75*(21), 6679-6687.

Fritz, C., Campbell, D. I., & Schipper, L. A. (2008). Oscillating peat surface levels in a restiad peatland, New Zealand—magnitude and spatiotemporal variability. *Hydrological Processes: An International Journal, 22*(17), 3264-3274.

Frolking, S., Roulet, N., & Fuglestvedt, J. (2006). How northern peatlands influence the Earth's radiative budget: Sustained methane emission versus sustained carbon sequestration. *Journal of Geophysical Research: Biogeosciences, 111*(G1).

Frolking, S., & Roulet, N. T. (2007). Holocene radiative forcing impact of northern peatland carbon accumulation and methane emissions. *Global Change Biology, 13*(5), 1079-1088.

Gedney, N., Cox, P., & Huntingford, C. (2004). Climate feedback from wetland methane emissions. *Geophysical Research Letters, 31*(20).

Glissman, K., Chin, K.-J., Casper, P., & Conrad, R. (2004). Methanogenic pathway and archaeal community structure in the sediment of eutrophic Lake Dagow: effect of temperature. *Microbial Ecology, 48*(3), 389-399.

Goodrich, J. P., Campbell, D. I., Roulet, N. T., Clearwater, M. J., & Schipper, L. A. (2015). Overriding control of methane flux temporal variability by water table dynamics in a Southern Hemisphere, raised bog. *Journal of Geophysical Research: Biogeosciences, 120*(5), 819-831.

Goodrich, J. P., Campbell, D. I., & Schipper, L. A. (2017). Southern Hemisphere bog persists as a strong carbon sink during droughts. *Biogeosciences, 14*(20), 4563-4576.

Gougoulias, C., Clark, J. M., & Shaw, L. J. (2014). The role of soil microbes in the global carbon cycle: tracking the below ‐ ground microbial processing of plant ‐ derived carbon for manipulating carbon dynamics in agricultural systems. *Journal of the Science of Food and Agriculture, 94*(12), 2362-2371.

Granberg, G., Mikkelä, C., Sundh, I., Svensson, B. H., & Nilsson, M. (1997). Sources of spatial variation in methane emission from mires in northern Sweden: A mechanistic approach in statistical modeling. *Global Biogeochemical Cycles, 11*(2), 135-150.

Günther, A., Barthelmes, A., Huth, V., Joosten, H., Jurasinski, G., Koebsch, F., & Couwenberg, J. (2020). Prompt rewetting of drained peatlands reduces climate warming despite methane emissions. *Nature Communications, 11*(1), 1-5.

Hamdi, S., Moyano, F., Sall, S., Bernoux, M., & Chevallier, T. (2013). Synthesis analysis of the temperature sensitivity of soil respiration from laboratory studies in relation to incubation methods and soil conditions. *Soil Biology & Biochemistry, 58*, 115-126.

Hamill, J. (2019). *Methane emission hotspots from a drained peat soil under dairy grazing.* The University of Waikato.

Hamilton, S. K. (2010). Biogeochemical implications of climate change for tropical rivers and floodplains. *Hydrobiologia, 657*(1), 19-35.

Hanson, P., Gill, A., Xu, X., Phillips, J., Weston, D., Kolka, R., Riggs, J., & Hook, L. (2016). Intermediate-scale community-level flux of CO_2 and CH_4 in a Minnesota peatland: putting the SPRUCE project in a global context. *Biogeochemistry, 129*(3), 255-272.

Hargreaves, K., & Fowler, D. (1998). Quantifying the effects of water table and soil temperature on the emission of methane from peat wetland at the field scale. *Atmospheric Environment, 32*(19), 3275-3282.

Hobbs, J. K., Jiao, W., Easter, A. D., Parker, E. J., Schipper, L. A., & Arcus, V. L. (2013). Change in heat capacity for enzyme catalysis determines temperature dependence of enzyme catalyzed rates. *ACS Chemical Biology, 8*(11), 2388-2393.

Hodgkins, S. B., Chanton, J. P., Langford, L. C., McCalley, C. K., Saleska, S. R., Rich, V. I., Crill, P. M., & Cooper, W. T. (2015). Soil incubations reproduce field methane dynamics in a subarctic wetland. *Biogeochemistry, 126*(1), 241-249.

Hopple, A., Wilson, R., Kolton, M., Zalman, C. A., Chanton, J. P., Kostka, J., Hanson, P. J., Keller, J. K., & Bridgham, S. (2020). Massive peatland carbon banks vulnerable to rising temperatures. *Nature Communications, 11*(1), 1-7.

Huang, Y., Ciais, P., Luo, Y., Zhu, D., Wang, Y., Qiu, C., Goll, D. S., Guenet, B., Makowski, D., & De Graaf, I. (2021). Tradeoff of CO_2 and CH_4 emissions from global peatlands under water-table drawdown. *Nature Climate Change*, 1-5.

Inglett, K., Inglett, P., Reddy, K., & Osborne, T. (2012). Temperature sensitivity of greenhouse gas production in wetland soils of different vegetation. *Biogeochemistry, 108*(1), 77-90.

Joosten, H., Tapio-Biström, M.-L., & Tol, S. (2012). *Peatlands: guidance for climate change mitigation through conservation, rehabilitation and sustainable use*. Food and Agriculture Organization of the United Nations Rome.

Kaat, A., & Joosten, H. (Compiler) (2009). *Factbook for UNFCCC policies on peat carbon emissions, Wetlands International, Wageningen, the Netherlands*.

Keller, J. K., & Bridgham, S. D. (2007). Pathways of anaerobic carbon cycling across an ombrotrophic‐minerotrophic peatland gradient. *Limnology and Oceanography, 52*(1), 96-107.

Keller, J. K., & Takagi, K. K. (2013). Solid‐phase organic matter reduction regulates anaerobic decomposition in bog soil. *Ecosphere, 4*(5), 1-12.

Kettunen, A., Kaitala, V., Lehtinen, A., Lohila, A., Alm, J., Silvola, J., & Martikainen, P. J. (1999). Methane production and oxidation potentials in relation to water table fluctuations in two boreal mires. *Soil Biology and Biochemistry, 31*(12), 1741-1749.

Kirschke, S., Bousquet, P., Ciais, P., Saunois, M., Canadell, J. G., Dlugokencky, E. J., Bergamaschi, P., Bergmann, D., Blake, D. R., & Bruhwiler, L. (2013). Three decades of global methane sources and sinks. *Nature geoscience, 6*(10), 813-823.

Knox, S. H., Bansal, S., McNicol, G., Schafer, K., Sturtevant, C., Ueyama, M., Valach, A. C., Baldocchi, D., Delwiche, K., & Desai, A. R. (2021). Identifying dominant environmental predictors of freshwater wetland methane fluxes across diurnal to seasonal time scales. *Global Change Biology*.

Kolton, M., Marks, A., Wilson, R. M., Chanton, J. P., & Kostka, J. E. (2019). Impact of Warming on Greenhouse Gas Production and Microbial Diversity in Anoxic Peat From a *Sphagnum* -Dominated Bog (Grand Rapids, Minnesota, United States). *Front Microbiol, 10*, 870.

Laine, J., Silvola, J., Tolonen, K., Alm, J., Nykänen, H., Vasander, H., Sallantaus, T., Savolainen, I., Sinisalo, J., & Martikainen, P. J. (1996). Effect of water-level drawdown on global climatic warming: Northern peatlands. *Ambio*, 179-184.

Le Mer, J., & Roger, P. (2001). Production, oxidation, emission and consumption of methane by soils: A review. *European Journal of Soil Biology, 37*(1), 25-50.

Lehmann, J. R., Münchberger, W., Knoth, C., Blodau, C., Nieberding, F., Prinz, T., Pancotto, V. A., & Kleinebecker, T. (2016). High-resolution classification of south patagonian peat bog microforms reveals potential gaps in up-scaled CH4 fluxes by use of Unmanned Aerial System (UAS) and CIR imagery. *Remote Sensing, 8*(3), 173.

Liang, L. L., Arcus, V. L., Heskel, M. A., O'Sullivan, O. S., Weerasinghe, L. K., Creek, D., Egerton, J. J., Tjoelker, M. G., Atkin, O. K., & Schipper, L. A. (2018). Macromolecular rate theory (MMRT) provides a thermodynamics rationale to underpin the convergent temperature response in plant leaf respiration. *Global Change Biology, 24*(4), 1538-1547.

Lin, X., Green, S., Tfaily, M., Prakash, O., Konstantinidis, K., Corbett, J., Chanton, J., Cooper, W., & Kostka, J. (2012). Microbial community structure and activity linked to contrasting biogeochemical gradients in bog and fen environments of the Glacial Lake Agassiz Peatland. *Applied and environmental Microbiology, 78*(19), 7023-7031.

Liu, Y., Yang, J., Ning, K., Wang, A., Wang, Q., Wang, X., Wang, S., Lv, Z., Zhao, Y., & Yu, J. (2021). Temperature sensitivity of anaerobic CO_2 production in soils of *Phragmites*

australis marshes with distinct hydrological characteristics in the Yellow River estuary. *Ecological Indicators, 124*, 107409.

Lloyd, J., & Taylor, J. (1994). On the temperature dependence of soil respiration. *Functional Ecology*, 315-323.

Loisel, J., Gallego-Sala, A., Amesbury, M., Magnan, G., Anshari, G., Beilman, D., Benavides, J., Blewett, J., Camill, P., & Charman, D. (2021). Expert assessment of future vulnerability of the global peatland carbon sink. *Nature climate change, 11*(1), 70-77.

Ma, S., Jiang, J., Huang, Y., Shi, Z., Wilson, R. M., Ricciuto, D., Sebestyen, S. D., Hanson, P. J., & Luo, Y. (2017). Data‐constrained projections of methane fluxes in a northern Minnesota peatland in response to elevated CO_2 and warming. *Journal of Geophysical Research: Biogeosciences, 122*(11), 2841-2861.

MacDonald, J., Fowler, D., Hargreaves, K., Skiba, U., Leith, I., & Murray, M. (1998). Methane emission rates from a northern wetland; response to temperature, water table and transport. *Atmospheric Environment, 32*(19), 3219-3227.

McGlone, M. (2009). Postglacial history of New Zealand wetlands and implications for their conservation. *New Zealand Journal of ecology, 33*(1).

McKenzie, C., Schiff, S., Aravena, R., Kelly, C., & Louis, V. S. (1998). Effect of temperature on production of CH_4 and CO_2 from peat in a natural and flooded boreal forest wetland. *Climatic Change, 40*(2), 247-266.

Megonigal, J. P., Hines, M. E., & Visscher, P. T. (Compiler) (2004). *Anaerobic metabolism: linkages to trace gases and aerobic processes*: Elsevier-Pergamon.

Metje, M., & Frenzel, P. (2005). Effect of temperature on anaerobic ethanol oxidation and methanogenesis in acidic peat from a northern wetland. *Applied and Environmental Microbiology, 71*(12), 8191-8200.

Metje, M., & Frenzel, P. (2007). Methanogenesis and methanogenic pathways in a peat from subarctic permafrost. *Environmental Microbiology, 9*(4), 954-964.

Mitsch, W., & Gosselink, J. (Compiler) (2000). *Wetlands Third Edition John Wiley & Sons*: Toronto.

Moore, T., & Dalva, M. (1993). The influence of temperature and water table position on carbon dioxide and methane emissions from laboratory columns of peatland soils. *Journal of Soil Science, 44*(4), 651-664.

Mukhtar, H., Lin, Y.-P., Lin, C.-M., & Petway, J. R. (2019). Assessing thermodynamic parameter sensitivity for simulating temperature responses of soil nitrification. *Environmental Science: Processes & Impacts, 21*(9), 1596-1608.

Myhre, G., Shindell, D., Bréon, F., Collins, W., Fuglestvedt, J., Huang, J., Koch, D., Lamarque, J., & Lee, D. (2013). Mendoza, 25 B. *Nakajima, T., Robock, A., Stephens, G., Takemura, T., and Zhang, H. Anthropogenic and natural radiative forcing. In: Stocker, T., Qin, D., Plattner, GK, Tignor, M., Allen, S., Boschung, J., Nauels, A., Xia, Y., Bex, V., and Midgley, P.(eds) Climate Change, 505*.

Neubauer, S. C., & Megonigal, J. P. (2015). Moving beyond global warming potentials to quantify the climatic role of ecosystems. *Ecosystems, 18*(6), 1000-1013.

Newnham, R., De Lange, P., & Lowe, D. (1995). Holocene vegetation, climate and history of a raised bog complex, northern New Zealand based on palynology, plant macrofossils and tephrochronology. *The Holocene, 5*(3), 267-282.

Numa, K. (2020). *The temperature response of soil respiration from labile and stable carbon.* The University of Waikato.

Numa, K. B., Robinson, J. M., Arcus, V. L., & Schipper, L. A. (2021). Separating the temperature response of soil respiration derived from soil organic matter and added labile carbon compounds. *Geoderma, 400*, 115128.

Portner, H., Bugmann, H., & Wolf, A. (2010). Temperature response functions introduce high uncertainty in modelled carbon stocks in cold temperature regimes. *Biogeosciences, 7*(11), 3669-3684.

Prentice, E., Hicks, J., Ballerstedt, H., Blank, L. M., Liang, L., Schipper, L., & Arcus, V. L. (2020). The inflection point hypothesis: The relationship between the temperature dependence of enzyme catalyzed reaction rates and microbial growth rates. *Biochemistry (Easton)*.

Pronger, J., Schipper, L. A., Hill, R. B., Campbell, D. I., & McLeod, M. (2014). Subsidence rates of drained agricultural peatlands in New Zealand and the relationship with time since drainage. *Journal of Environmental Quality, 43*(4), 1442-1449.

Reddy, K., Clark, M., DeLaune, R., & Kongchum, M. (2013). Physicochemical characterization of wetland soils. *Methods in Biogeochemistry of Wetlands, 10*, 41-54.

Riley, W. J., Subin, Z. M., Lawrence, D. M., Swenson, S. C., Torn, M. S., Meng, L., Mahowald, N. M., & Hess, P. (2011). Barriers to predicting changes in global terrestrial methane fluxes: analyses using CLM4Me, a methane biogeochemistry model integrated in CESM. *Biogeosciences, 8*(7), 1925-1953.

Rinklebe, J., & Langer, U. (2013). Soil microbial biomass and phospholipid fatty acids. *Methods in Biogeochemistry of Wetlands, 10*, 331-348.

Robinson, J., O'Neill, T., Ryburn, J., Liang, L., Arcus, V., & Schipper, L. (2017). Rapid laboratory measurement of the temperature dependence of soil respiration and application to changes in three diverse soils through the year. *Biogeochemistry, 133*(1), 101-112.

Saunois, M., Stavert, A. R., Poulter, B., Bousquet, P., Canadell, J. G., Jackson, R. B., Raymond, P. A., Dlugokencky, E. J., Houweling, S., & Patra, P. K. (2020). The global methane budget 2000–2017. *Earth System Science Data, 12*(3), 1561-1623.

Schädel, C., Beem-Miller, J., Aziz Rad, M., Crow, S. E., Hicks Pries, C. E., Ernakovich, J., Hoyt, A. M., Plante, A., Stoner, S., Treat, C. C., & Sierra, C. A. (2020). Decomposability of soil organic matter over time: the Soil Incubation Database (SIDb, version 1.0) and guidance for incubation procedures. *Earth System Science Data, 12*(3), 1511-1524.

Schimel, J., & Holland, E. A. (2005). Global gases. *Principles and Applications of Soil Microbiology*, 491-494.

Schipper, L. A., Hobbs, J. K., Rutledge, S., & Arcus, V. L. (2014). Thermodynamic theory explains the temperature optima of soil microbial processes and high Q10 values at low temperatures. *Glob Chang Biol, 20*(11), 3578-3586.

Schipper, L. A., Petrie, O. J., O'Neill, T. A., Mudge, P. L., Liang, L. L., Robinson, J. M., & Arcus, V. L. (2019). Shifts in temperature response of soil respiration between adjacent irrigated and non-irrigated grazed pastures. *Agriculture, Ecosystems & Environment, 285*, 106620.

Schulz, S., Matsuyama, H., & Conrad, R. (1997). Temperature dependence of methane production from different precursors in a profundal sediment (Lake Constance). *FEMS Microbiology Ecology, 22*(3), 207-213.

Schuur, E. A., McGuire, A. D., Schädel, C., Grosse, G., Harden, J. W., Hayes, D. J., Hugelius, G., Koven, C. D., Kuhry, P., & Lawrence, D. M. (2015). Climate change and the permafrost carbon feedback. *Nature, 520*(7546), 171-179.

Schwärzel, K., Šimůnek, J., van Genuchten, M. T., & Wessolek, G. (2006). Measurement modeling of soil ‐ water dynamics evapotranspiration of drained peatland soils. *Journal of Plant Nutrition and Soil Science, 169*(6), 762-774.

Scott, D. A. (1996). *A directory of wetlands in New Zealand*. Department of Conservation.

Segers, R., & Kengen, S. (1998). Methane production as a function of anaerobic carbon mineralization: a process model. *Soil Biology and Biochemistry, 30*(8-9), 1107-1117.

Sierra, C. A. (2012). Temperature sensitivity of organic matter decomposition in the Arrhenius equation: some theoretical considerations. *Biogeochemistry, 108*(1), 1-15.

Sierra, C. A., Trumbore, S. E., Davidson, E. A., Vicca, S., & Janssens, I. (2015). Sensitivity of decomposition rates of soil organic matter with respect to simultaneous changes in temperature and moisture. *Journal of Advances in Modeling Earth Systems, 7*(1), 335-356.

Sjögersten, S., Aplin, P., Gauci, V., Peacock, M., Siegenthaler, A., & Turner, B. (2018). Temperature response of ex-situ greenhouse gas emissions from tropical peatlands: Interactions between forest type and peat moisture conditions. *Geoderma, 324*, 47-55.

Smemo, K., & Yavitt, J. (2011). Anaerobic oxidation of methane: an underappreciated aspect of methane cycling in peatland ecosystems? *Biogeosciences, 8*(3), 779-793.

Smith, J. (2003). *Fluxes of carbon dioxide and water vapour at a Waikato peat bog.* Thesis (Ph.D.)--University of Waikato, 2003.

Sorrell, B. K., & Brix, H. (2013). Gas transport and exchange through wetland plant aerenchyma. *Methods in Biogeochemistry of Wetlands, 10*, 177-196.

Svensson, B. H. (1984). Different temperature optima for methane formation when enrichments from acid peat are supplemented with acetate or hydrogen. *Applied and Environmental Microbiology, 48*(2), 389-394.

Tfaily, M. M., Cooper, W. T., Kostka, J. E., Chanton, P. R., Schadt, C. W., Hanson, P. J., Iversen, C. M., & Chanton, J. P. (2014). Organic matter transformation in the peat column at Marcell Experimental Forest: Humification and vertical stratification. *Journal of Geophysical Research. Biogeosciences, 119*(4), 661-675.

Tiner, & Ralph, W. (2016). *Wetland Indicators: A Guide to Wetland Formation, Identification, Delineation, Classification, and Mapping, Second Edition*. (2 ed. ed.). Baton Rouge: Baton Rouge: CRC Press Inc.

Treat, C. C., Natali, S. M., Ernakovich, J., Iversen, C. M., Lupascu, M., McGuire, A. D., Norby, R. J., Roy Chowdhury, T., Richter, A., & Šantrůčková, H. (2015). A pan ‐ Arctic synthesis of CH_4 and CO_2 production from anoxic soil incubations. *Global Change Biology, 21*(7), 2787-2803.

Treat, C. C., Wollheim, W. M., Varner, R. K., Grandy, A. S., Talbot, J., & Frolking, S. (2014). Temperature and peat type control CO_2 and CH_4 production in Alaskan permafrost peats. *Global Change Biology, 20*(8), 2674-2686.

Turetsky, M. R., Kotowska, A., Bubier, J., Dise, N. B., Crill, P., Hornibrook, E. R. C., Minkkinen, K., Moore, T. R., Myers-Smith, I. H., Nykänen, H., Olefeldt, D., Rinne, J., Saarnio, S., Shurpali, N., Tuittila, E.-S., Waddington, J. M., White, J. R., Wickland, K. P., & Wilmking, M. (2014). A synthesis of methane emissions from 71 northern, temperate, and subtropical wetlands. *Glob Chang Biol, 20*(7), 2183-2197.

Turner, A. J., Frankenberg, C., & Kort, E. A. (2019). Interpreting contemporary trends in atmospheric methane. *Proceedings of the National Academy of Sciences, 116*(8), 2805-2813.

Tveit, A. T., Urich, T., Frenzel, P., & Svenning, M. M. (2015). Metabolic and trophic interactions modulate methane production by Arctic peat microbiota in response to warming. *Proceedings of the National Academy of Sciences, 112*(19), E2507-E2516.

Updegraff, K., Bridgham, S. D., Pastor, J., & Weishampel, P. (1998). Hysteresis in the temperature response of carbon dioxide and methane production in peat soils. *Biogeochemistry, 43*(3), 253-272.

Van Huissteden, J., van den Bos, R., & Alvarez, I. M. (2006). Modelling the effect of water-table management on CO_2 and CH_4 fluxes from peat soils. *Netherlands Journal of Geosciences, 85*(1), 3-18.

van Winden, J. F., Reichart, G.-J., McNamara, N. P., Benthien, A., & Damsté, J. S. S. (2012). Temperature-Induced Increase in Methane Release from Peat Bogs: A Mesocosm Experiment. *PLoS One, 7*(6), e39614.

Waddington, J., Rotenberg, P., & Warren, F. (2001). Peat CO_2 production in a natural and cutover peatland: implications for restoration. *Biogeochemistry, 54*(2), 115-130.

Wagstaff, S., & Clarkson, B. (Compiler) (2012). *Systematics and ecology of the Australasian genus*: Empodisma.

Watson, A., Stephen, K. D., Nedwell, D. B., & Arah, J. R. (1997). Oxidation of methane in peat: kinetics of CH_4 and O_2 removal and the role of plant roots. *Soil Biology and Biochemistry, 29*(8), 1257-1267.

Wecking, A. R., Cave, V. M., Liáng, L. L., Wall, A. M., Luo, J., Campbell, D. I., & Schipper, L. A. (2020). A novel injection technique: using a field-based quantum cascade laser for the analysis of gas samples derived from static chambers. *Atmospheric Measurement Techniques, 13*(11), 5763-5777.

Weedon, J. T., Aerts, R., Kowalchuk, G. A., van Logtestijn, R., Andringa, D., & van Bodegom, P. M. (2013). Temperature sensitivity of peatland C and N cycling: Does substrate supply play a role? *Soil Biology and Biochemistry, 61*, 109-120.

Whalen, S. (2005). Biogeochemistry of methane exchange between natural wetlands and the atmosphere. *Environmental Engineering Science, 22*(1), 73-94.

Wilson, D., Blain, D., Couwenberg, J., Evans, C., Murdiyarso, D., Page, S., Renou-Wilson, F., Rieley, J., Sirin, A., & Strack, M. (2016a). Greenhouse gas emission factors associated with rewetting of organic soils. *Mires and Peat, 17*.

Wilson, R. M., Hopple, A. M., Tfaily, M. M., Sebestyen, S. D., Schadt, C. W., Pfeifer-Meister, L., Medvedeff, C., McFarlane, K. J., Kostka, J. E., Kolton, M., Kolka, R. K., Kluber, L. A., Keller, J. K., Guilderson, T. P., Griffiths, N. A., Chanton, J. P., Bridgham, S. D., & Hanson, P. J. (2016b). Stability of peatland carbon to rising temperatures. *Nat Commun, 7*, 13723.

Wilson, R. M., Tfaily, M. M., Rich, V. I., Keller, J. K., Bridgham, S. D., Zalman, C. M., Meredith, L., Hanson, P. J., Hines, M., & Pfeifer-Meister, L. (2017). Hydrogenation of organic matter as a terminal electron sink sustains high CO_2: CH_4 production ratios during anaerobic decomposition. *Organic Geochemistry, 112*, 22-32.

Yang, W. H., McNicol, G., Teh, Y. A., Estera‐Molina, K., Wood, T. E., & Silver, W. L. (2017). Evaluating the classical versus an emerging conceptual model of peatland methane dynamics. *Global Biogeochemical Cycles, 31*(9), 1435-1453.

Yao, H., & Conrad, R. (2000). Effect of temperature on reduction of iron and production of carbon dioxide and methane in anoxic wetland rice soils. *Biology and Fertility of Soils, 32*(2), 135-141.

Yavitt, J. B., Basiliko, N., Turetsky, M. R., & Hay, A. G. (2006). Methanogenesis and methanogen diversity in three peatland types of the discontinuous permafrost zone, boreal western continental Canada. *Geomicrobiology Journal, 23*(8), 641-651.

Yavitt, J. B., & Seidman-Zager, M. (2006). Methanogenic conditions in northern peat soils. *Geomicrobiology Journal, 23*(2), 119-127.

Ye, R., Jin, Q., Bohannan, B., Keller, J. K., McAllister, S. A., & Bridgham, S. D. (2012). pH controls over anaerobic carbon mineralization, the efficiency of methane production,

and methanogenic pathways in peatlands across an ombrotrophic–minerotrophic gradient. *Soil Biology and Biochemistry, 54*, 36-47.

Yu, Z., Loisel, J., Brosseau, D. P., Beilman, D. W., & Hunt, S. J. (2010). Global peatland dynamics since the Last Glacial Maximum. *Geophysical Research letters, 37*(13).

Yvon-Durocher, G., Allen, A. P., Bastviken, D., Conrad, R., Gudasz, C., St-Pierre, A., Thanh-Duc, N., & Del Giorgio, P. A. (2014). Methane fluxes show consistent temperature dependence across microbial to ecosystem scales. *Nature, 507*(7493), 488-491.

Zalman, C., Keller, J. K., Tfaily, M., Kolton, M., Pfeifer-Meister, L., Wilson, R., Lin, X., Chanton, J., Kostka, J., & Gill, A. (2018). Small differences in ombrotrophy control regional-scale variation in methane cycling among *Sphagnum*-dominated peatlands. *Biogeochemistry, 139*(2), 155-177.

Zhang, C., & Wang, Y. (2017). Projected future changes of tropical cyclone activity over the western North and South Pacific in a 20-km-mesh regional climate model. *Journal of Climate, 30*(15), 5923-5941.

Appendices

Appendix A

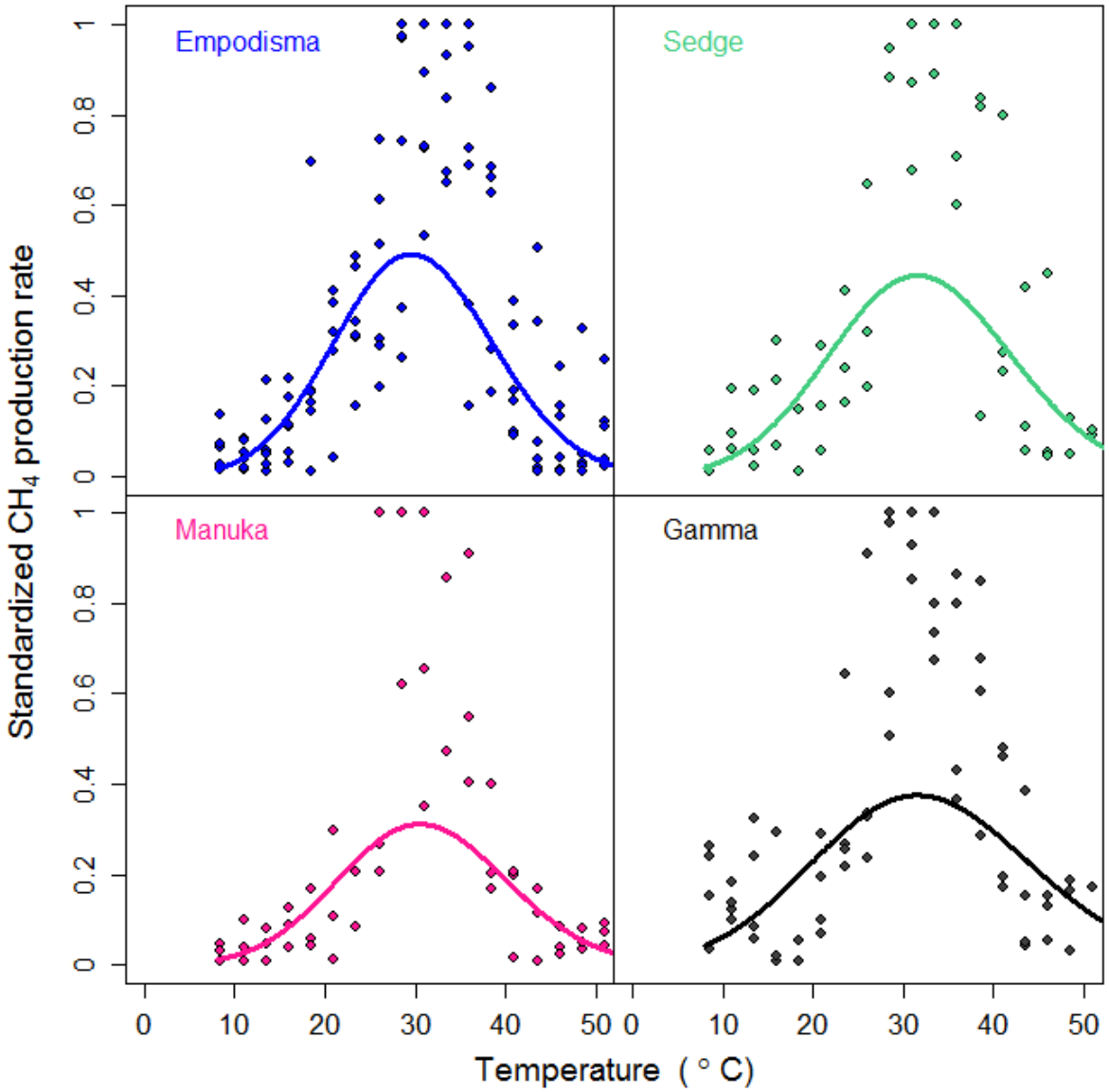

Figure A1 MMRT v.1 curve fit for all sites across temperatures between 8.5 to 51°C to show the lack of fit in comparison to Figure 4.7. Clearly, including the full temperature range in the fit does not accurately capture peak values at any site. Code for using R to plot MMRT to data across a list of temperatures is given in Appendix B.

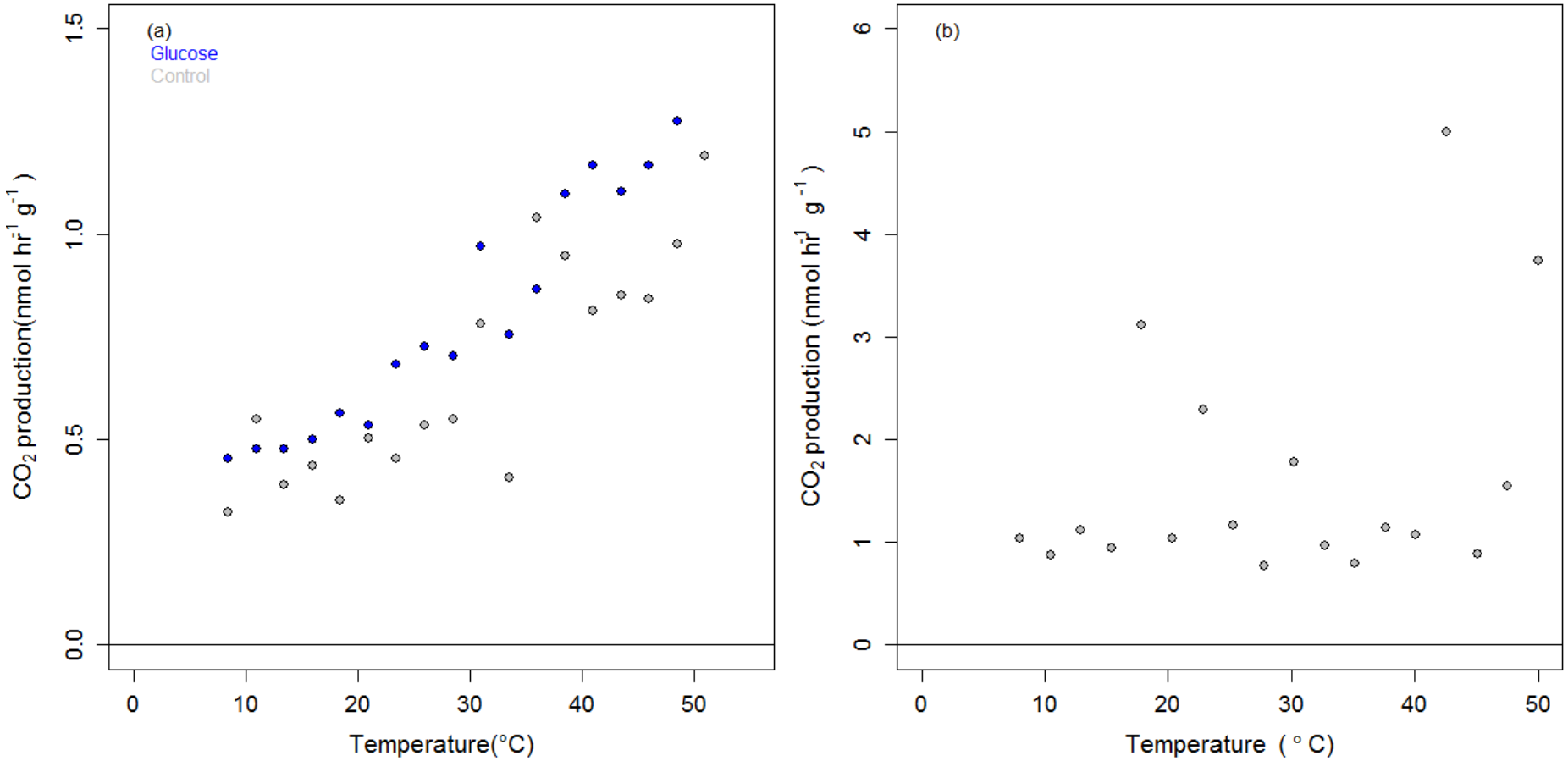

Figure A2 CO_2 production rates for a drained peat soil (Site DP) across a temperature gradient (8.5-51°C) for samples collected (a) at 30–35 cm with glucose additions (b) from beneath the existing water table at –100 cm.

Table 5 Interactions between site temperature curve characteristics for CH_4 production across a temperature gradient (8.5-51°C)

Site interactions	Difference in means	95% CI [LL, UL]	P value	Curve parameter
DP-IE	2.67	[–2,7.33]	0.37	
IM-IE	0.35	[–4.76, 5.46]	1	
IS-IE	2.45	[–2.65, 7.56]	0.51	T_{opt}
IM-DP	–2.32	[–7.84, 3.2]	0.61	
IS-DP	–0.21	[–5.73, 5.3]	1	
IS-IM	2.1	[–3.8, 8]	0.72	
DP-IE	2.26	[–1.11, 5.63]	0.25	
IM-IE	0.35	[–3.34, 4.05]	0.99	
IS-IE	1.52	[–2.18, 5.22]	0.63	T_{inf}
IM-DP	–1.91	[–5.9, 2.09]	0.51	
IS-DP	–0.74	[–4.73, 3.25]	0.94	
IS-IM	1.17	[–3.10, 5.43]	0.85	
DP-IE	132.64	[–11455.7, 11720.98]	1	
IM-IE	797.74	[–11896.66, 13492.13]	1	
IS-IE	4464.31	[–8230.08, 17158.7]	0.73	$\Delta C_P^{\ddagger}$ J mol^{-1} K^{-1}
IM-DP	665.09	[–13046.42, 18043.18]	1	
IS-DP	4331.67	[–9379.84, 18043.18]	0.79	
IS-IM	3666.57	[–10991.65, 18324.8]	0.88	
DP-IE	37788.5	[–20232.9, 95809.81]	0.27	
IM-IE	11048.1	[–52511.08, 74607.34]	0.95	
IS-IE	37735.2	[–25824.03, 101294.39]	0.34	$\Delta H_{T_0}^{\ddagger}$ J mol^{-1} K^{-1}
IM-DP	–26740	[–95392.12, 41911.47]	0.66	
IS-DP	–53.28	[–68705.07, 68598.52]	1	
IS-IM	26687.1	[–46704.81, 100078.91]	0.71	
DP-IE	123.88	[–65.31, 313.07]	0.26	
IM-IE	31.64	[–175.61, 238.89]	0.97	
IS-IE	121.67	[–85.58, 328.93]	0.35	$\Delta S_{T_0}^{\ddagger}$ J mol^{-1} K^{-1}
IM-DP	–92.24	[–316.09, 131.62]	0.62	
IS-DP	–2.21	[–226.06, 221.65]	1	
IS-IM	90.03	[–149.28, 329.34]	0.69	

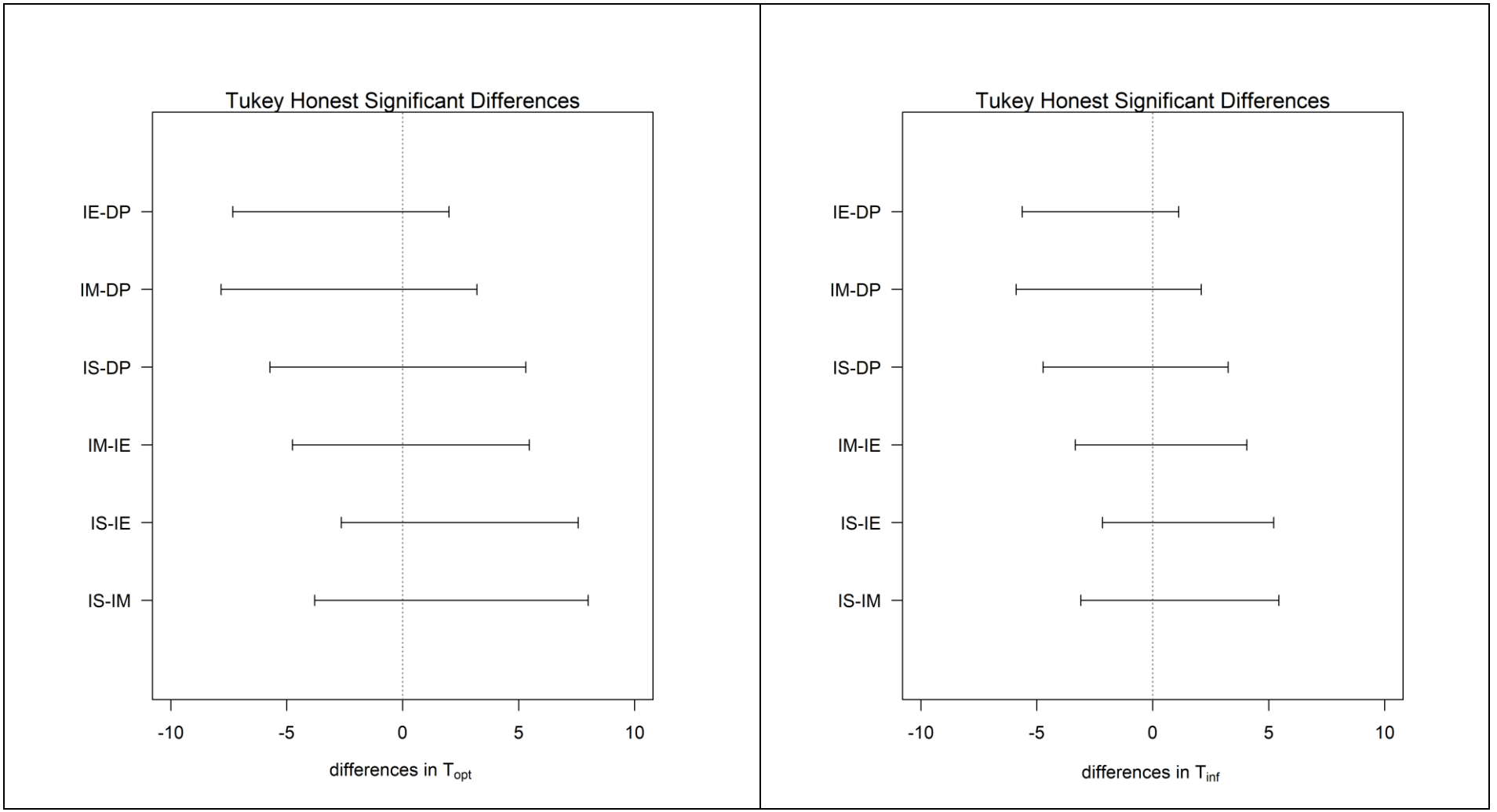

Figure A.3 Tukey's Honest Significance Difference demonstrating the differences in T_{opt} and $\underline{T}_{inf}$ across sites based on 95% confidence intervals.

Autoclave experiment

We considered carrying out an abiotic experiment to differentiate the biotic and abiotic temperature response of the peat. However, we decided against pursuing this experiment because after a few simple experiments, peat microbes proved to be very difficult to kill using an autoclave and after supposedly killing all microbial populations (2 cycles in the autoclave at 121°C = low CO_2), there was no temperature response from 10, 20, and 30°C or in the temperature block (1 replicate). Additionally, we decided kill controls were too indiscriminate as you cannot target specific microbial populations and could instead be measuring CO_2 output from other processes such as the denaturation of enzymes.

Appendix B

#R code for fitting MMRT to a rate versus temperature dataset

```
rm(list=ls())
#==================================
# some user input required here
#==================================
# for scaling data between ~0 and 1
newmin=0.01
newmax=1
# for limiting the range of temperature within which to fit MMRT
mint=14
maxt=44

#==================================
# sample data
#==================================
rdat=c(3.7,3.9,5.1,7.6,9.5,13.9,21.2,32.2,40.9,
        42.1,29.3,17.9,10.4,6.7,4.6,3.5,4.3,4.5)
temp=c(8.0,10.5,12.9,15.4,17.9,20.4,22.8,25.3,
        27.8,30.2,32.7,35.2,37.6,40.1,42.6,45.1,47.5,50.0)
# scale the data [0,1]
oldmin=min(rdat,na.rm=T)
oldmax=max(rdat,na.rm=T)
```

```
r=(rdat-oldmin)/(oldmax-oldmin)*(newmax-newmin)+newmin


#==================================

# prepare to fit MMRT

#==================================

# convert T from C to K

T=temp[temp>mint & temp<maxt]+273.15

# definte To as the midpoint of temperature range

To=mean(range(T))

# take the log of the rates

lnk=log(r[temp>mint & temp<maxt])

# define constants used in MMRT

kb    = 1.38064852e-23

h    = 6.626070040e-34

R    = 8.314


#==================================

# fit MMRT

#==================================

ifit=nls(lnk ~ log((kb*T)/h) - ((delH+(delCp*(T-To)))/(R*T)) + ((delS+(delCp*(log(T)-
log(To))))/(R)),

                start=list(delCp=-1000,delH=50000,delS=-
50),control=nls.control(maxiter=500))


#==================================
```

```
# plot the result
#==================================
# generate lots of new x for drawing a line
xs<-seq(mint+273.15, maxt+273.15, length.out=10000);
# use the predict() function to apply the model to the generated temperature
dev.new(width=5,height=3)
par(mar=c(4,4,1,1))
plot(temp,r,ylim=c(0,1.25),xlim=c(0,60),cex=1.1,pch=21,bg='grey',
        xlab=expression('Temperature'~ ~'('~degree~'C)'),
        ylab=expression('Scaled CH'[4]~'production'))
points(T-273.15,exp(lnk),cex=1.1,pch=21,bg='dodgerblue')
lines(xs-273.15, exp(predict(ifit, data.frame(T=xs))),col='dodgerblue',lwd=2)
abline(h=0)
```